

# **AN EXPERIMENTAL STUDY ON SETTLEMENT RESPONSE OF FOUNDATION ON REINFORCED SAND**

*A Thesis*

*Submitted in Partial Fulfillment of the Requirements  
for the Degree of*

**MASTER OF TECHNOLOGY**

By

**Sudhir Kumar Saxena**

*to the*

**Department of Civil Engineering  
INDIAN INSTITUTE OF TECHNOLOGY KANPUR  
JULY 2005**

TH

CE/2005/M

Sa 98e

13 OCT 2005 | CE

पुरषोत्तम लाल शर्मा केन्द्रीय पुस्तकालय  
भारतीय न्यायिक शिक्षा संस्थान कानपुर  
वर्षादि ६० A... 153060



A153060

# CERTIFICATE

It is to certify that the work contained in this thesis entitled "**An Experimental Study on Settlement Response of Foundation on Reinforced Sand** " by Sudhir Kumar Saxena has been carried out under my supervision and this work has not been submitted elsewhere for a degree.



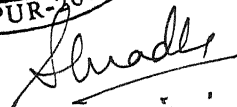
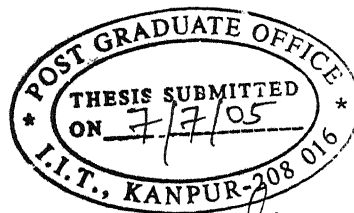
(Dr. Sarvesh Chandra)

Professor

Department of Civil Engineering

IIT Kanpur - 208016

July 2005



# ACKNOWLEDGEMENTS

I express my deep gratitude and sincere thanks to my thesis supervisor Dr. Sarvesh Chandra for his valuable guidance and encouragement through all the stages of my thesis work.

I am sincerely thankful to Dr. P. K. Basudhar and Dr. N.R. Patra for imparting valuable instructions during the course and encouragement during my thesis work.

My special thanks to Shri A. K. Srivastava, Shri Gulab Chand, Shri Kishan Pal Yadav and Shri Parashuram for their cooperation during my entire experimental work.

I would like to express my sincere thanks to all my course mates namely Mr. Abhik Datta, Mr. Arindam Dey, Mr. Bappaditya Manna, Mr. Paritosh Kumar, Mr. Pradipta Kundu, Mr. Shyam Vihari, Ms. Sutapa Hazra and Ms. Meera. for their help, support and friendly approach during the course. I would also like to thank Mr. Shanker and Mr. Kaushik Deb (both pursuing PhD) not only for their support and encouragement but also for their suggestions during my thesis.

I would also like to thank sincerely Mr. Susheel Kumar Yadav, Project Assistant who always willingly extended his helping hand during the compilation of my thesis whenever I got stuck up.

I am grateful to my parents for their encouragement and invaluable blessings.

Last but not the least, I am indebted to my wife, son and daughter for their encouragement and whole hearted support during the entire course.

Sudhir Kumar Saxena



**DEDICATED  
TO  
MY PARENTS**

# ABSTRACT

In this study, model tests have been conducted on Ennore sand to study the load-settlement response of reinforced sand bed. Two types of geosynthetic namely geotextile and geogrid were used for the model tests. The load-settlement response has been studied for different geotextile and geogrid with varying tensile strength. The tensile strength was varied by pasting two layers of geotextile and geogrid each. A dimensionless parameter Bearing Capacity Ratio ( $BCR_u$ ), which is the ratio of ultimate bearing capacity of the reinforced sand to the ultimate bearing capacity of the unreinforced sand, has been determined for single layer reinforced sand bed at various depth ratios to evaluate the performance of geotextile and geogrid as reinforcement with reference to their individual tensile strength. Also Bearing Capacity Ratio with respect to settlement ( $BCR_s$ ), which is the ratio of bearing pressure of the reinforced sand to the bearing pressure of the unreinforced sand at a given settlement  $s$ ,  $s \leq s_u$  where  $s_u$  is the ultimate settlement, has been obtained for single layer as well as for multiple layer reinforced sand bed. Effective depth and the optimum embedment depth for single layer reinforcement have been determined. Percentage Reduction in Settlement (PRS) has been determined to ascertain the reduction in settlement for single layer and multiple layer reinforced sand bed. Modulus of Subgrade Reaction ( $k$ ) has also been determined from the load-settlement curves.

# CONTENTS

<b>List of Symbols</b>	<b>i</b>
<b>List of Figures</b>	<b>iii</b>
<b>List of Tables</b>	<b>vii</b>
<b>List of Photographs</b>	<b>viii</b>
<b>Chapter 1 INTRODUCTION</b>	<b>1</b>
1.1 General	1
1.2 Scope of the present Work	2
<b>Chapter 2 LITERATURE REVIEW</b>	<b>3</b>
2.1 General	3
2.11 Experimental Studies	3
2.12 Analytical Studies	15
<b>Chapter 3 DETAILS OF EXPERIMENTAL STUDIES</b>	<b>21</b>
3.1 Introduction	21
3.2 Materials used	21
3.2.1 Sand	21
3.2.2 Reinforcement	22
3.2.2.1 Procedure for Adhesion of Reinforcement	22
3.2.2.2 Tensile Strength Test on Reinforcement	23
3.3 Direct Shear Test	23
3.4 Model Test Arrangements and Test Procedure	24
3.4.1 Model Tank and Model Footing	24
3.4.2 Experimental Set-Up	25
3.4.2.1 Preparation of Sand Bed	25
3.4.2.2 Loading Arrangement and Test Procedure	26
3.4.2.3 Details of Tests conducted on Reinforced sand bed	29
<b>Chapter 4 EXPERIMENTAL RESULTS AND DISCUSSIONS</b>	<b>33</b>
4.1 General	33
4.2 Properties of Sand	33

4.2.1	Grain Size Distribution Curve	33
4.2.2	Specific Gravity	34
4.2.3	Relative Density of Sand	34
4.3	Direct Shear Test	35
4.4	Properties of Reinforcements	35
4.4.1	Tensile Strength of Geotextile	35
4.4.2	Angle of Friction between Geotextile and Sand	36
4.4.3	Tensile Strength of Geogrid	37
4.5	Model Tests Results	37
4.6	Effect of Placement Depth of Reinforcement	40
4.7	Bearing Capacity Ratio (BCR)	43
4.8	Percentage Reduction in Settlement (PRS)	48
4.9	Effect of Multiple Layers on Settlement Response	50
4.10	Effect of Multiple Layers on BCR <sub>s</sub>	52
4.11	Effect of Multiple Layers on PRS	54
4.12	Determination of Modulus of Subgrade Reaction (k)	55
<b>Chapter 5</b>	<b>CONCLUSIONS</b>	<b>57</b>
	Scope for Further Studies	59
Appendix – A		60
Appendix – B		75
References		84

# LIST OF SYMBOLS AND ABBREVIATIONS

$B$	Width of Footing
$D_r$	Relative Density of Sand Fill
$\gamma_{d \max}$	Dry unit weight of sand in the densest condition
$\gamma_{d \min}$	Dry unit weight of sand in the loosest condition
$\gamma_d$	Dry unit weight of sand used in the test
$e_{\max}$	Void ratio of sand in the loosest condition
$e_{\min}$	Void ratio of sand in the densest condition
$D_{10}$	Effective size
$D_{30}$	Diameter at which 30 % soil is finer
$D_{60}$	Diameter at which 60 % soil is finer
$C_u$	Uniformity coefficient
$C_c$	Coefficient of curvature
$G_s$	Specific gravity of sand
BCR	Bearing Capacity Ratio
UBC	Ultimate Bearing capacity
$q_u$	Ultimate Bearing Capacity of unreinforced sand in kPa
$q_{u(R)}$	Ultimate Bearing Capacity of reinforced sand in kPa
$BCR_u$	Ratio of ultimate bearing capacity of reinforced sand to the ultimate bearing capacity of unreinforced sand ie. $q_{u(R)} / q_u$
$s$	Settlement of footing
$s_u$	Ultimate settlement ie. settlement at ultimate bearing capacity
$q_R$	Bearing pressure of reinforced sand at a settlement $s \leq s_u$ in kPa

$BCR_s$	Ratio of bearing pressure of reinforced sand to the bearing pressure of unreinforced sand at a settlement $s \leq s_u$ , ie. $q_R/q$ , where $s_u$ is the settlement at ultimate bearing capacity i.e. $q_R/q$
$\phi$	Angle of internal friction
$\delta$	Angle of friction between sand and geotextile
$\tau$	Shear stress
$\sigma$	Normal stress
$u$	Depth of first layer of reinforcement from the bottom of the footing
$N$	Number of reinforcing layers
$d$	Depth of the bottom most layer from the bottom of the footing in case of multiple layers of reinforcement
$h$	Vertical spacing between two consecutive layers of reinforcement
$u/B$	Depth Ratio
$s_o$	Settlement of unreinforced sand to its ultimate bearing capacity
$s_r$	Settlement of reinforced sand corresponding to bearing pressure equal to the ultimate bearing capacity of unreinforced sand
PRS	Percentage reduction in settlement = $\frac{s_o - s_r}{s_o}$

# LIST OF FIGURES

Fig. No.	Description	Page No.
3.1	Experimental Set-Up	26
3.2	Geometric Parameters for the Square Footing Supported by Reinforced Soil	27
3.3	Elevation and Plan View of Hopper	28
3.4	Penetrometer	29
4.1	Grain Size Distribution Curve for Ennore Sand	33
4.2	Direct Shear Test for Angle of Internal Friction of Sand	35
4.3	Direct Shear Test for Angle of Friction between Geotextile and Sand	36
4.4	Typical Load-Settlement Curve for Distinguishable Shear Failure	38
4.5	Typical Load-Settlement Curve for Undistinguishable Shear Failure	39
4.6	Typical Load-Settlement Curve for Determination of Bearing Pressure	39
4.7	Load-Settlement Curves at Different Depth Ratios ( $u/B$ ) for GT-1	40
4.8	Load-Settlement Curves at Different Depth Ratios ( $u/B$ ) for GT-2	41
4.9	Load-Settlement Curves at Different Depth Ratios ( $u/B$ ) for GG-1	41
4.10	Load-Settlement Curves at Different Depth Ratios ( $u/B$ ) for GG-2	42
4.11	Plot between $BCR_u$ and $u/B$ for GT-1, GT-2, GG-1 and GG-2	44
4.12	Plot between $BCR_s$ and Settlement Ratio for GT-1	45
4.13	Plot between $BCR_s$ and Settlement Ratio for GT-2	46
4.14	Plot between $BCR_s$ and Settlement Ratio for GG-1	46

4.15	Plot between $BCR_s$ and Settlement Ratio for GG-2	47
4.16	Plot between PRS and $u/B$ for GT-1, GT-2, GG-1 and GG-2	49
4.17	Load-settlement Curve for Multilayer Reinforcement (GT-1)	50
4.18	Load-settlement Curve for Multilayer Reinforcement (GT-2)	51
4.19	Load-settlement Curve for Multilayer Reinforcement (GG-1)	51
4.20	Load-settlement Curve for Multilayer Reinforcement (GG-2)	52
4.21	Plot between $BCR_s$ and Number of Layers for GT-1, GT-2, GG-1 and GG-2	53
4.22	Plot between PRS and Number of Layers for GT-1, GT-2, GG-1 and GG-2	54
A.1	Load-Settlement curve for Unreinforced Sand Bed	60
A.2	Load-Settlement Curve for GT-1 at $u/B = 0.15$	60
A.3	Load-Settlement Curve for GT-1 at $u/B = 0.3$	61
A.4	Load-Settlement Curve for GT-1 at $u/B = 0.5$	61
A.5	Load-Settlement Curve for GT-1 at $u/B = 0.7$	62
A.6	Load-Settlement Curve for GT-1 at $u/B = 0.85$	62
A.7	Load-Settlement Curve for GT-1 at $u/B = 1.0$	63
A.8	Load-Settlement Curve for GT-1 at $u/B = 1.2$	63
A.9	Load-Settlement Curve for GT-2 at $u/B = 0.15$	64
A.10	Load-Settlement Curve for GT-2 at $u/B = 0.3$	64
A.11	Load-Settlement Curve for GT-2 at $u/B = 0.5$	65
A.12	Load-Settlement Curve for GT-2 at $u/B = 0.7$	65
A.13	Load-Settlement Curve for GT-2 at $u/B = 0.85$	66
A.14	Load-Settlement Curve for GT-2 at $u/B = 1.0$	66
A.15	Load-Settlement Curve for GG-1 at $u/B = 0.15$	67
A.16	Load-Settlement Curve for GG-1 at $u/B = 0.3$	67



A.17	Load-Settlement Curve for GG-1 at $u/B = 0.5$	68
A.18	Load-Settlement Curve for GG-1 at $u/B = 0.7$	68
A.19	Load-Settlement Curve for GG-1 at $u/B = 0.85$	69
A-20	Load-Settlement Curve for GG-1 at $u/B = 1.0$	69
A-21	Load-Settlement Curve for GG-1 at $u/B = 1.2$	70
A.22	Load-Settlement Curve for GG-2 at $u/B = 0.15$	71
A.23	Load-Settlement Curve for GG-2 at $u/B = 0.3$	71
A.24	Load-Settlement Curve for GG-2 at $u/B = 0.5$	72
A.25	Load-Settlement Curve for GG-2 at $u/B = 0.7$	72
A.26	Load-Settlement Curve for GG-2 at $u/B = 0.85$	73
A.27	Load-Settlement Curve for GG-2 at $u/B = 1.0$	73
B.1	Load-Settlement Curve for One Layer for GT-1 at $u/B = 0.5$ and $h/B = 0$	75
B.2	Load-Settlement Curve for Two Layers for GT-1 at $u/B = h/B = 0.5$	75
B.3	Load-Settlement Curve for Three Layers for GT-1 at $u/B = h/B = 0.33$	76
B.4	Load-Settlement Curve for Four Layers for GT-1 at $u/B = h/B = 0.25$	76
B.5	Load-Settlement Curve for One Layer for GT-2 at $u/B = 0.5$ and $h/B = 0$	77
B.6	Load-Settlement Curve for Two Layers for GT-2 at $u/B = h/B = 0.5$	77
B.7	Load-Settlement Curve for Three Layers for GT-2 at $u/B = h/B = 0.33$	78
B.8	Load-Settlement Curve for Four Layers for GT-2 at $u/B = h/B = 0.25$	78
B.9	Load-Settlement Curve for One Layer for GG-1	79

	at $u/B = 0.5$ and $h/B = 0$	
B.10	Load-Settlement Curve for Two Layers for GG-1 at $u/B = h/B = 0.5$	79
B.11	Load-Settlement Curve for Three Layers for GG-1 at $u/B = h/B = 0.33$	80
B.12	Load-Settlement Curve for Four Layers for GG-1 at $u/B = h/B = 0.25$	80
B.13	Load-Settlement Curve for One Layer for GG-2 at $u/B = 0.5$ and $h/B = 0$	81
B.14	Load-Settlement Curve for Two Layers for GG-2 at $u/B = h/B = 0.5$	81
B.15	Load-Settlement Curve for Three Layers for GG-2 at $u/B = h/B = 0.33$	82
B.16	Load-Settlement Curve for Four Layers for GG-2 at $u/B = h/B = 0.25$	82

# LIST OF TABLES

Table No.	Description	Page No.
3.1	Tests Conducted on Sand	21
3.2	Symbols for Different Types of Reinforcement	22
3.3	Tests Conducted with Single Layer of Reinforcement	30
3.4	Tests Conducted with Multi Layer of Reinforcement	30
4.1	Properties of Sand Used for the Test	34
4.2	Properties of GT-1 and GT-2	36
4.3	Properties of GG-1 and GG-2	37
4.4	Modulus of Subgrade Reaction for all types of Reinforcement at all Depth Ratios	56
A.1	UBC and $BCR_u$ of Reinforced Sand Bed for Single Layer for all types of Model Tests	74
B.1	UBC and $BCR_u$ of Reinforced Sand Bed for Multiple Layers for all Types of Model Tests	83

# LIST OF PHOTOGRAPHS

Plate No.	Description	Page No.
1	Experimental Set-Up	31
2	Checking Density with Penetrometer	31
3	Geotextile Placed in a Filled Tank	32
4	Geogrid Placed in a Filled Tank	32

# **AN EXPERIMENTAL STUDY ON SETTLEMENT RESPONSE OF FOUNDATION ON REINFORCED SAND**

## **INTRODUCTION**

### **1.1 GENERAL**

Ground Improvement is one of the recent techniques adopted during the last few decades. Due to the rapid growth of civilization across the world, often the sites to be used for the construction of a structure may not be ideal from the view point of geotechnical engineering. Soils having low bearing capacity are not able to withstand heavy loads and cause excessive settlements, which may not only adversely affect the proper functioning of the structures but may also cause early damage thus rendering them unstable. Geotechnical engineers, therefore, are forced to improve the site condition so that the site can be suitably used for various types of constructional works. Depending on the type and the soil conditions various ground improvement techniques have been developed. Among them Reinforced Earth is one of the effective methods.

Major areas of application of reinforced earth using geosynthetics (such as geotextile, geogrid, geomembranes etc.) are foundations, earth retaining structures, highway/road embankments, erosion control etc. For geotechnical purposes, the geosynthetic materials used can perform four major functions ie. separation, reinforcement, filtration and drainage. The most common use is as reinforcement. The main advantage of using geosynthetic as a reinforcing material is, its chemical inertness and non-biodegradability coupled with its relatively high tensile strength. The purpose of ground improvement is mainly

to reduce settlement, increase bearing capacity, to change the dynamic response of soil and to reduce the risk of liquefaction of soil at site. Soil improvement was pioneered by Henri Vidal (1966) who worked with galvanized metal strips as reinforcing material. Binquet and Lee (1975) were the first to study the effects of reinforcement on bearing capacity of soil in shallow foundations. After that a number of analytical and experimental studies have been done on the beneficial effects of reinforcement on ultimate bearing capacity by various researchers.

## **1.2 SCOPE OF THE PRESENT WORK**

A number of studies have been conducted to study the effect of geosynthetic in load-settlement behaviour of reinforced foundation using mainly geogrid and geotextile. The optimum width of reinforcement, depth of first layer of reinforcement, optimum number of layers of reinforcement, vertical and horizontal spacing between two layers of reinforcement, etc. has been studied extensively. Most of these aspects have been studied from bearing capacity point of view only. Hardly any researchers have done the study from bearing capacity as well as from settlement point of view and with geotextile and geogrid both. In the present study, the aspect of settlement along with bearing capacity aspect has been studied on geotextile and geogrid, both with two different tensile strengths (by pasting two layers) of each. The parameters of study include the effect of depth of reinforcement on bearing capacity and reduction in settlement for single layer as well as multi layer of reinforcement. Modulus of subgrade reaction of reinforced bed has also been studied from the load-settlement curves for single layer reinforcement.

# LITERATURE REVIEW

## 2.1 GENERAL

In this chapter the literature related to reinforced soils subjected to loads has been presented. Literature review has been divided into experimental studies and analytical studies and the same has been presented in the succeeding paragraphs.

### 2.1.1 EXPERIMENTAL STUDIES

**Binquet and Lee (1975)** conducted model tests with strip footings on reinforced sand foundations for three conditions. (1) Homogeneous deep sand (2) sand above an extensive layer of very soft material simulating soft clay and (3) sand above a finite size pocket of very soft material. Results showed that the load settlement and the ultimate bearing capacities of the footings can be improved by a factor of about 2-4 times on the same load settlement or bearing capacity of an unreinforced soil for otherwise same conditions. This improvement was obtained for a relatively light amount of reinforcement: linear density ratio, (LDR) = 42.5 % (defined as the ratio of the tank footing covered by reinforcing strips to the length of the footing and is expressed in percentage); relative vertical spacing  $\Delta H/B = 0.3$  where  $\Delta H$  is vertical spacing between two consecutive reinforcement layers and B is the width of model footing; and N = 4 - 6 layers of reinforcing strips. It was also shown that the bearing capacity continued to improve with increasing number of layers up to at least six to eight, beyond which little additional improvement was noticed. In most cases, for any given number of layers, the greatest improvement was obtained for an arrangement with the reinforcing layers beginning near the base of the footing.

**Akinmusuru and Akinbolade (1981)** conducted bearing capacity model tests on square footing on a homogeneous sand bed reinforced with strips of a local rope material.

Results showed that the bearing capacity of footing depends on horizontal spacings between strips, vertical spacings between layers, depth below the footing of the first layer and number of layers of reinforcement. It was also shown that depending on the strip arrangement, ultimate bearing capacity values can be improved by a factor up to three times that of the unreinforced soil.

**Fragaszy and Lawton (1984)** conducted a series of laboratory model tests designed to determine the influence of soil density ( $D_r = 51$  to  $98\%$ ) and reinforcing strip length of the load settlement behaviour of reinforced sand. The results showed that when bearing capacity ratio was calculated at a settlement equal to  $10\%$  of the footing width, the percentage increase in bearing capacity ratio was independent of soil density. When calculated at a percentage of  $4\%$  of the footing width, the percentage increase in bearing capacity appears to be less for loose sands than for dense sands. Failure of rectangular footings on dense reinforced sand occurs at a larger settlement than an identical footing on unreinforced sand at the same density. As the strip length increases from three to seven times the footing width, the bearing capacity ratio increased rapidly. Additional strip length did not significantly affect bearing capacity.

**Guido et al. (1986)** carried out a series of laboratory plate loading tests using either geogrid or geotextile as reinforcement in sand and drawn a comparison between geogrid and geotextile reinforced slabs. The parameters studied were the coefficient of friction between the geotextile and the soil, pull-out resistance between the geogrid and the soil, depth below the footing of the first layer of reinforcement, vertical spacing of the layers, width size of the square sheet of reinforcement and the tensile strength of the reinforcement. The results have shown that the bearing capacity of a reinforced earth slab can increase substantially with the insertion of either type of reinforcement. After an optimum number of layers or width of reinforcement, the bearing capacity did not increase for both geogrids and geotextiles. In



addition, the bearing capacity was the largest for those geogrid and geotextile reinforced earth slabs where the first layer was closest to the footing and the spacing between the layers was the smallest. Bearing capacity increased directly with increasing reinforcement tensile strength for the geotextile; however for the geogrid, aperture size and the reinforcement tensile strength both have to be considered simultaneously. It was pointed out that for geotextiles to function

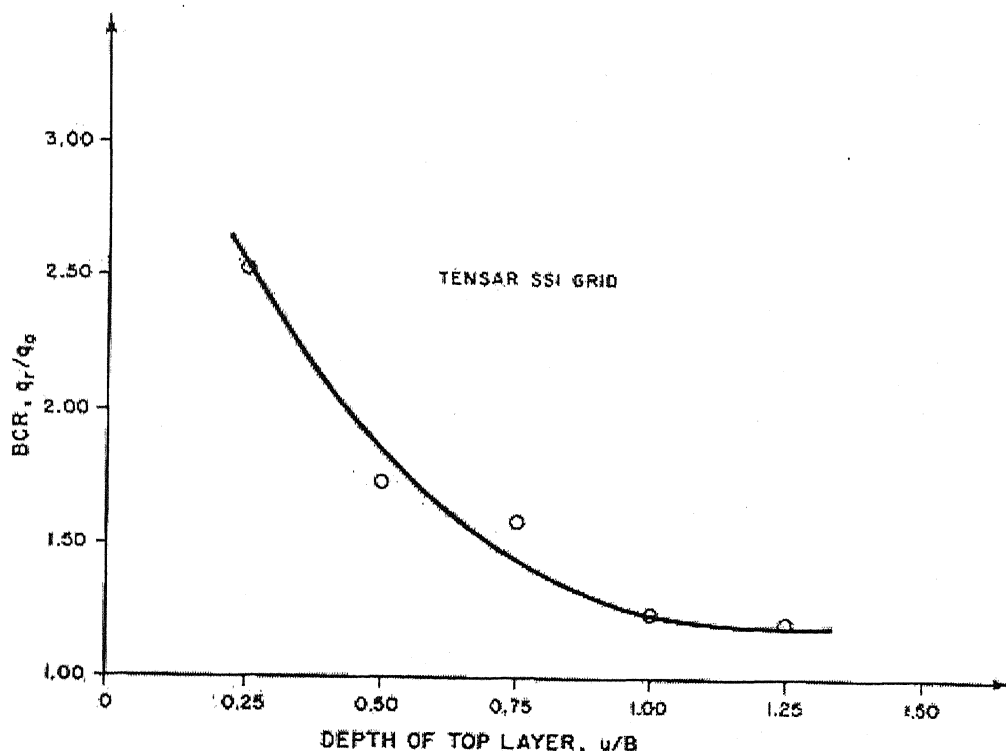


Fig. 2.1: BCR variation with vertical spacing of reinforcement,  
 $u/B = 0.25$ ,  $N = 2$  and  $b/B = 3$

properly as reinforcement, friction must develop between the soil and reinforcement to prevent sliding; whereas for grids, it is interlocking of the soil through the apertures of the grid that achieves an efficient anchoring effect.

**Dembicki et al. (1986)** conducted model tests of rigid strip foundation on subsoil reinforced by horizontally placed geotextile. The two layer subsoil system was used ie. mud covered by sand wherein two types of geotextile for different inclination and eccentricity of load and two different lengths of geotextile anchorage were used. All parameters influenced

independently the bearing capacity, these are thickness of the sand layer equal to depth of geotextile, length of geotextile band, type of geotextile, inclination of load and eccentricity of load.

Love et al. (1987) conducted model tests in the laboratory to study the effectiveness of the geogrid reinforcement, placed at a base of a layer of granular fill and on the surface of soft clay. In the tests, monotonic loading was applied by a rigid footing under plane strain conditions to the surface of the reinforced and unreinforced systems, using a range of fill thickness and subgrade strengths. Performance of reinforced systems was found to be superior even at small deformations, owing to the significant change in the pattern of the shear forces acting on the surface of the clay, brought about by the presence of the reinforcement. Membrane action of the reinforcement only became significant at large deformations. The model and analytical studies had shown that geogrid reinforcement tends to reduce the shear stresses transmitted to the surface of the clay subgrade. The amount of reduction depends primarily on the strength of the clay and the thickness and the stiffness of the granular layer. The failure mechanism in the clay is mobilized at quite small deformations of the fill, and the large deformations are therefore not necessary for benefits of reinforcement to be felt. At large deformations, where these are permissible, additional benefit is obtained from the membrane action of the reinforcement. To have the desired effect, the reinforcement has to be stiff and strong enough to take tension induced by the shear stresses from the granular layer above (and also the shear stresses from the clay beneath) without failing.

Huang and Tatsuoka (1988) developed a method of predicting the bearing capacity of sandy ground reinforced with tensile reinforcement layers horizontally placed beneath a footing. A series of plane strain model tests with a strip footing were performed to study the effects of the length, the arrangement, rigidity and rupture strength of reinforcement. The strain fields in sand, the tensile forces in reinforcement and the distribution of contact

pressure on footing were measured. The bearing capacity was found to increase remarkably even by means of reinforcement layers with a length similar to the footing width,. Also, the portions of reinforcement layers located outside the footing width contributed to the increase in the bearing capacity only marginally. The bearing capacity of reinforced sand found was equal to the smaller of the following two values; the one controlled by the failure of the reinforced zone immediately beneath the footing and the other by the failure of sand beneath the reinforced zone.

**Samtani and Sonpal (1989)** conducted model laboratory tests to investigate the bearing-capacity aspects of cohesive soil reinforced with metal strips. The aim was to study the increase in bearing capacity of reinforced cohesive soil over unreinforced cohesive soil and the failure mechanism and failure profile in reinforced cohesive soil. Results showed that the bearing capacity of cohesive soils can be improved by reinforcing the soil with strips. For a given linear density ratio (LDR) of ties, increase in length of ties does not significantly increase the bearing capacity. Linear Density Ratio (LDR) is defined as the ratio of the tank footing covered by reinforcing strips to the length of the footing and is expressed in percentage.

**Das (1989)** conducted model tests for the ultimate bearing capacity of strip and square shallow foundations supported by a compact sand layer underlain by a soft clay layer with and without a geotextile at the sand-clay interface. It was found that the maximum bearing capacity ratio of a foundation increases with the use of geotextile at the sand-clay interface. The increase is about 24% for square foundations and about 8% for the strip foundation. With the use of geotextile, the critical value of the  $H/B$  ratio at which maximum bearing capacity ratio occurs is about 0.75 for strip foundation and about 0.5 for square foundation where  $H$  is the depth from the bottom of the footing to the bottom of the sand layer and  $B$  is the width of the footing. The optimum width of the geotextile layer for deriving

the maximum possible bearing capacity ratio was found to be 4 B for strip foundation and 3B for square foundations.

**Mandal and Sah (1992)** carried out tests on model footings on clay subgrades with geogrids placed horizontally to show the effectiveness of the geogrid reinforcement on bearing capacity of subgrades. Results showed that with the introduction of geogrid reinforcement the bearing capacity improved significantly and the maximum bearing capacity ratio was 1.36 at  $u/B = .175$  for a square foundation where  $u$  is the depth of the first layer from the base of the footing and  $B$  is the foundation width. The improvements occurred at all levels of settlements.. However, the settlement reduction was found to be significant in the range of  $u/B = 0-.25$ . The maximum percentage reduction in settlement with the use of geogrid reinforcement below the compacted and saturated clay was found to be about 45% and it occurred at a distance of  $.25 B$  from the base of the square foundation.

**Khing et al. (1993)** conducted laboratory model tests for the bearing capacity of a strip foundation supported by a sand layer reinforced with layers of geogrid. Based on the tests results, the bearing capacity ratio with respect to the ultimate bearing capacity and at all levels of settlement of the foundation was determined. For practical design purposes, it appeared that the bearing capacity ratio at limited levels of settlement is about 67-70% of the bearing capacity ratio calculated on the basis of the ultimate bearing capacity. Since the inside width of the box was equal to the length of the model foundation, a plain strain condition was maintained. The maximum benefit of geogrid reinforcement in increasing the bearing capacity was obtained when the ratio of the depth of the first reinforcing layer to the foundation width was less than unity. For the case of strip foundation, a reinforcement placed below the foundation at a depth of more than 2.25 times the foundation width did not contribute to any increase in bearing capacity. For maximum benefit, the minimum width of the geogrid layers should be about six times the foundation width.

**Omar et al. (1993a)** conducted laboratory model tests for the ultimate bearing capacity of shallow rectangular foundations supported by geogrid reinforced sand. The width-to-length ratio ( $B/L$ ) of the foundations was varied as 0.33, 0.5 and 1.0. Test was also conducted for a strip foundation. The width,  $B$  of each model foundation was the same. For a given sand at a given relative density and type of geogrid, the critical depth of reinforcement for mobilization of maximum possible ultimate bearing capacity ratio decreases with the width-to-length ratio of the foundation. It is about  $2B$  for strip foundations and  $1.2B$  for square foundations. The optimum size of the reinforcing geogrid layers will vary based on the  $B/L$

ratio and can be approximated by  $\left(\frac{b}{B}\right)_{cr} = 8 - 3.5\left(\frac{B}{L}\right)^{0.51}$  and  $\left(\frac{L}{B}\right)_{cr} = 3.5\frac{B}{L} + \frac{L}{B}$

where  $B$  and  $L$  are the width and length of the rectangular foundation respectively and  $b$  is the width of the geogrid.

**Omar et al. (1993b)** performed laboratory model tests for the ultimate bearing capacity of strip and square foundations supported by sand reinforced with geogrid layers. The critical depth of reinforcement and the dimensions of the geogrid layers for mobilizing the maximum bearing capacity ratio were determined and compared. Results showed that for the development of maximum bearing capacity, the effective depth of reinforcement is about  $2B$  for the strip foundation and  $1.4B$  for the square foundations. Maximum widths of reinforcement layers required for mobilization of maximum bearing capacity ratio is about  $8B$  for strip foundations and  $4.5B$  for square foundations. The maximum depth of the placement of the first layer of geogrid should be less than about  $B$  to take advantage of reinforcement.

**Khing et al. (1994)** carried out a number of laboratory model tests for the ultimate bearing capacity of a surface strip foundation supported by a strong sand layer of limited thickness underlain by weak clay with a layer of geogrid at the sand-clay interface. The tests were conducted at one relative density of compaction of sand and one undrained shear strength

of clay. Two types of geogrid were used. Based on the test results presented, it was found that the optimum height of the strong sand layer should be about two thirds of the foundation width for obtaining the maximum benefit from the geogrid reinforcement. For  $H/B \geq 1.5$ , where  $H$  is the depth from the bottom of the footing to the geogrid layer, the contribution of the geogrid reinforcement to the bearing capacity improvement is practically negligible. The optimum width of the geogrid layer required to mobilize the maximum possible bearing capacity for a given sand, geogrid, clay combination is about six times the width of the foundation.

**Das and Khing (1994)** conducted laboratory model tests to determine the ultimate bearing capacity variation of a strip foundation on a stronger sand layer underlain by a near saturated weaker clay layer with and without geogrid reinforcement at the sand-clay interface to include in the study the effect of the presence of a void with a rectangular cross-section in the weaker clay layer immediately below and parallel to the central axis of the foundation. The width of the geogrid was kept six times the foundation width ( $b = 6B$ ) and the depth of the sand layer was kept two third times the foundation width throughout the test program. The results showed that the bearing capacity was generally reduced due to the existence of a void in the clay below the foundation. For a given void size and given  $H/B$ , the variation of the bearing capacity efficiency with  $d/B$  for reinforced and unreinforced cases was practically the same. The bearing capacity ratio (for a given  $B'/B$ ,  $H'/B$  and  $H/B$ ) increased with  $d/B$  to a maximum at  $d/B = 0.75$  to  $0.8$  and then decreased to a constant value at a greater depth. Where  $H$  is the depth of the geogrid from the bottom of the footing,  $H'$  and  $B'$  are the height and width of the void respectively,  $d$  is the depth from the geogrid layer to top of the void,  $b$  is the width of the geogrid and  $B$  is the width of the foundation.

**Das and Shin (1994)** conducted laboratory model tests to determine the permanent settlement of a surface strip foundation supported by geogrid reinforced saturated clay and subjected to a low frequency cyclic load. In conducting the tests, the foundation was

initially subjected to an allowable static load. The variation of the maximum settlement with the intensity of the static load and the intensity of the amplitude of the cyclic load were presented. The tests results showed that for a given cyclic load intensity, the maximum permanent settlement increases with the increase in the intensity of the static load. For a given intensity of the static loading, the maximum permanent settlement increases with the increase in the amplitude of the cyclic load intensity. Full depth of geogrid reinforcement may reduce the permanent settlement of a foundation by about 20% to 30% compared to one without reinforcement.

**Yetimoglu et al. (1994)** undertook a study to investigate the bearing capacity of rectangular footings on geogrid-reinforced sand by performing laboratory model tests as well as by finite element analysis. The effect of the depth to the first layer of the reinforcement, vertical spacing of the reinforcement layers and the size of the reinforcement sheet on the bearing capacity was investigated. Both the experimental and analytical studies indicated that there was an optimum reinforcement embedment depth at which the bearing capacity was the highest when single layer reinforcement was used. Also there appeared to be an optimum reinforcement spacing for multi-layer reinforced sand. The bearing capacity was also found to increase with increase in number of reinforcement layers and reinforcement size when the reinforcement was placed within a certain effective zone. For the conditions investigated, the extent of the effective zone lies approximately within  $1.5B$  from both base and edges of the footing. In addition, the analysis indicated that increasing reinforcement stiffness beyond a certain value did not bring about further increase in the bearing capacity. They found that for the single layer of reinforcement the optimum embedment depth was approximately 0.3 of the footing width. The analysis indicated that the optimum depth would be somewhat larger for settlement ratios (settlement/footing width) greater than 6%. For multi layer reinforced sand, the highest bearing capacity occurs at an embedment depth of approximately  $0.25 B$ . For

multilayer reinforced sand, there is an optimum vertical spacing of reinforcement layers. The optimum spacing for the reinforced sand investigated was between  $0.2 B$  and  $0.4 B$ .

**Das et al. (1998)** conducted laboratory model tests for the settlement of a square surface foundation supported by a geogrid reinforced sand and subjected to transient load. The tests were conducted with one model foundation at one relative density of compaction using only one type of geogrid. A fine silica sand was used for the test. In all tests, the results showed that the peak value of the transient load per unit area of the foundation exceeded the ultimate bearing capacity of the foundation supported by unreinforced sand. Geogrid reinforcement reduces the settlement due to transient loading.

**Huang and Hong (2000)** predicted the bearing capacity ratio of reinforced sandy ground at ultimate footing load condition using high tensile stiffness reinforcement in a series of model tests. Settlement of reinforced ground at ultimate footing load condition was also investigated using a series of model tests. Linear relationships between  $SR_f$  and  $BCR_m$  were found for all the tests in which a semi rigid reinforcement zone was successfully developed under ultimate footing load condition where  $SR_f = S_{f(\text{reinforced})}/S_{f(\text{unreinforced})}$  and  $S_{f(\text{unreinforced})}$ ,  $S_{f(\text{unreinforced})}$  are the vertical settlements at the ultimate loading condition for the reinforced and unreinforced ground, respectively. The values of  $SR_f$  for reinforced ground may also be a linear function of bearing capacity ratio generated by the deep footing effect ( $BCR_D$ ) and bearing ratio generated by the wide slab effect ( $BCR_S$ ). The bearing capacity ratio for reinforced ground,  $BCR_R$  is equal to  $BCR_D$  plus  $BCR_S$ . This implies that the settlement of footing required for reaching the failure of the reinforced ground may increase with the increase of the degrees of 'deep-footing' and 'wide slab' effects.

**Shin et al. (2000)** conducted laboratory model tests to determine the ultimate bearing capacity of a strip foundation supported by sand with geogrid reinforcement in multiple layers. Tests were conducted with one type of geogrid and one relative density of



sand. The embedment ratio of the foundation was varied from 0 to 0.6. Results showed that the critical depth-reinforcement ratio below the bottom of the foundation  $(d/B)_{cr}$  for deriving the maximum benefit from reinforcement was about two. For a given reinforcement depth ratio,  $u/B$ ,  $h/B$  and  $b/B$ , the bearing capacity ratio with respect to the ultimate load ( $BCR_u$ ) increases with the embedment ratio of the foundation ( $D_f/B$ ) where  $u$  is the depth of the first reinforcement layer from the bottom of the footing,  $h$  is the vertical spacing between two consecutive layers,  $b$  is the width of the reinforcement layer and  $B$  is the foundation width. For similar soil and type of configuration of geogrid reinforcement, the bearing capacity ratio ( $BCR_s$ ) at a limited level of settlement ( $s/B \geq 5\%$ ) is smaller than  $BCR_u$ . The ratio of  $BCR_s/BCR_u$  at  $s/B \leq 5\%$  and  $(d/B)_{cr} \approx 2$  decreases from about 0.9 at  $D_f/B = 0$  to about 0.75 at  $D_f/B = 1$ .

**Dash et al. (2001)** conducted laboratory model tests on a strip footing supported by a sand bed reinforced with geocell mattress. The parameters in the testing program included pattern of geocell formation, pocket size, height and width of geocell mattress, the depth to the top of geocell mattress, tensile stiffness of the geogrids used to fabricate geocell mattress and the relative density of the sand. Based on the model tests, the depth of placement and the dimensions of the geocell layer for mobilizing maximum bearing capacity improvement were determined. In addition to the tensile strength of the reinforcement, the aperture size and orientation of the ribs of the geogrid used to fabricate geocell mattress must be taken into account while evaluating its contribution to the improvement in the performance. It was concluded that the pressure settlement behaviour of strip footing resting on geocell-reinforced sand is approximately linear even up to a settlement of about 50% of the footing width and a load as high as 8 times the ultimate capacity of the unreinforced one. Very good improvement in the footing performance can be obtained even with geocell mattress of width equal to the width of the footing. The performance improvement is significant up to a geocell

height equal to 2 times the width of the footing. Beyond that height, the improvement is marginal. To obtain maximum benefit, the top of geocell mattress should be at a depth of  $0.1 B$  from the bottom of the footing. Better performance of the footing can be obtained by filling the geocell denser soils because of dilation induced load transfer from soil to geocell. The optimum width of the geocell layer is around four times the footing width at which stage, the geocell would intercept all the potential rupture planes formed in the foundation soil. The optimum aspect ratio of geocell pockets for supporting strip footings was to be around 1.67.

Yoo (2001) studied the bearing capacity behaviour of a strip footing on a reinforced soil slope by conducting laboratory model tests as well as by finite element analysis. A wide range of boundary conditions were considered by varying the geogrid parameters. Based on the results of the investigation, both qualitative and quantitative relationships were established between the bearing capacity of a surface strip footing on the reinforced soil slope and the geogrid layout. Results showed that for the reinforced slope loaded with a footing, the failure zone tends to become wider and deeper than that for the unreinforced slope. The bearing capacity of a footing situated on a crest of sloping ground can be significantly increased by the inclusion of the layers of geogrid as in the level ground. The effect of geogrid reinforcements on the footing performances is more effectively mobilized under more aggressive slope environments. Full effect of the geogrid stiffness can be achieved when the geogrid layers are arranged so as to maximize the reinforcing effect. Significant benefit of geogrid reinforcements in terms of footing performance can be derived by the inclusion of the short geogrid layers directly below the footing. A close agreement between the experimental and the numerical results on the critical values of the geogrid parameters was found.

Unnikrishnan et al. (2002) studied the strength improvement due to the provision of the sand layers on either side of the reinforcement within reinforced clay soils. The

behaviour of reinforced clay was examined in triaxial compression tests under both static and cyclic conditions. Effect of the sand layer thickness, moisture content and reinforcement types (namely woven geotextile, non-woven geotextile and micro grid) were studied. All the triaxial compression tests were conducted under unconsolidated-undrained (UU) conditions. The results of the tests indicated that a thin layer of high-strength sand provided on both sides of the reinforcement is effective in improving the strength and deformation behaviour of reinforced clay soils under both static and cyclic type loadings. It was found that the grid type geosynthetic reinforcements are more effective than the sheet type reinforcement in increasing the strength and stiffness of the clay soils because of inter locking of sand within grid openings. Needle punched non-woven geotextile was less effective in arresting the deformations with or without sandwich layers compared to other types of geosynthetic reinforcements such as woven geotextile and grids. The benefit due to the sandwich layers was found to be higher at lower confining pressures than at higher confining pressures. At high confining pressures, the influence of reinforcement and that of sand layer is relatively less due to smaller relative movements between the soil and the reinforcement. For a particular soil, reinforcement, loading conditions and confining pressure, an optimum sand layer thickness exists which gives the maximum benefit. The provision of thicker sand layers will not lead to further improvement in the performance of the system.

### 2.1.2 ANALYTICAL STUDIES

**Meyerhof (1974)** investigated the ultimate bearing capacity of footings resting on subsoils consisting of two layers for the cases of dense sand on soft clay and loose sand on stiff clay. The analysis for the ultimate bearing capacity of footings of different modes of soil failure were compared with the results of the model tests on circular and strip footings and some field observations of foundation failures. It was concluded that the ultimate bearing capacity of footings on sand layers overlying clay can be expressed by punching shear

coefficients for the case of dense sand on soft clay and by modified bearing capacity coefficients or an empirical interaction relationship for the case of loose sand on stiff clay. If the shearing resistance of the sand layer approaches that of the clay, the bearing capacity does not vary significantly from that of the individual strata. Theory and test results show that influence of the sand layer thickness beneath the footing depends mainly on the bearing capacity ratio of the clay to the sand, the friction angle of the sand, the shape and depth of the foundation.

**Poorooshasb (1991)** investigated the effect of a cavity in the subgrade that may appear at some stage after the construction of a reinforced (geosynthetic) granular fill. In contrast to the majority of the works published so far, situation was treated as an instability problem. However, the study regards it as an equilibrium problem which is a more realistic representation of the actual case. According to this model the granular medium is a hardening plastic material obeying a non-associative flow rule. The geosynthetic is assumed to remain linearly elastic during the entire loading process. The subgrade supporting the reinforced fill is represented by a Winkler's foundation with a constant modulus of subgrade reaction. It was found that the proposed analysis appears to be a strong and simple tool in analyzing similar system. The boundary condition that is not satisfied is at the surface of the fill where the analysis predicts a measure of shear stress. The magnitudes of these unbalanced stresses, however are very small and will not introduce errors of any significance. The extension of the analysis to cover the cases of non-linear membrane behaviour, non-linear subgrade reaction is straight forward and may be incorporated in the computer program with little effort.

**Shukla and Chandra (1994)** proposed a foundation model to incorporate the compressibility of the granular fill by attaching a layer of Winkler springs to the Pasternak shear layer. The study showed that the effect of compressibility of the granular fill on the load settlement characteristics of geosynthetic reinforced granular fill-soft soil system is observed

to be significant at all load intensities except for very small values of the load. With the increase in the compressibility of the granular fill, the order of the increase in the settlement is more at the edge than at the centre of the loaded region. For any degree of compressibility of the granular fill, the geosynthetic-reinforced granular fill-soft soil system behaves as a much stiffer system at higher load intensities. The order of increase in the settlement with increase in the compressibility of the granular fill at any location within the loaded region is greater for lower values of shear parameter. The order of increase in the settlement with the consideration of compressibility of the granular fill varied from 5% to 10% within the loaded region for the set of parameters studied. Even when the granular fill is considered 50 times stiffer than the soft soil, there is increase in the settlement of the order of 1% to 2%.

**Ghosh and Madhav (1994a)** developed a new mathematical model for the analysis of a reinforced foundation bed by incorporating the confinement effect of a single layer of reinforcement. It is quantified in terms of the average increase in confining pressure due to the reinforcement from which modified shear stiffness of the granular soil surrounding the reinforcement were obtained. Parametric studies for a plain strain case showed that the confinement effect improves the load carrying capacity of the foundation significantly. The parametric results are sensitive to the methods used for obtaining the modified shear stiffness of the granular fill. The confinement effect is more pronounced when the shear stiffness of the granular fill is large. The modified shear stiffness below the centre of the footing increased by two to five times the initial value of  $G^*$ .

**Ghosh and Madhav (1994b)** proposed a new model by incorporating the rough membrane element for a single layer reinforcement. Mechanics of the rough membrane element with the assumption of horizontal shear stress transfer at the soil/reinforcement interfaces were explained and formulated. The model is generalized by incorporating non-linear responses of the soft soil and the granular fill under plain strain loading condition. The

membrane effect is quantified in terms of the improvement in the load-responses of the composite foundation system over the unreinforced one. Parametric results indicated that reinforcement while in tension spreads the load over a large area, leading to a reduction in the settlement beneath the footing. The reinforcement was either placed at the interface or at a certain depth from the surface. The membrane effect is significant at low values of shear stiffness of the granular fill. A reinforcement length of  $3B$  is sufficient to improve the foundation response to a significant degree where  $B$  is the foundation width. With increased soil-reinforcement interface friction coefficient ( $\mu$ ), the membrane effect improves the load-settlement response.

**Benrabah and Gielly (1996)** explored the changes in stress distribution for a medium reinforced by flexible geomembrane layers. The experimental results were compared to the theoretical results obtained using the Boussinesq method and numerical results obtained using the Fast Lagrangian Analysis of Continua calculation program, (FLAC). The tests carried out on analogical medium, which consisted of a stack of small rollers. It was shown that , despite the discrete nature of the model used, the distribution of vertical stresses follow theory, and the agreement increases with increasing stress applied to the soil, and with a measurement point chosen near the foundation. This may be due to the fact that, in the foundation, the soil grains are structured in such a way that they closely approximate a continuous medium. In the case of loaded reinforced soil, the distribution of the vertical stress,  $\sigma_s$ , appears not to be linked to the presence of reinforcing layers and always follow Boussinesq theory. However, the horizontal stress,  $\sigma_x$ , increases considerably with the tensile loading of the reinforcing layers and the sandwiched soil layers.

**Kurian et al. (1997)** carried out a detailed analysis by paying individual attention to soil, reinforcement and the interface between the two. A three-dimensional, nonlinear finite element analysis was done that used a three-dimensional, nonlinear soil-reinforcement

interface friction element, along with other three dimensional elements to model the system. The predicted results were compared with those from laboratory tests and were found to be in fair agreement. The settlement of the reinforced soil system was found to be much less than that of the unreinforced soil, particularly at values close to working loads, which proved effectiveness of the reinforcement in reducing settlement. The axial forces in the reinforcement are found to be maximum near the center, gradually reducing towards the end. The principal stresses at higher depths get reduced in the reinforced case. The stress contours shift downwards in the reinforced case, spreading the stresses deeper, thereby strengthening of the soil brought about by the reinforcement.

**Maheshwari et al. (2004)** presented a model for estimating the flexural response of beams resting on reinforced beds with reinforcing elements, such as geogrids, which are idealized as beams with smooth surface characteristics. The lower poor strata and the upper dense soil are modeled using Winkler springs of different stiffnesses. Taking a surcharge load on the reinforcing elements has incorporated the effect of depth of placement of the reinforced layer. The governing differential equations to find the response of the model were derived and closed form analytical solutions were found subjected to appropriate boundary and continuity conditions. Results showed that there was practically no change observed in the normalized deflection of the upper and lower beams when the normalized length ratio of beams exceeds 1.5 for the range of parameters considered. The normalized depth of placement of the lower beam has a significant effect on the deflection of the beams. The relative flexural rigidity of the beams affects the deflection at the edge of the beams more than at the centre. The relative stiffness of the soils, has a significant influence on the normalized net deflection of the upper beam as well as that on the lower beam. The maximum normalized positive bending moment occurs at the centre for the upper and lower beams whereas at the edge it is zero.

**Dey and Basudhar (2005)** studied the flexural response of a strip footing resting on a reinforced granular foundation bed overlying a poor granular soil. The footing and the reinforcement were idealized as free-ended beams and the granular soil media were idealized as Winkler springs. Considering the effect of distribution of confining pressure in the beam-soil interface, a parabolic variation of the subgrade modulus, maximum at the centre and progressively decreasing to minimum at the edges, was assumed. The resulting differential equations were discretized by using the Finite Difference Method (FDM) and the set of linear equations so obtained were solved by the Gauss-Seidel iterative technique. Results showed that the nature of distribution of confining pressure on the beam-soil interface had a significant effect on the settlement response of a footing placed on a reinforced soil bed. Observation of the above results indicates that considering variable subgrade reaction, there was a significant deviation of 5%-15% over and above the same obtained with uniform subgrade reaction. Parametric studies indicated that the settlement response of beams is influenced by the shape and nature of distribution of subgrade reaction at the beam-soil interface.

## **2.2 CONCLUDING REMARKS**

Literature review of experimental studies and analytical studies was presented in this chapter. Details of the present study will be presented in the next chapter.



## DETAILS OF EXPERIMENTAL STUDIES

### 3.1 INTRODUCTION

In this chapter, the details regarding materials used in this study, tests conducted on the materials to determine the basic properties, experimental set-up used, the loading arrangements and the tests procedures that have been followed are described.

### 3.2 MATERIALS USED

Details of sand, geosynthetic (Geotextile & Geogrid) and tests conducted on these materials for the study have been presented below.

#### 3.2.1 SAND

Fully dried Ennore (Tamilnadu) sand was used for the model tests. Table 3.1 gives the details of tests conducted on sand. Results of the tests conducted on sand have been discussed in chapter 4.

**Table 3.1**

Tests Conducted on Sand

S.No	Types of Tests Conducted	No. of Tests Conducted
1.	Grain Size Distribution	1
2.	Specific Gravity	1
3.	Maximum Unit Weight of Sand	1
4.	Minimum Unit Weight of Sand	1
5.	Direct Shear Tests	4

### 3.2.2 REINFORCEMENT

For the present study, two types of geosynthetic namely geotextile (woven) and geogrid (punched sheet drawn type) were used for the model tests. The size of the reinforcement (geotextile and geogrid) was kept six times of the footing width i.e. 60 cm x 60 cm to mobilize the full tensile force in the reinforcement through friction in case of geotextile and through soil reinforcement interlock in case of geogrid. Geotextile used was of woven type and geogrid used was punched sheet drawn type. Two single layers of geotextile and geogrid were pasted with an adhesive (fevicol) to increase the thickness and thereby the tensile strength of the geotextile and geogrid.

#### 3.2.2.1 PROCEDURE FOR ADHESION OF REINFORCEMENT LAYERS

Two layers (60 cm x 60 cm each) of geotextile were spread on ground, wrinkles removed and adhesive applied uniformly on one side of the layers. These were left to dry for 15-20 minutes before the layers were pasted by applying mild pressure with hands to ensure proper adhesion. 30-35 kgs of weight was applied uniformly on the pasted layers and left for 24 hours before they were used for testing. Same procedure was followed to paste two layers of geogrid. However, an extra care was taken while pasting the layers of geogrid to ensure that aperture size does not get overlapped and remains the same. The symbols used for single and pasted layers of geotextiles and geogrids in the discussion henceforth is given in Table 3.2.

**Table 3.2**

Symbols for different types of reinforcement used for tests

Type of Reinforcement	Symbol
Geotextile	GT-1
Pasted Layers of Geotextile	GT-2
Geogrid	GG-1
Pasted Layers of Geogrid	GG-2

### 3.2.2.2 TENSILE STRENGTH TEST ON REINFORCEMENT

Tensile strength of all types of reinforcement mentioned above was determined through Universal Testing Machine, AIMIL, India. Four samples of size 20 cm x 8 cm each were taken for all types of reinforcements. Strain controlled loading was used for the tests and the load was measured electronically directly in kN. Load was increased at the rate of 80 mm/min till the sample failed. Reading at failure was noted in kN which was divided by the width of the sample (8 cm) to get the tensile strength in kN/m. Elongation was also measured at the time of failure to find out the failure strain. Average of four readings was taken to determine the tensile strength of the reinforcement. The results of tensile strength tests and physical properties of single and pasted layers of geotextile and geogrid are given in chapter 4.

### 3.3 DIRECT SHEAR TEST

Four direct shear tests were conducted to determine the angle of internal friction of sand used for the model test as per IS: 2720-XIII, 1972. The tests were conducted in a shear box of size 6 cm x 6 cm at four normal stresses of 50, 100, 150 & 200 kN/m<sup>2</sup>. Strain controlled loading was applied and the rate of loading for all the tests was kept as 0.25 mm/min. To ascertain the value of interfacial friction angle  $\delta$ , between sand and geotextile, one side of wooden piece of size equal to half of the shear box size was pasted with a layer of geotextile. The geotextile pasted on the wooden block was then brought in contact with sand by placing it upside down in the other half of shear box filled with sand. Thereafter, similar tests as in the case of determination of angle of internal friction of sand were repeated to determine the value of  $\delta$ . Angle of friction between geogrid and sand was not determined as forces and strains transmitted from the soil to the geogrid depend on soil reinforcement interlock and not on soil reinforcement friction. The results

for angle of internal friction of sand,  $\phi$  and angle of friction between sand and geotextile,  $\delta$  have been discussed in chapter 4.

### **3.4 MODEL TEST ARRANGEMENTS AND TEST PROCEDURES**

Details about model tank, model footing are covered under model test arrangements whereas preparation of the sand bed, loading arrangements and test procedures etc. are covered under experimental set-up.

#### **3.4.1 MODEL TANK AND MODEL FOOTING**

Model tests were performed in a steel tank of 60 cm x 60 cm x 60 cm size. Since the length and the width of the tank are six times the size of the footing, end effects can be neglected. The inside wall of the tank was kept smooth hence the frictional effect were neglected for all practical purposes. The model footing used for the tests was made of mild steel and measured 10 cm x 10 cm x 1.25 cm. The plate had a recess in the centre for placing a solid steel ball of 2 cm diameter through which load was applied on the footing.

#### **3.4.2 EXPERIMENTAL SET-UP**

##### **3.4.2.1 PREPARATION OF SAND BED**

The technique of sand placement plays an important role in the process of achieving the desired density of the sand bed as the reliability of results would depend upon the uniformity of density. The sand was poured in the tank by rainfall technique keeping the height of fall as 30 cm to maintain the same relative density throughout the bed. Elevation and plan view of hopper used to pour the sand is shown in fig 3.3. The tank was filled up to the height of 50-52 cm in order to adjust the height of extension rod, plate, ball, proving ring and the loading device. After the desired height was reached, reinforcement (geotextile(s) or geogrid(s)) was/were placed and the sand was poured again to achieve the required height of 50-52 cm in the tank. The tank was emptied and

refilled after each test. This method of sand pouring from a height of 30 cm gave the predetermined dry density of 1.58 gm/cc and the relative density of 54.2 %.

Density of the sand bed was checked at the end of each test using a penetrometer. Fig 3.4 shows the sketch of the penetrometer. It consists of 0.95 cm diameter mild steel rod with a conical tip at the bottom for the ease of penetration. It is provided with a platform (11.5 cm x 10 cm x 1 cm) fixed to the rod for free fall of a rectangular mild steel weight (8.5 cm x 8 cm x 1 cm) of 590g. The weight was dropped from a height of 30 cm on to the platform and the depth of penetration was recorded after four and eight number of drops (Plate No. 2) The depth of penetration was recorded close to all corners in the tank after each test which was found almost same for four and eight number of drops indicating uniformity of density during sand filling. Typical values of penetration depth measured on the steel rod for four and eight number of drops were found to be 21.5 cm and 26.5 cm respectively. It is mentioned that whenever the desired penetration values were not achieved, the test was shelved and repeated.

#### **3.4.2.2 LOADING ARRANGEMENTS AND TEST PROCEDURE**

The loading arrangement and the experimental set up is shown in Fig. 3.1 as well as in Plate 1. Geometric parameters for the square footing supported by reinforced soil is given in Fig. 3.2. Geotextile and geogrid placed in filled tank has been shown in Plate No. 3 and Plate No. 4 respectively. Strain controlled loading was applied at a strain rate of 0.51 mm/min and the load was measured with the help of a proving ring (Proving Ring Constant being 1130.2 divisions = 5 kN) and the readings were taken at regular intervals.

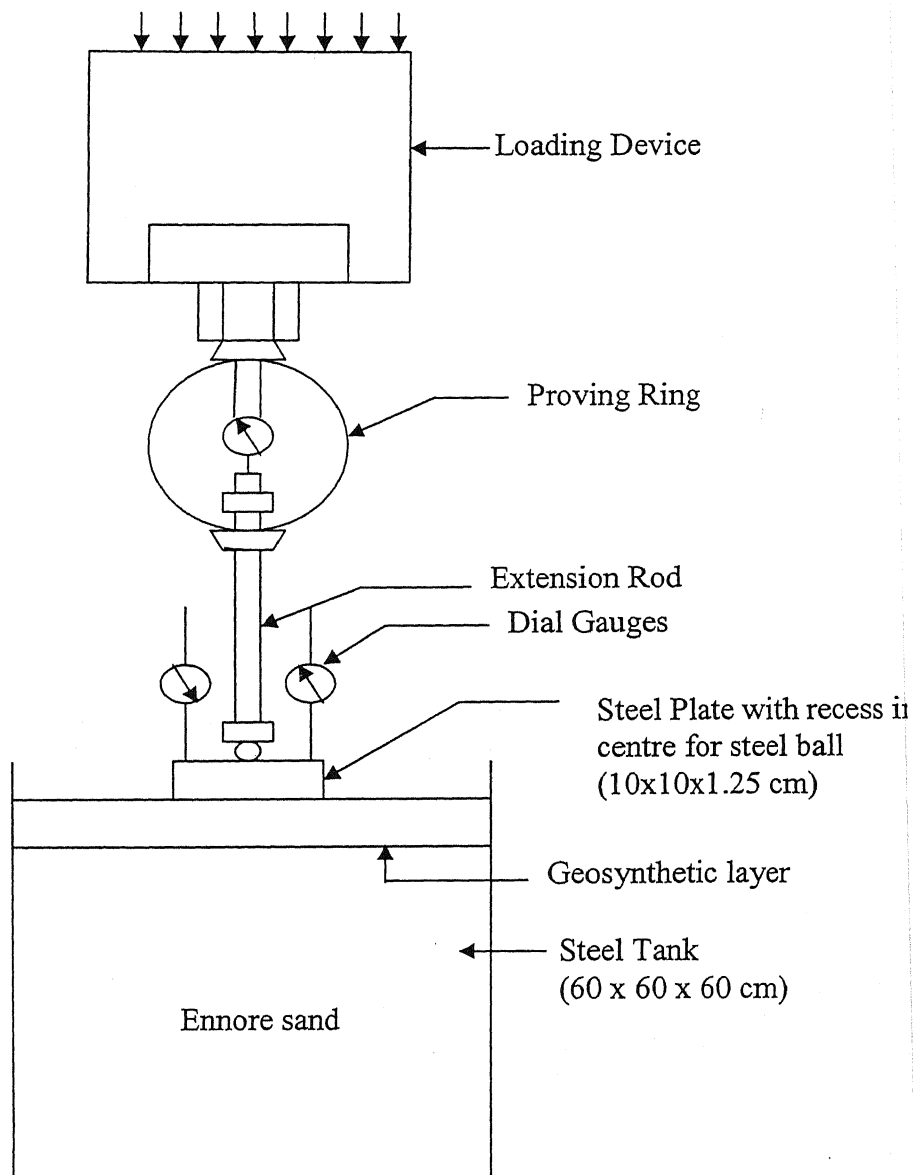


**Figure3.1:** Experimental Set- Up

An extension rod of 30.5 cm long, joined with a circular plate with recess on one side and external threads on the other side, was used between the proving ring and the steel ball. The external threads of rod were joined with the internal threads of the proving ring and the rod was brought down to make the recess of the circular plate rest centrally and vertically on the steel ball. A thin layer of sand was pasted on the bottom surface of the plate with the help of glue to avoid slip between the sand and the steel plate. The footing

was centrally and vertically loaded at a constant rate until the ultimate bearing capacity was reached. The settlement of the sand bed was measured by placing two dial gauges on the plate diagonally. The settlements reported were the average of the two dial gauges readings, which were nearly identical throughout the tests. The dial gauges had a least count of 0.01 mm each.

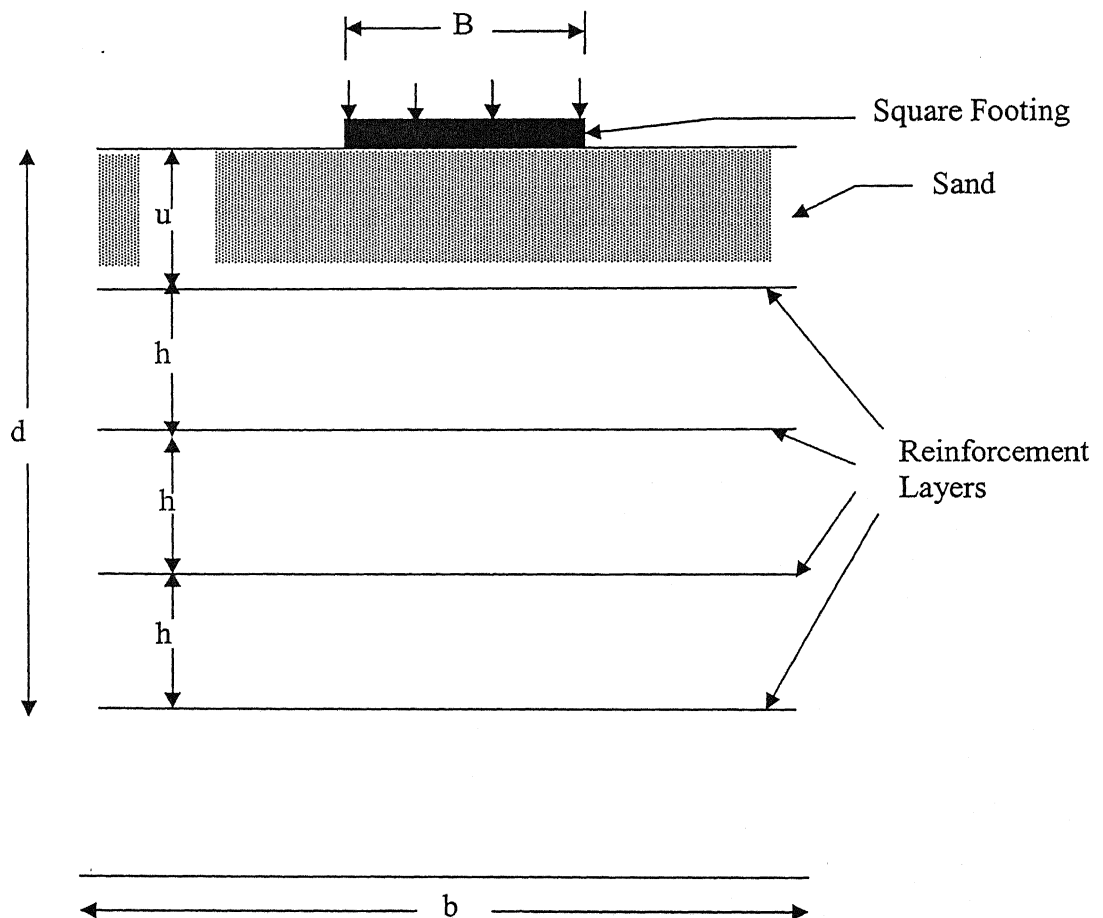


**Fig 3.2:** Geometric Parameters for the Square Footing Supported by Reinforced Soil

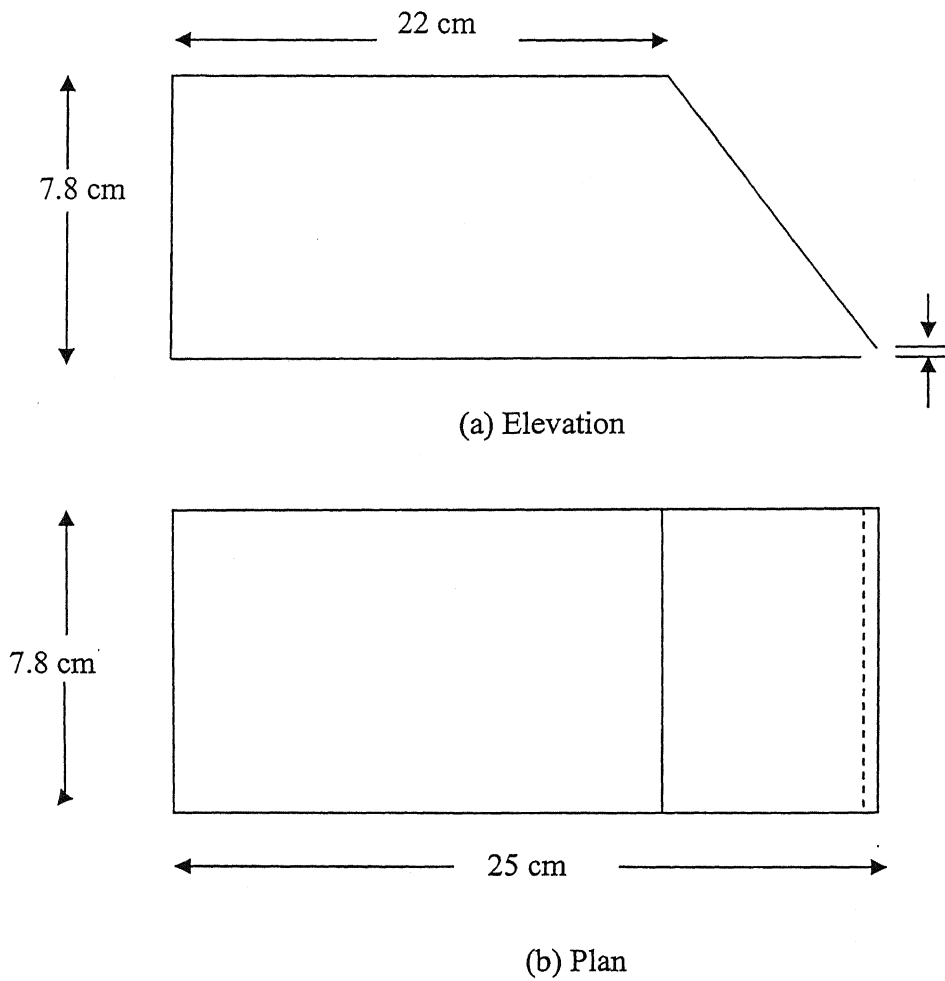
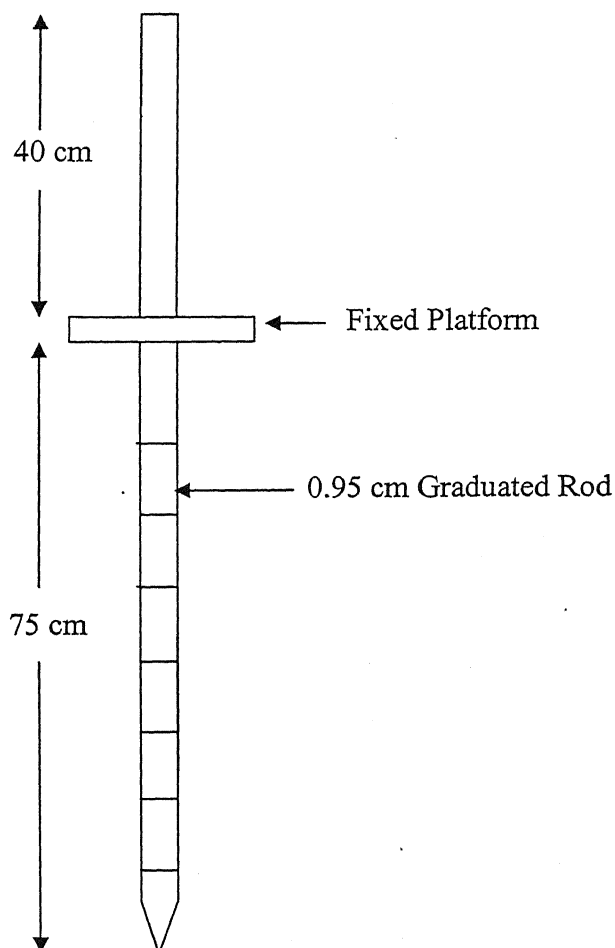


Fig. 3.3: (a) Elevation and (b) Plan View of Hopper





**Fig. 3.4: Penetrometer**

### **3.4.2.3 DETAILS OF TESTS CONDUCTED ON REINFORCED SAND**

One model test was conducted on unreinforced sand whereas 26 No. of tests were conducted with single layer of reinforcement and 12 with multiple layer of reinforcement thus making a total of 38 model tests on reinforced sand. Details of tests conducted with single layer and multi layer of reinforcement are given in Table 3.3 and Table 3.4 respectively.

**Table: 3.3**

Details of Tests Conducted with Single Layer of Reinforcement

<b>u/B</b>	<b>GT-1</b>	<b>GT-2</b>	<b>GG-1</b>	<b>GG-2</b>
0.15	✓	✓	✓	✓
0.3	✓	✓	✓	✓
0.5	✓	✓	✓	✓
0.7	✓	✓	✓	✓
0.85	✓	✓	✓	✓
1.0	✓	✓	✓	✓
1.2	✓	—	✓	—
<b>No. of Tests</b>	<b>7</b>	<b>6</b>	<b>7</b>	<b>6</b>

**Table: 3.4**

Details of Tests Conducted with Multi Layer of Reinforcement

<b>No. of Layers</b>	<b>u/B</b>	<b>h/B</b>	<b>GT-1</b>	<b>GT-2</b>	<b>GG-1</b>	<b>GG-2</b>
1	0.5	0	✓	✓	✓	✓
2	0.5	0.5	✓	✓	✓	✓
3	0.33	0.33	✓	✓	✓	✓
4	0.25	0.25	✓	✓	✓	✓

### 3.5 CONCLUDING REMARKS

The results obtained by the execution of the test programs described in this chapter will be presented in the next chapter.

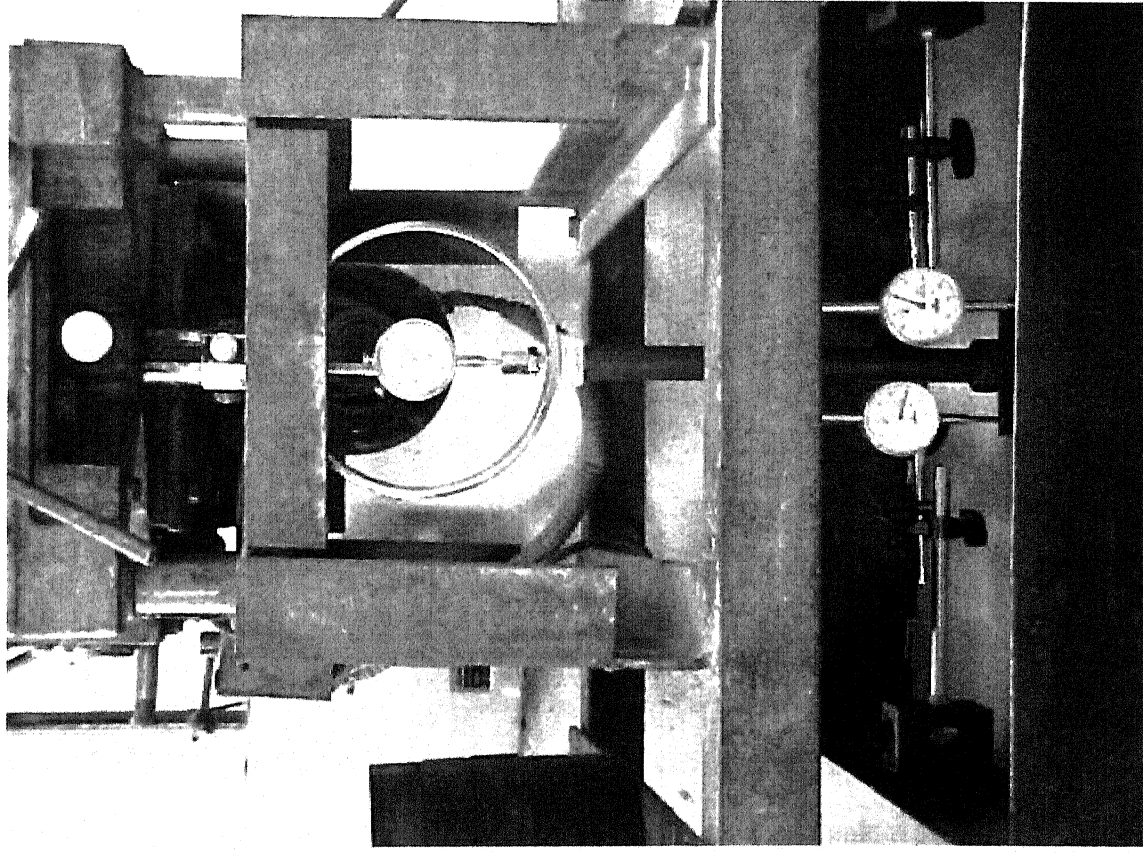


**Plate No. 1: Experimental Setup**

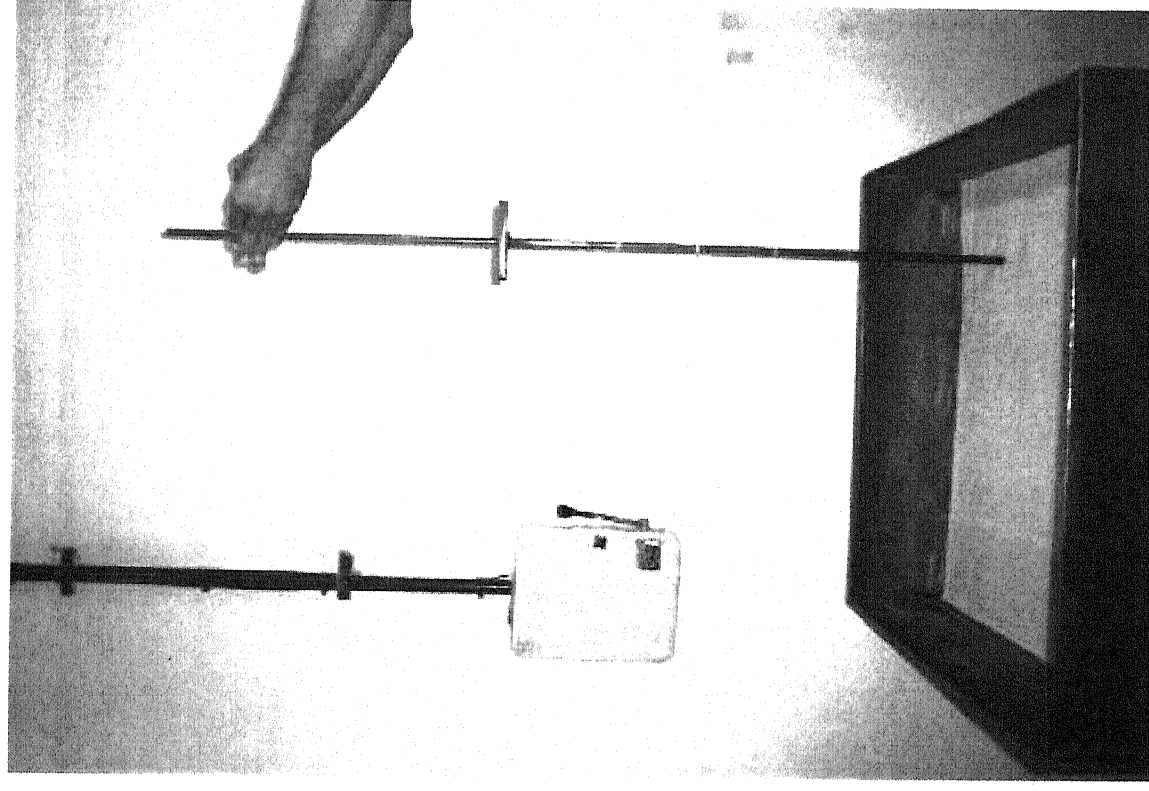


**Plate No. 2: Checking Density with Penetrometer**

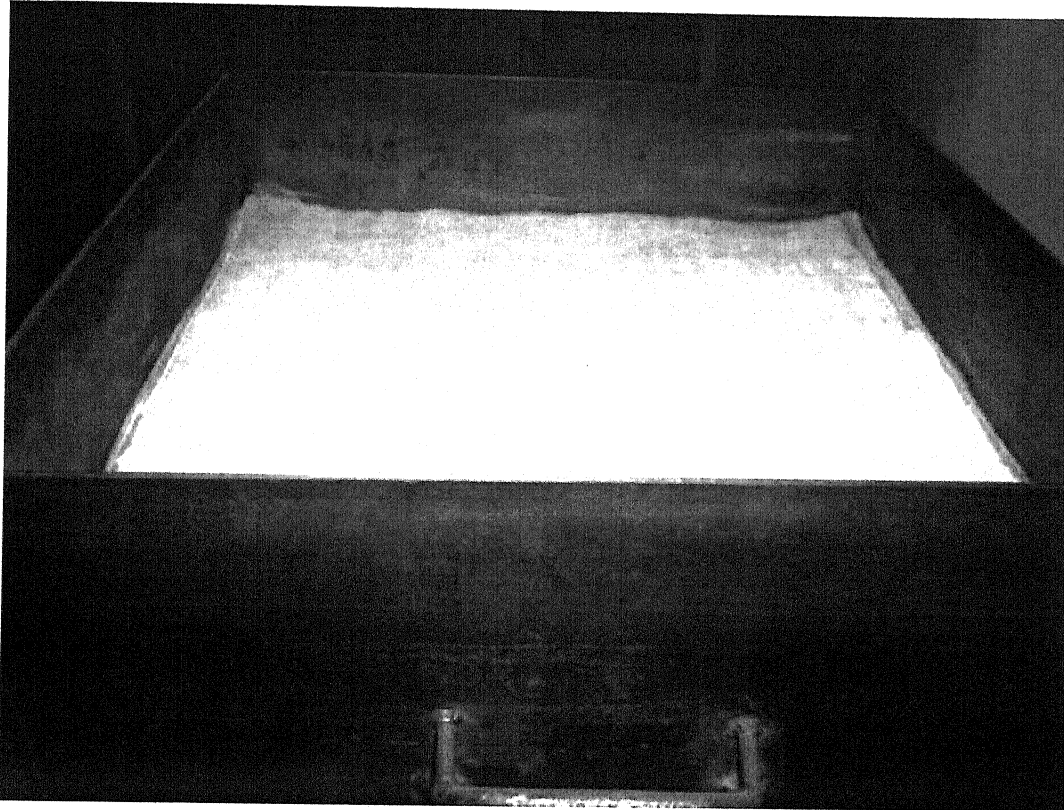


**Plate No. 3:** Geotextile Placed in a Filled Tank

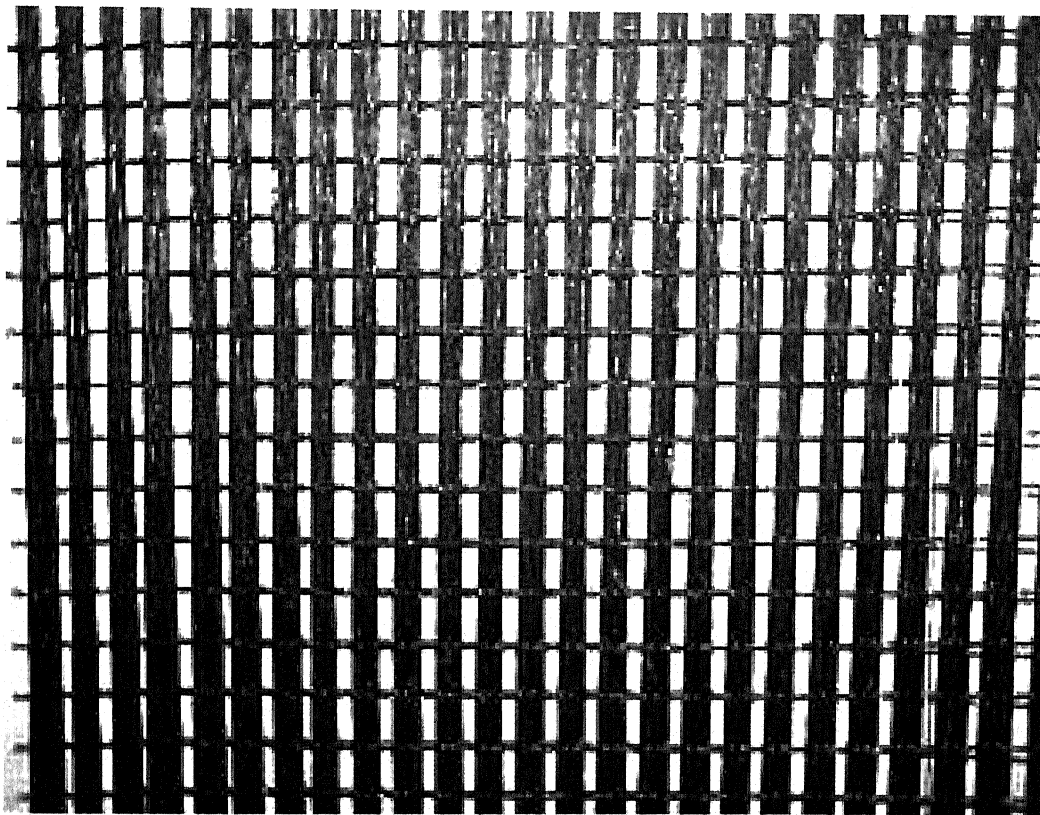


**Plate No. 4:** Geotgrid Placed in a Filled Tank

## RESULTS AND DISCUSSION

### 4.1 GENERAL

Results of model tests conducted on unreinforced and reinforced Ennore sand are presented in this chapter. Tests results on sand and reinforcements (geotextile & geogrid) and their properties are also presented. Results have also been discussed to reach a logical conclusion.

### 4.2 PROPERTIES OF ENNORE SAND

#### 4.2.1 Grain Size Distribution Curve

Grain size distribution test on sand was conducted as per IS: 2720: Part IV, 1975. The grain size distribution of Ennore sand is shown in Fig.4.1.  $D_{10}$ ,  $D_{50}$ , uniformity coefficient ( $C_u$ ) and coefficient of curvature ( $C_c$ ) were found out to be 0.44, 0.63, 1.59 and 0.98 respectively as given in Table 4.1 which is matching with the test results of other researchers. From the grain size distribution curve it is found that the sand is uniformly graded medium dense sand.

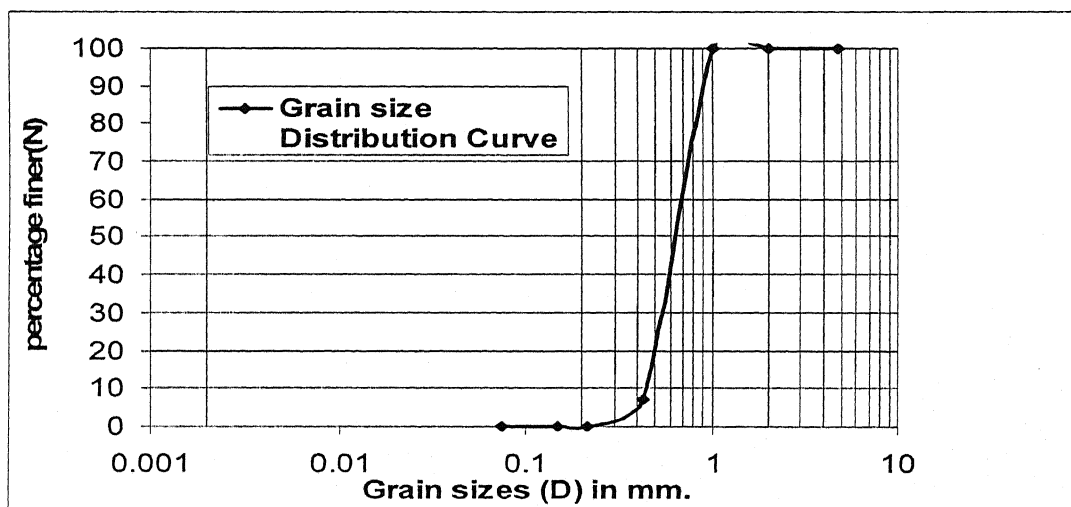


Fig.4.1: Grain Size Distribution Curve for Ennore Sand

### 4.2.2 Specific Gravity

Specific gravity of sand was determined by the density bottle method as per IS: 2720: Part III, 1980. Specific gravity so obtained was found to be 2.657.

### 4.2.3 Relative Density of Sand

Test of relative density of sand was conducted as per IS: 2720-XIV, 1968. Maximum and minimum dry unit weights of sand were determined as  $16.8 \text{ kN/m}^3$  and  $14.76 \text{ kN/m}^3$  respectively. For a 30 cm height of fall, the relative density was obtained as 54.2%. Various properties including, void ratios etc. are presented in Table 4.1. Properties of the sand are almost matching with the results of tests conducted by other researchers.

**Table 4.1**  
Properties of Sand used for the Tests

Uniformity Coefficient ( $C_u$ )	1.59
Coefficient of Curvature ( $C_c$ )	.95
Effective size, $D_{10}$ (mm)	0.44
Median size, $D_{50}$ (mm)	0.63
Specific Gravity, $G_s$	2.657
Dry unit weight, $\gamma_d$ ( $\text{kN/m}^3$ )	15.8
Max. dry unit weight, $\gamma_{d \text{ max}}$ ( $\text{kN/m}^3$ )	16.8
Min. dry unit weight, $\gamma_{d \text{ min}}$ ( $\text{kN/m}^3$ )	14.76
Minimum void ratio, $e_{\text{min}}$	0.5815
Maximum void ratio, $e_{\text{max}}$	0.8
Void ratio, $e_{\text{nat}}$	0.6816
Relative Density, $D_r$	54.2 %

### 4.3 DIRECT SHEAR TEST

Four direct shear tests were conducted to determine the angle of internal friction of sand used for the model test as per IS: 2720-XIII, 1986. The results are plotted in Fig.4.2 and the angle of internal friction of sand was found to be  $38.3^\circ$ .

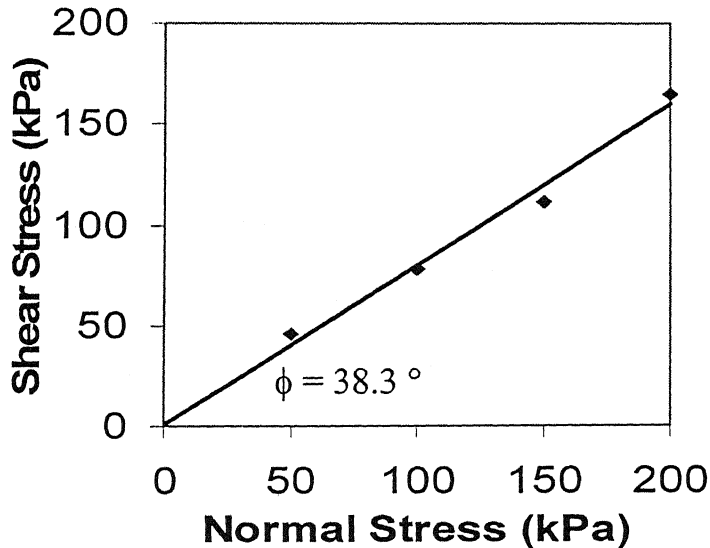


Fig. 4.2: Direct Shear Test for Angle of Internal Friction of Sand

### 4.4 PROPERTIES OF REINFORCEMENTS

Properties of all types of reinforcements i.e. GT-1, GT-2, GG-1 and GG-2 have been discussed in subsequent paragraphs.

#### 4.4.1 TENSILE STRENGTH OF GEOTEXTILE

Uniaxial tensile test was conducted on geotextile (GT-1) and pasted geotextile (GT-2) on Universal Testing Machine, AIMIL, India. The tensile strength of GT-1 and GT-2 were found to be 4.13 kN/m and 10.63 kN/m respectively. Properties of geotextile (GT-1) and pasted geotextile (GT-2) are presented in Table 4.2.

**Table: 4.2**  
Properties of GT-1 and GT-2

Parameter	GT-1	GT-2
Chemical composition	Polypropylene	Polypropylene
Structure	Woven	Woven
Thickness	0.61 (mm)	1.25 (mm)
Weight	5.36 N/m <sup>2</sup>	10.90 (N/m <sup>2</sup> )
Tensile Strength	4.13(kN/m)	10.63 (kN/m)

#### 4.4.2 ANGLE OF FRICTION BETWEEN GEOTEXTILE AND SAND

Direct shear test was conducted to determine angle of friction between geotextile and sand as described in chapter 3. The results are plotted in Fig. 4.3 and the angle of friction between geotextile and sand was found to be 30.3 °.

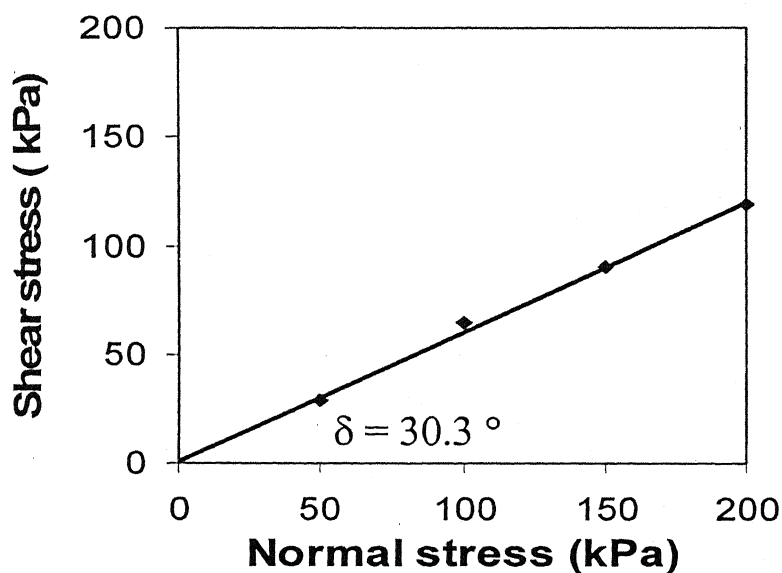


**Fig. 4.3: Direct Shear Test for Angle of Friction between Geotextile and Sand**



#### 4.4.3 TENSILE STRENGTH OF GEOGRID

Uniaxial tensile test was conducted on geogrid (GG-1) and pasted geogrid (GG-2) on Universal Testing Machine, AIMIL, India. The tensile strength of GG-1 and GG-2 were found to be 10.0 kN/m and 23.2 kN/m respectively. Properties of geogrid (GG-1) and pasted geogrid (GG-2) are presented in Table 4.3.

**Table: 4.3**  
Properties of GG-1 and GG-2

Parameter	GG-1	GG-2
Structure	Punched sheet drawn	Punched sheet drawn
Polymer	Polypropylene-HDPE copolymer	Polypropylene-HDPE copolymer
Aperture Size (MD/XMD)	12.54 mm / 30.50 mm	12.54 mm / 30.50 mm
Rib Thickness	1.71 (mm)	3.45 (mm)
Junction Thickness	2.33 (mm)	4.69 (mm)
Weight	6.76 (N/m <sup>2</sup> )	13.92 (N/m <sup>2</sup> )
Tensile Strength	10.0 (kN/m)	23.2 (kN/m)

#### 4.5 MODEL TESTS RESULTS

Load-Settlement curves obtained from the model tests for unreinforced and reinforced sand bed (GT-1, GT-2, GG-1, GG-2) for single layer of reinforcement placed at different depth ratios ( $u/B$ ) are given in Appendix A (Fig. A.1 to Fig. A.27). Load-settlement plots for multiple layers of reinforcement (GT-1, GT-2, GG-1, GG-2) are given in Appendix B (Fig. B.1 to Fig. B.16). Typical plots of load versus settlements are shown in Fig. 4.4 to Fig. 4.6 and the method of determining UBC in this study is described as under.

The ultimate bearing capacity (UBC) with distinguishable shear failure with single layer of reinforcement has been shown by a filled circle (Fig. 4.4). In case there is no distinct point observed, UBC has been determined by drawing double-tangents (Fig. 4.5). Bearing pressure for multiple layers of reinforcement has been obtained by drawing a vertical line corresponding to 6 mm settlement (Fig. 4.6).

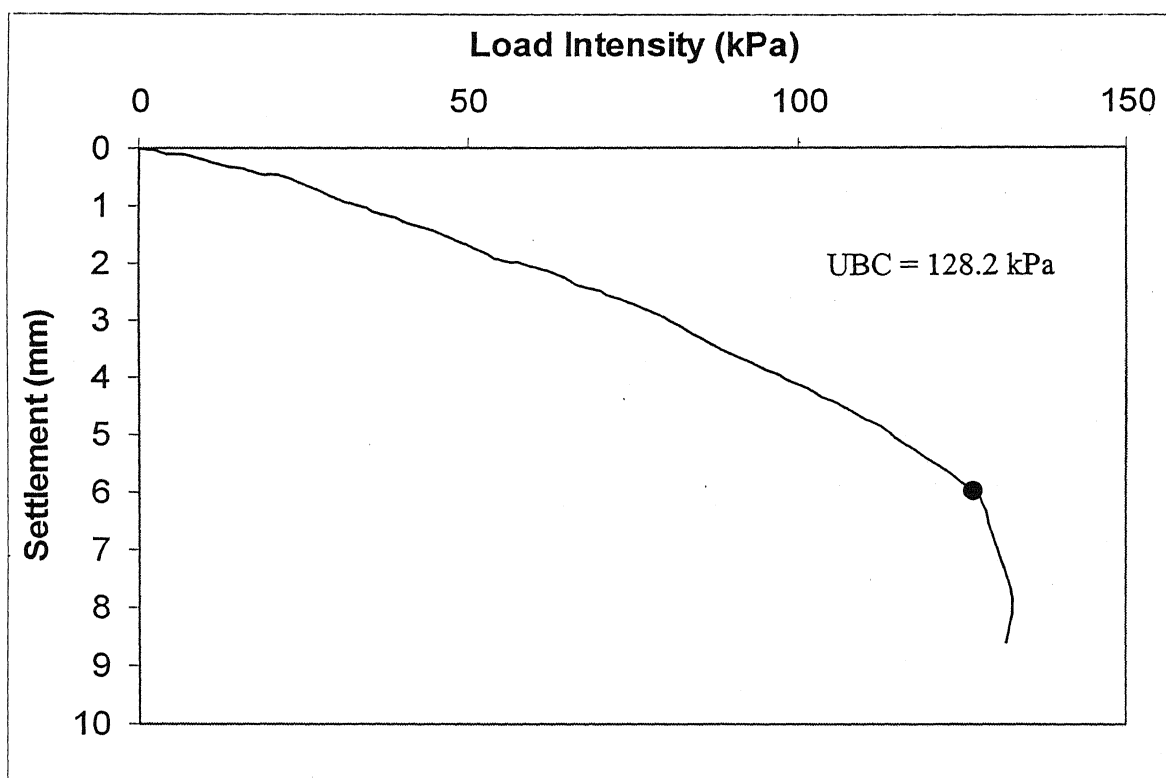


**Fig. 4.4:** Load-Settlement curve for GT-1 at  $u/B = 0.7$

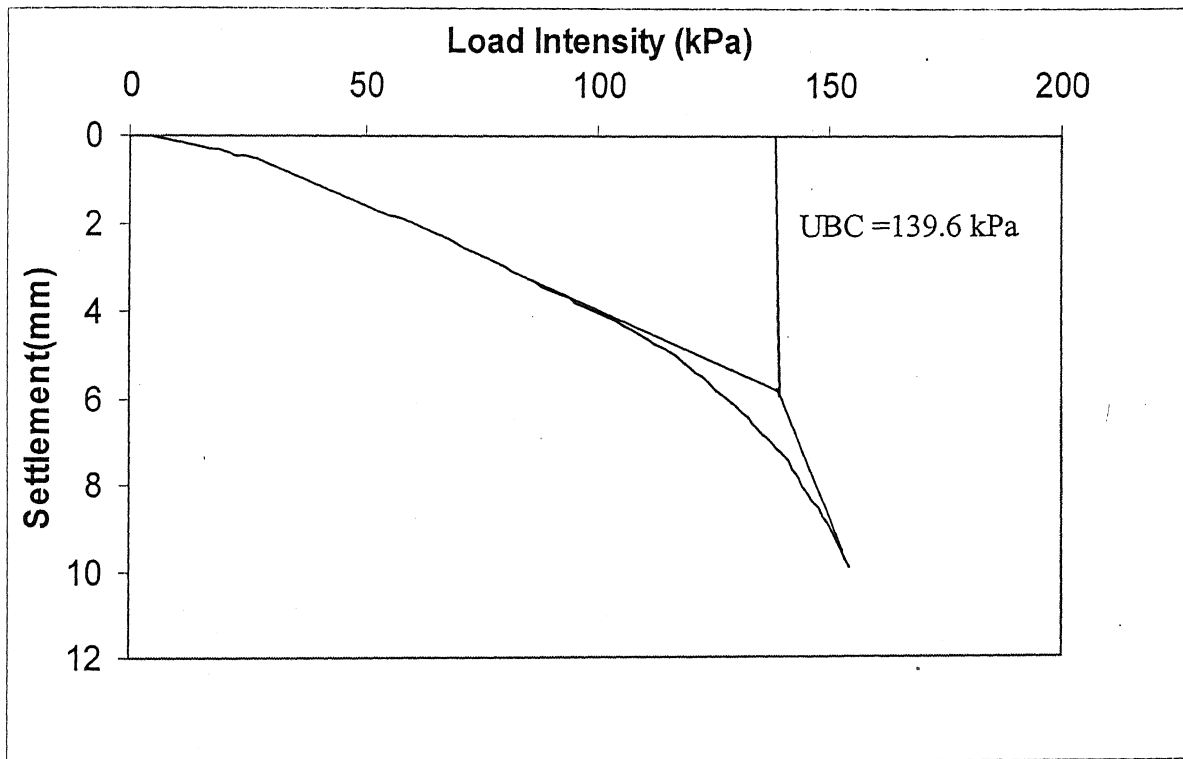


Fig 4.5: Load-Settlement curve for GT-1 at  $u/B = 0.5$

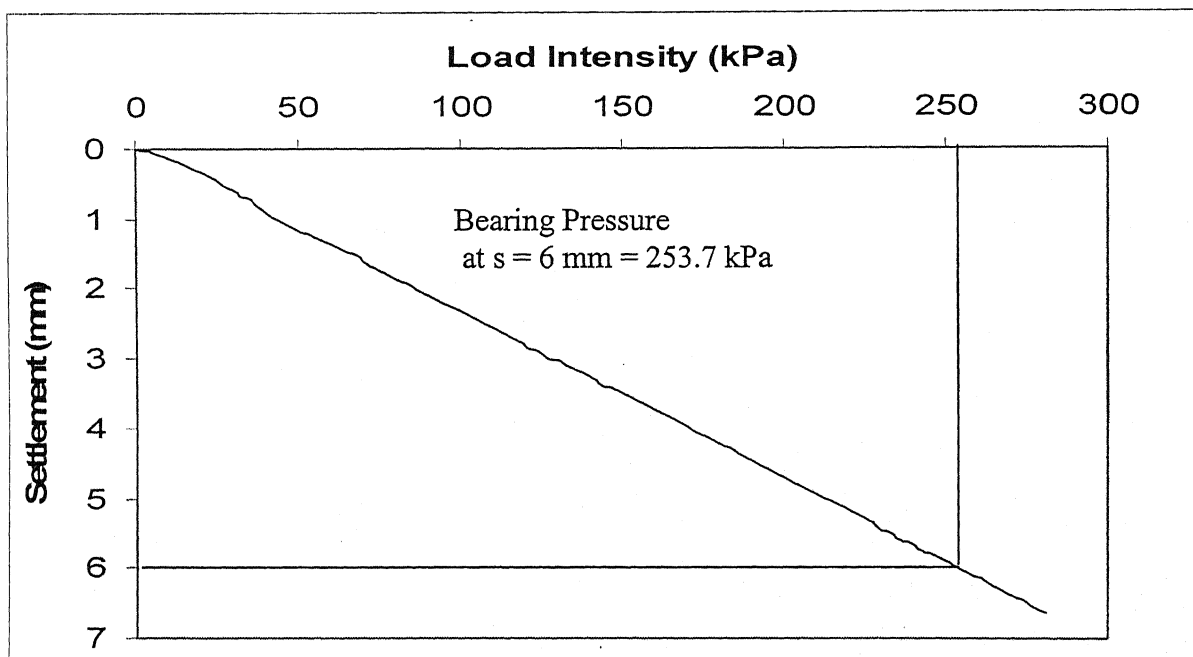
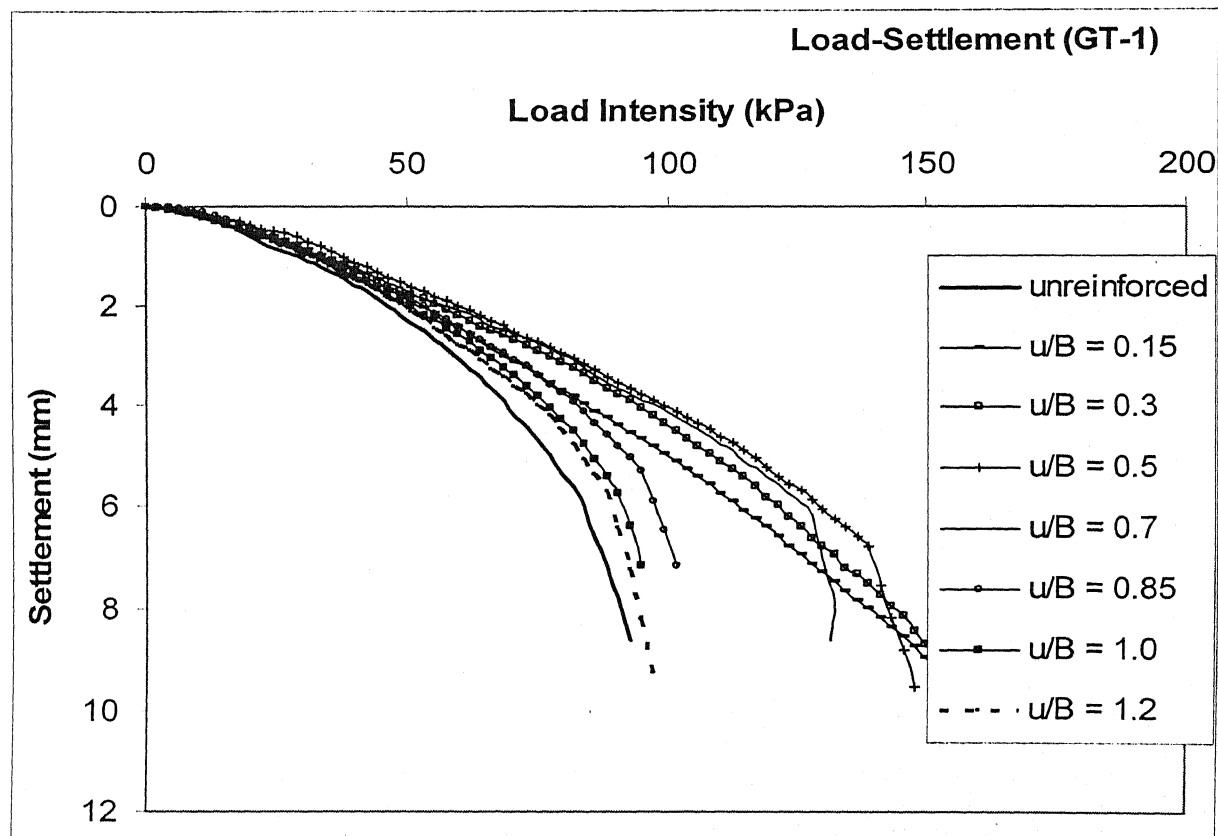


Fig 4.6: Load-Settlement curve for GT-2 at  $u/B = 0.25, 0.5, 0.75$  and  $1$

The ultimate bearing capacity of unreinforced sand bed ( $q_u$ ) determined from load-settlement curve is 84 kPa and the corresponding settlement for unreinforced sand bed is 6 mm. Ultimate bearing capacity ( $q_{u(R)}$ ) and bearing capacity ratio of reinforced sand bed for all types of model tests for single layer as determined by load-settlement curves is given in Table A.1 of Appendix A. Bearing pressure corresponding to 6 mm settlement for reinforced sand bed ( $q_R$ ) for all types of model tests for multiple layers of reinforcement is given in Table B.1 of Appendix B.

#### 4.6 EFFECT OF PLACEMENT DEPTH OF REINFORCEMENT

To study the effect of depth of placement of the reinforcement, combined plots for all individual depth ratios ( $u/B$ ) have been drawn from Figures 4.7 to 4.10 for GT-1, GT-2, GG-1 and GG-2 respectively.



**Fig. 4.7:** Load-Settlement curves at different depth ratios ( $u/B$ ) for GT-1

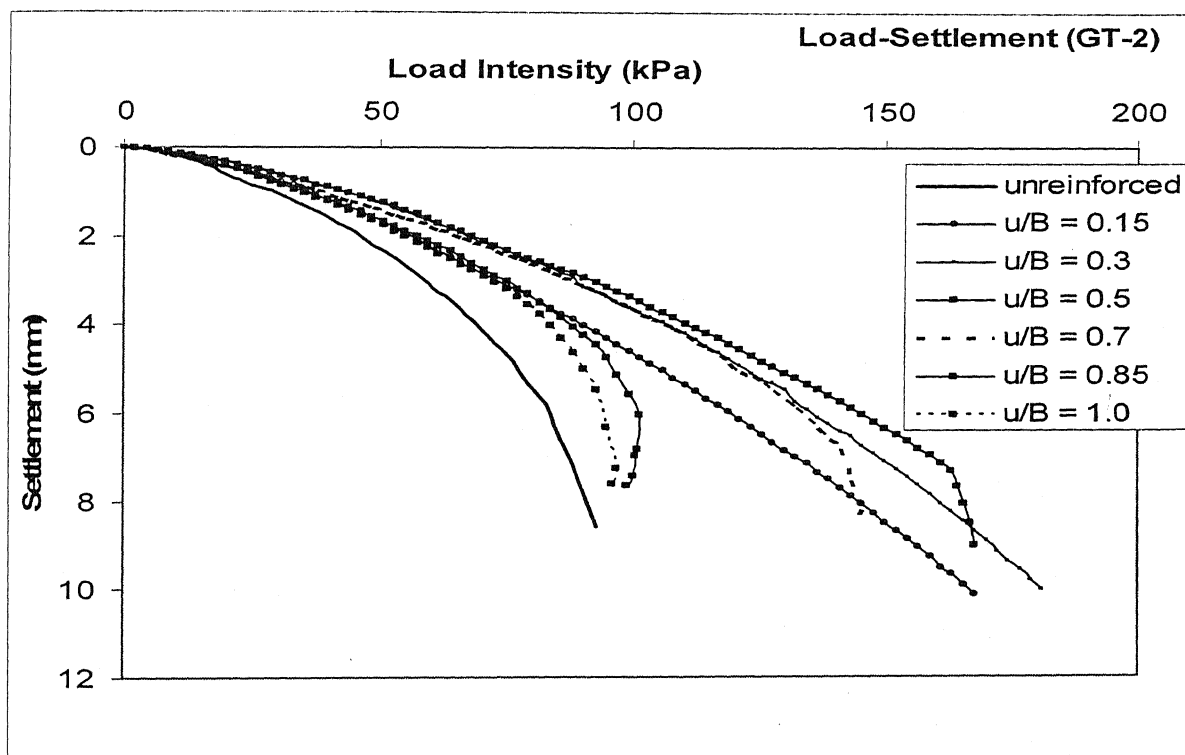


Fig. 4.8: Load-Settlement curves at different depth ratios ( $u/B$ ) for GT-2

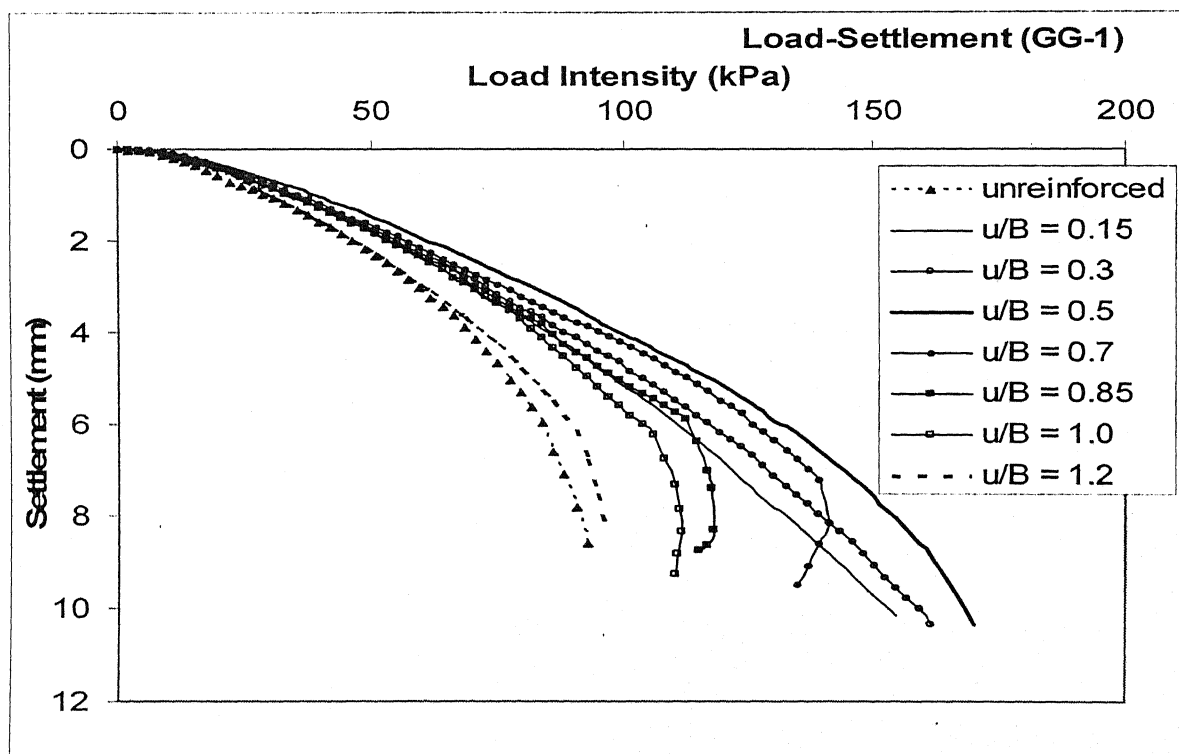


Fig. 4.9: Load-Settlement curves at different depth ratios ( $u/B$ ) for GG-1

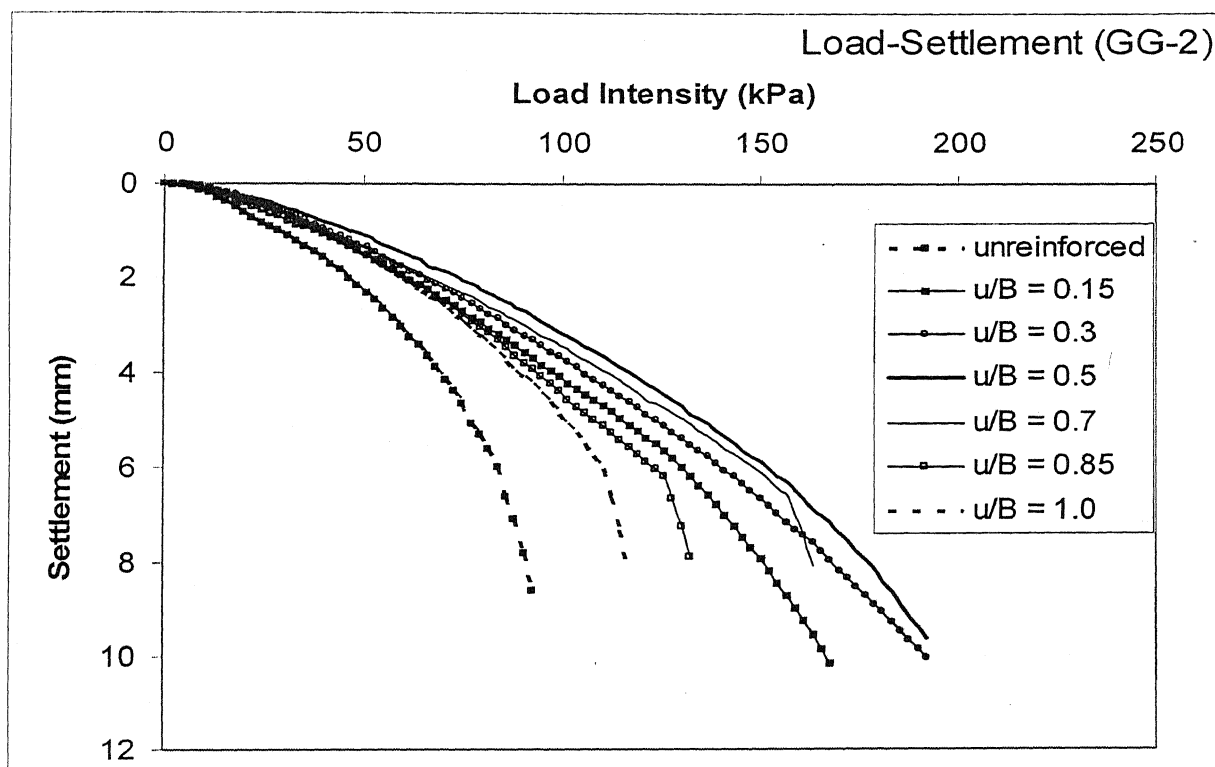


Fig. 4.10: Load-Settlement curves at different depth ratios ( $u/B$ ) for GG-2

As can be seen from the plot for GT-1 in Fig 4.7 that placement of reinforcing layer at different depth ratios ( $u/B$ ) does not contribute much to the settlement reduction up to the load intensity of 50 kPa whereas settlement reduction for GT-2 in Fig. 4.8 starts showing up after 20 kPa and is more prominent as the load increases. As regards plot for GG-1 in Fig. 4.9, placement of reinforcing layer at different depth ratio ( $u/B$ ) contributes towards settlement reduction after 30 kPa whereas for GG-2 in Fig. 4.10 it contributes after 15 kPa and is more prominent as the load increases. For a particular settlement the bearing pressure is maximum at  $u/B = 0.5$  for all types of reinforcement i.e. GT-1, GT-2, GG-1 and GG-2. The optimum depth, therefore, is 5 cm from the bottom of the footing for all types of reinforcement for the size of footing studied.

As can be observed from Fig. 4.7 and 4.9, load-settlement curves for  $u/B = 1.2$  for GT-1 and GG-1 show decrease in bearing pressure for a particular settlement if compared to the curve at  $u/B = 1$  for the same settlement. Also the bearing pressure at a particular settlement for  $u/B = 1.2$  is only marginally higher ( $< 10\%$ ) than that of unreinforced sand bed in case of GT-1 as well as for GG-1 thereby indicating the effective depth for placement of reinforcing layer to be 10 cm i.e.  $u/B = 1.0$ . This substantiates results reported by Guido (1985) that the placement of reinforcement below a depth  $B$  from the base of the footing is not beneficial. There is a significant improvement in the load-settlement response at depth ratios ( $u/B$ ) from 0.3 to 0.7 for GT-1 and GT-2. Significant improvement in load-settlement response for GG-1 and GG-2 is found at all depth ratios. However, it is more prominent from  $u/B = 0.3$  to 0.7.

#### 4.7 BEARING CAPACITY RATIO (BCR)

The bearing capacity ratio with respect to ultimate bearing capacity can be defined as  $BCR_u = q_{u(R)} / q_u$ ,

where  $q_{u(R)}$  = ultimate bearing capacity of reinforced sand

and  $q_u$  = ultimate bearing capacity of unreinforced sand.

The bearing capacity ratio with respect to settlement can be defined as

$$BCR_s = q_R / q,$$

where  $q_R$  = bearing pressure of reinforced sand at a settlement  $s \leq s_u$

and  $q$  = bearing pressure of unreinforced sand at a settlement  $s \leq s_u$ .

Bearing pressure of unreinforced and reinforced sand at a settlement  $s$ , is determined from the load-settlement curve with respect to any settlement  $s \leq s_u$ .

Plots between bearing capacity ratio ( $BCR_u$ ) and depth ratios ( $u/B$ ) for GT-1, GT-2, GG-1 and GG-2 are given in Fig. 4.11.

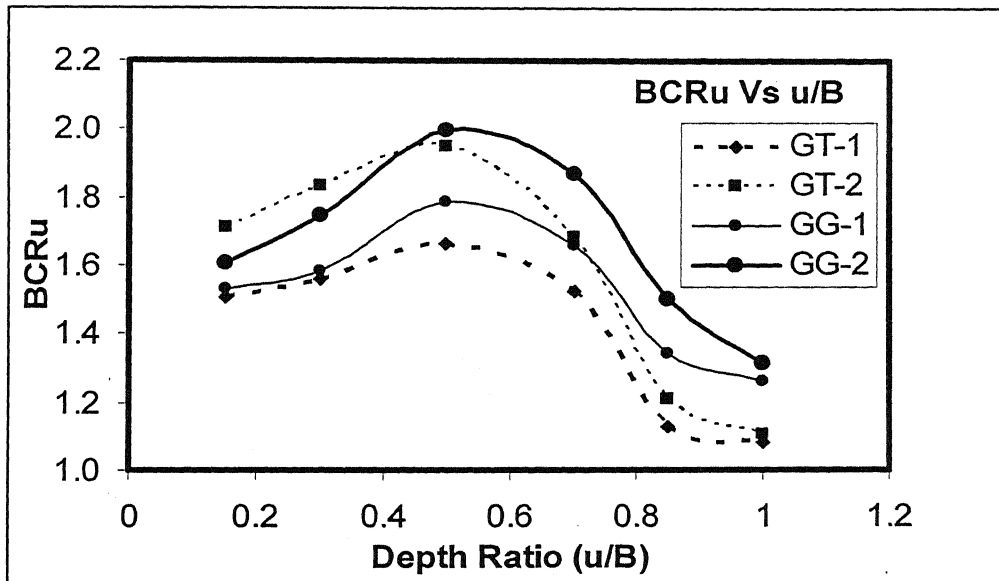


Fig. 4.11: Plot between  $BCR_u$  and  $u/B$  for GT-1, GT-2, GG-1 and GG-2

It is observed from Fig. 4.11 that  $BCR_u$  increases as  $u/B$  increases from 0.15 to 0.5 and then decreases until  $u/B = 1$ , however, significant increase in bearing capacity ratio is observed only from  $u/B = 0.15$  to 0.7 for GT-1 as well as for GT-2. The  $BCR_u$  at  $u/B = 0.5$  is found to be 1.66 and 1.95 for GT-1 and GT-2 respectively. As can also be seen that the increase in  $BCR_u$  from GT-1 to GT-2 corresponding to different depth ratios ( $u/B$ ) is not found very significant (7 to 18 %) even if the tensile strength of GT-2 is more than 2.5 times than that of GT-1. The reason for this is that mobilization of tensile force depends on the interfacial friction between sand and geotextile and that remains the same. However, the increase in  $BCR_u$  can be attributed to increased stiffness of pasted geotextile.

Significant increase in bearing capacity ratio is observed throughout the depth ratio i.e. from  $u/B = 0.15$  to 1.0 for GG-1 as well as for GG-2. However,  $BCR_u$  increases as  $u/B$  increases from 0.15 to 0.5 and then decreases until  $u/B = 1$ . The  $BCR_u$  at  $u/B = 0.5$  is found to be 1.79 and 2.0 for GG-1 and GG-2 respectively. As can be seen from the plot that the increase in  $BCR_u$  from GG-1 to GG-2 corresponding to different depth ratios ( $u/B$ ) is not found very significant (10 to 12 %) even if the



tensile strength of GG-2 is more than 2.3 times than that of GG-1. The reason for this is that mobilization of tensile force depends on effective bond due to interlock of sand particles in the aperture of geogrid and the aperture size remains the same for GG-1 and GG-2. However, the slight increase in  $BCR_u$  can be attributed to increased stiffness of geogrid. Pattern of the relationship between  $BCR_u$  and  $u/B$  is observed to be same for all types of reinforcement i.e. GT-1, GT-2, GG-1 and GG-2.

Plots between  $BCR_s$  and the Settlement Ratio ( $s/B$ ) for GT-1, GT-2, GG-1 and GG-2 are given in Figs. 4.12 to 4.15 respectively.

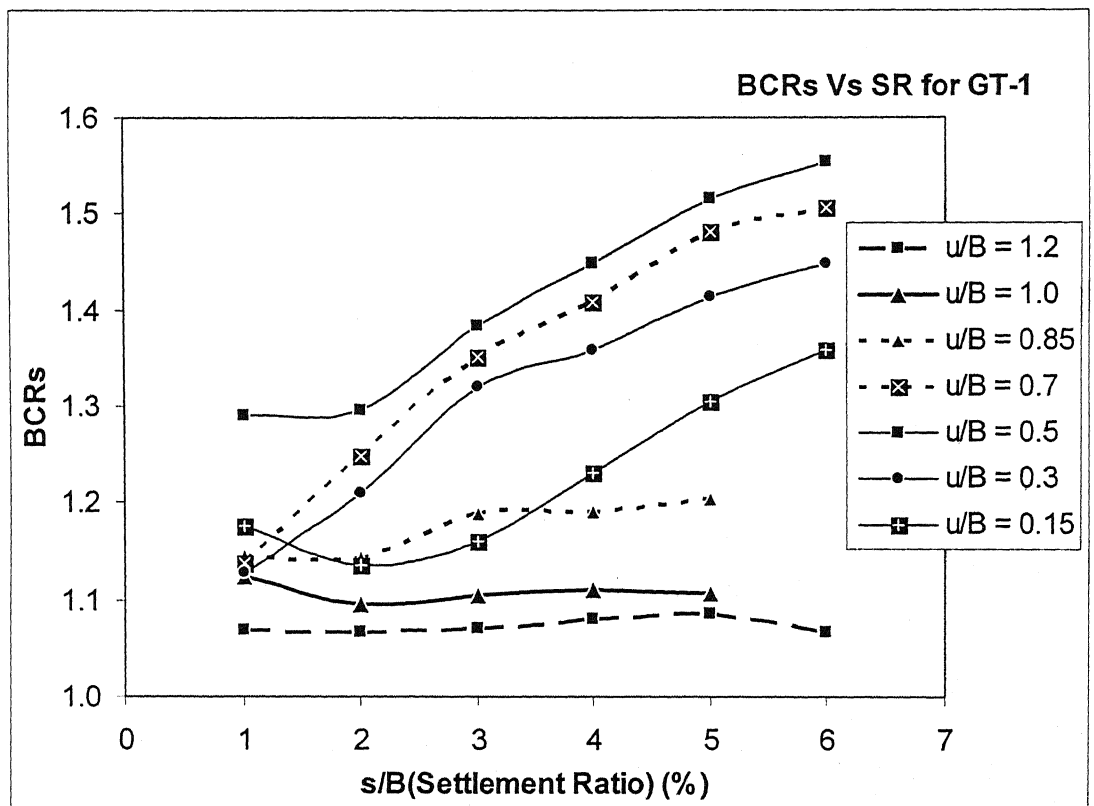


**Fig. 4.12:** Plot between  $BCR_s$  and Settlement ratio for GT-1

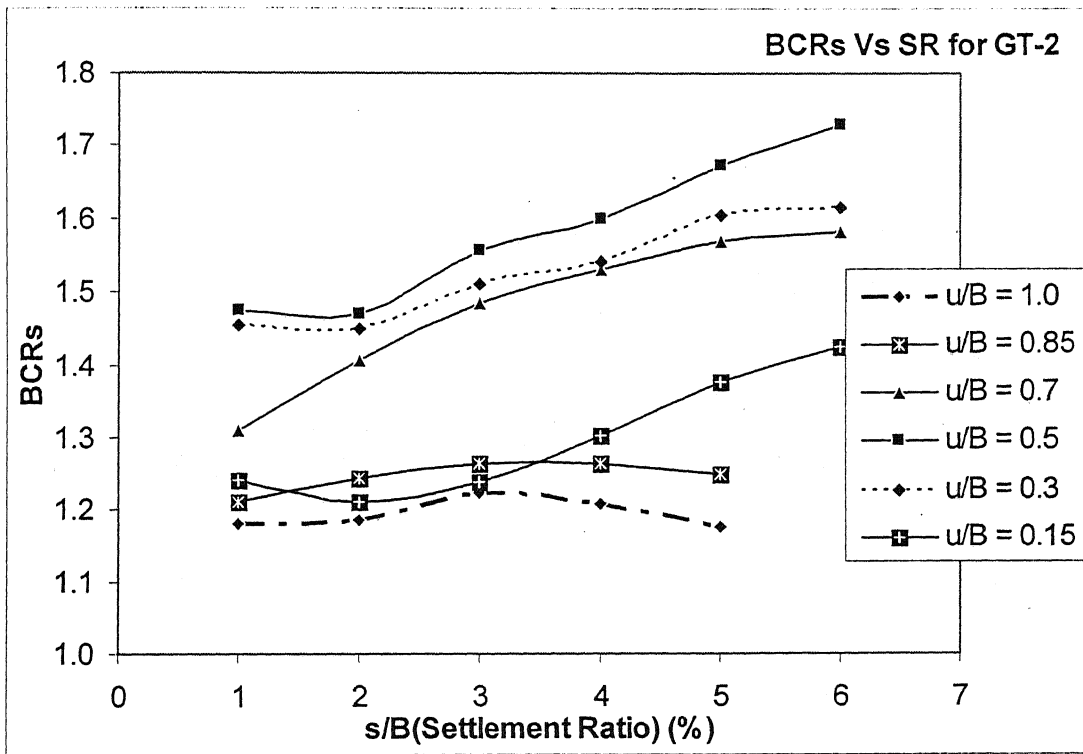


Fig. 4.13: Plot between  $BCR_s$  and Settlement ratio for GT-2

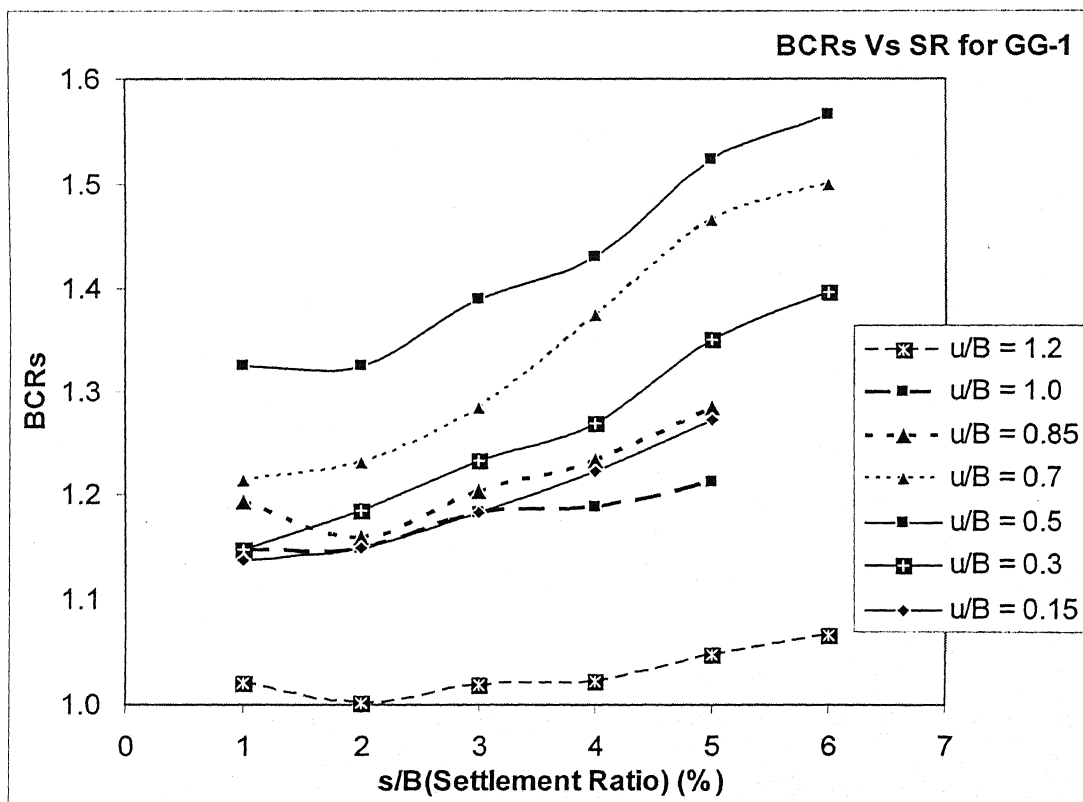


Fig. 4.14: Plot between  $BCR_s$  and Settlement ratio for GG-1

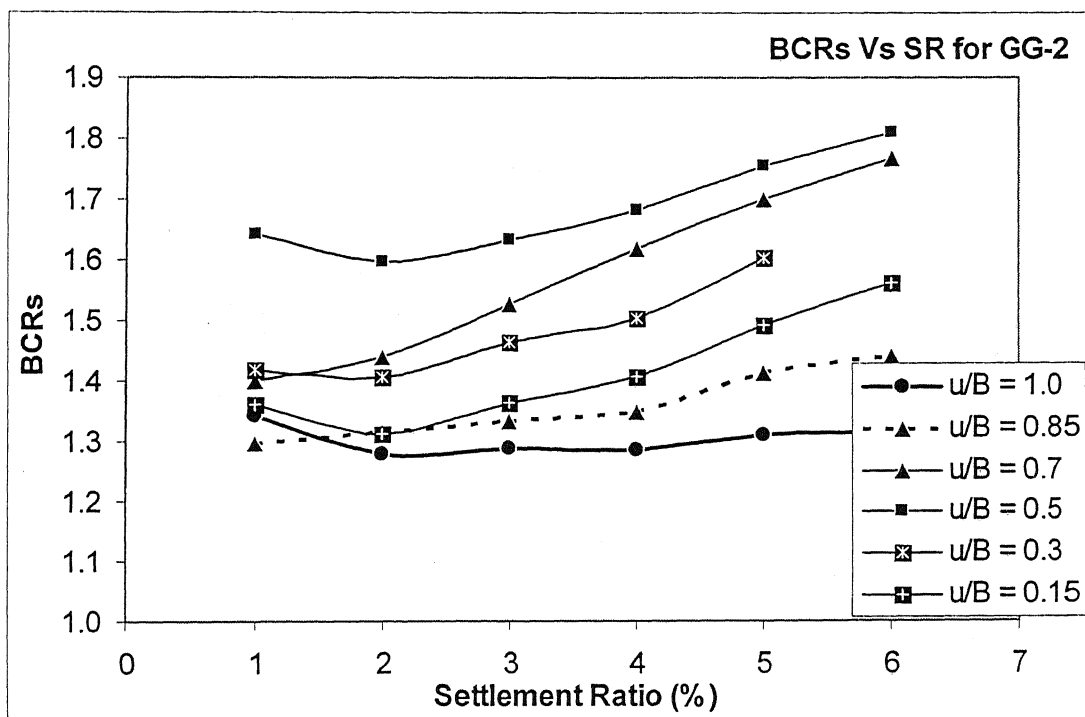


Fig. 4.15: Plot between  $BCR_s$  and Settlement ratio for GG-2

As can be seen from the plots in Figs. 4.12 and 4.13 that  $BCR_s$  is maximum at all settlement ratios ( $s/B$ ) at the depth ratio ( $u/B$ ) = 0.5 for GT-1 as well as for GT-2.  $BCR_s$  for  $u/B = 0.5$  and  $s/B = 5$  is observed to be 1.516 for GT-1 and 1.673 for GT-2. For GT-1 and GT-2, significant improvement is observed in  $BCR_s$  at all settlement ratios ( $s/B$ ) for  $u/B = 0.3, 0.5$  and  $0.7$  than for other depth ratios. However,  $BCR_s$  is more prominent for  $s/B \geq 3$ .  $BCR_s$  at all settlement ratios is higher for  $u/B = 1$  than for  $u/B = 1.2$  for GT-1. Also  $BCR_s$  for  $u/B = 1.2$  at all settlement ratios is marginally higher than 1 indicating the effective depth for placing the reinforcing layer to be 10 cm i.e.  $u/B = 1$ .

As can be seen from the plots in Figs. 4.14 and 4.15 that  $BCR_s$  is maximum at all settlement ratios ( $s/B$ ) at depth ratio ( $u/B$ ) = 0.5 for GG-1 as well as for GG-2.  $BCR_s$  for  $u/B = 0.5$  and  $s/B = 5$  is observed to be 1.523 for GG-1 and 1.755 for GG-2.

Significant improvement is observed in  $BCR_s$  at all settlement ratios ( $s/B$ ) and at all depth ratios for GG-1 and GG-2. However, it is more prominent for  $s/B \geq 3$ .  $BCR_s$  at all settlement ratios is higher for  $u/B = 1$  than for  $u/B = 1.2$  for GG-1. Also  $BCR_s$  for  $u/B = 1.2$  at all settlement ratios is marginally higher than 1 indicating the effective depth for placing the reinforcing layer to be 10 cm i.e.  $u/B = 1$ .

#### 4.8 PERCENTAGE REDUCTION IN SETTLEMENT (PRS)

By placing a layer of geosynthetic, not only there is an increase in the ultimate bearing capacity but also a reduction in the settlement. This reduction in settlement has been worked out for all types of model tests (given in section 3.4.2.3 of chapter 3) as percentage reduction in settlement (PRS). The same has been defined and determined as under :-

$$\text{Percentage reduction in settlement (PRS)} = \frac{(s_o - s_r)}{s_o} \dots\dots\dots(4.1)$$

where,

$s_o$  - Settlement of unreinforced sand corresponding to its ultimate bearing capacity

$s_r$  - Settlement of reinforced sand corresponding to bearing pressure equal to the ultimate bearing capacity of unreinforced sand

(Mandal & Sah (1992) defined the reduction in settlement in the same manner.)

Settlement ( $s_o$ ) of unreinforced sand to its ultimate bearing capacity ( $q_u = 83.98 \approx 84$  kPa) is determined from the load-settlement curve and found to be  $5.985 \approx 6$  mm. Settlement of reinforced sand ( $s_r$ ) corresponding to bearing pressure equal to the ultimate bearing capacity of unreinforced sand ( $q_u = 84$  kPa) is

determined from various load-settlement curves and the percentage reduction in settlement is found out by using Equation 4.1.

Plots between percentage reduction in settlement and depth ratio ( $u/B$ ) for GT-1, GT-2, GG-1 and GG-2 are given in Fig 4.16.

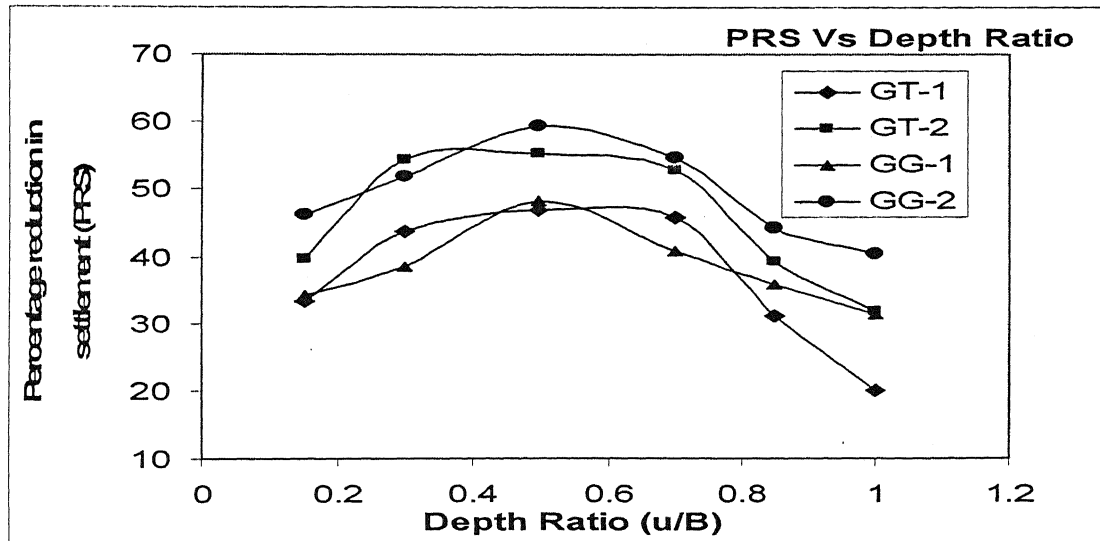


Fig. 4.16: Plot between PRS and  $u/B$  for GT-1, GT-2, GG-1 and GG-2

Based on the plot, it can be observed that the percentage reduction in settlement (PRS) increases from  $u/B = 0.15$  to  $0.5$  and then decreases until  $u/B = 1$  for GT-1 and GT-2. PRS ranges from 21 to 47 % for GT-1 and 32 to 55 % for GT-2. Maximum PRS is observed at  $u/B = 0.5$  and found to be 47 % and 56 % for GT-1 and GT-2 respectively. Increase in PRS from GT-1 to GT-2 is in the range of 6-11% for different depth ratios ( $u/B$ ).

For GG-1 and GG-2, the percentage reduction in settlement (PRS) increases from  $u/B = 0.15$  to  $u/B = 0.5$  and then decreases until  $u/B = 1$ . PRS ranges from 31 to 48 % for GG-1 and 40 to 59 % for GG-2. Maximum PRS is observed at  $u/B = 0.5$  and found to be 48 % and 59 % for GG-1 and GG-2 respectively. Increase in PRS from GG-1 to GG-2 is in the range of 9-14 % for different depth ratios ( $u/B$ ).

## 4.9 EFFECT OF MULTIPLE LAYERS ON SETTLEMENT RESPONSE

Load-settlement plots at different depth ratios ( $u/B$ ) for GT-1, GT-2, GG-1 and GG-2 are given from Figs. 4.17 to 4.20. Single layer was placed at a depth ratio ( $u/B$ ) of 0.5 thereafter layers were placed at equal spacing ie.  $u/B = h/B$  in all the cases. Details of model tests conducted are given in para 3.4.2.3 of chapter 3.

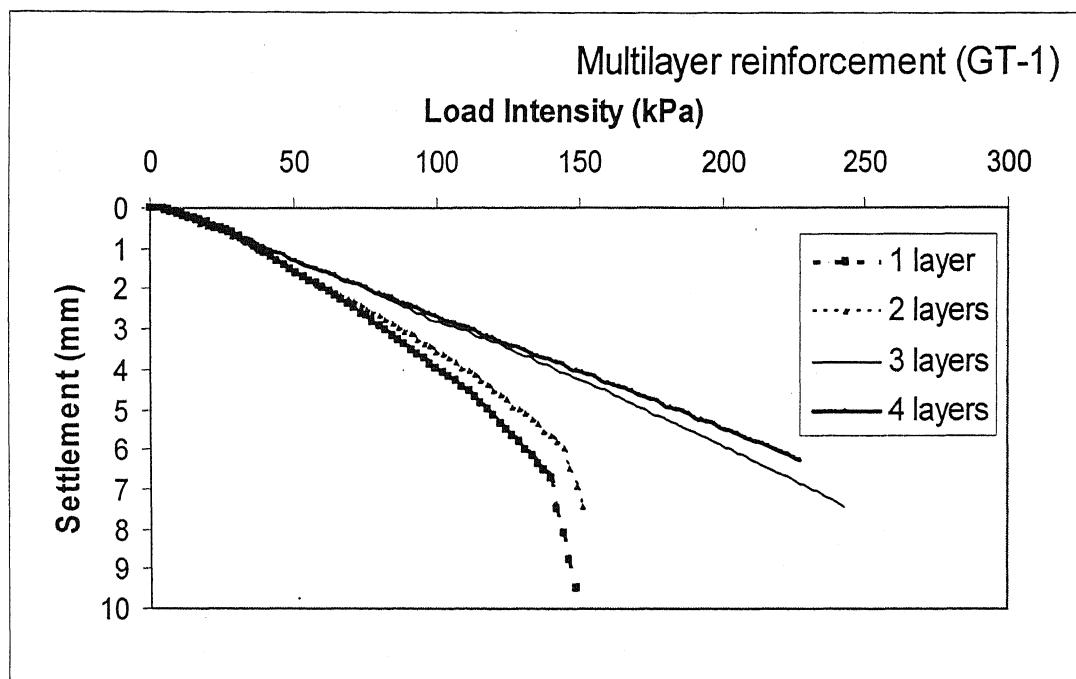
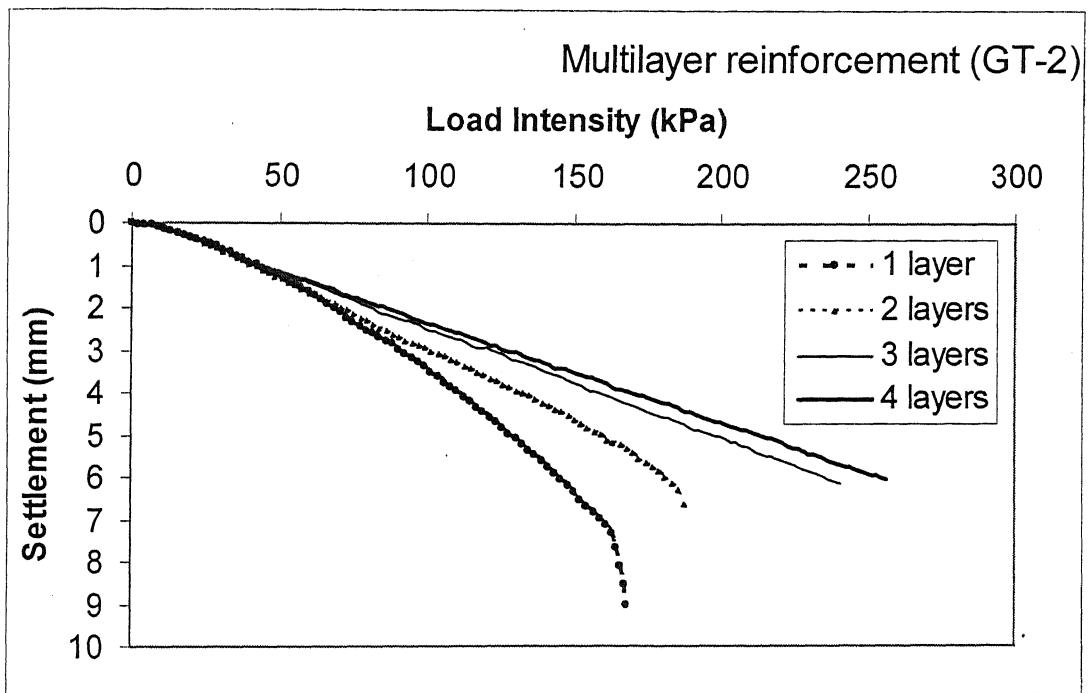
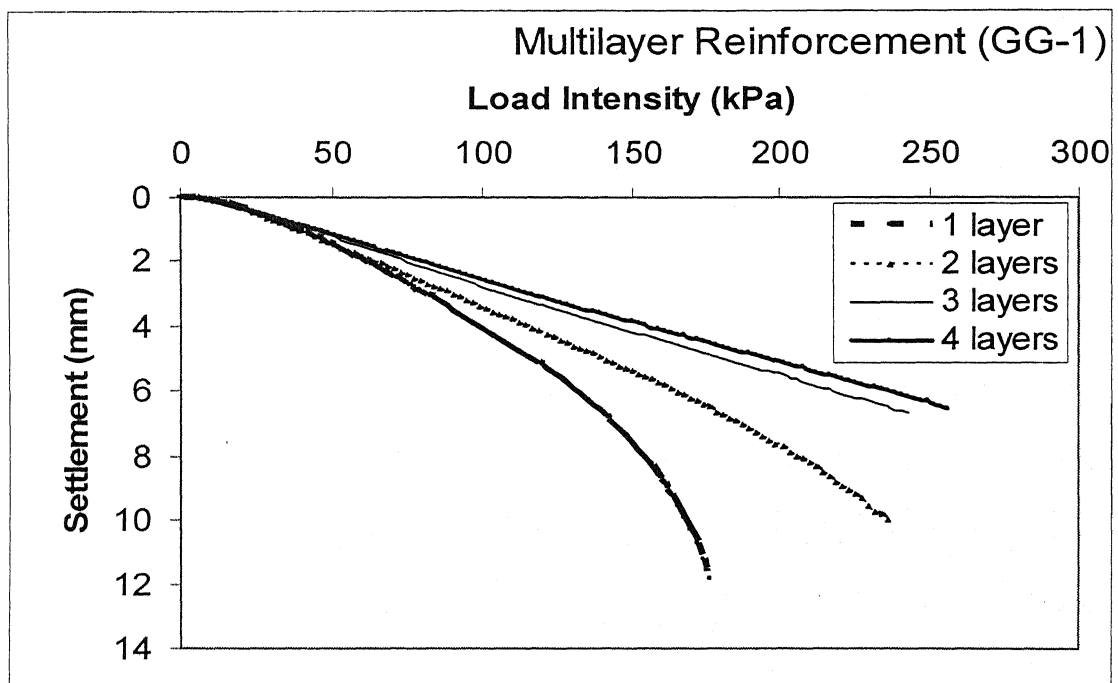


Fig. 4.17: Load-settlement Curve for Multilayer Reinforcement (GT-1)



**Fig. 4.18: Load-settlement Curve for Multilayer Reinforcement (GT-2)**



**Fig. 4.19: Load-settlement Curve for Multilayer Reinforcement (GG-1)**

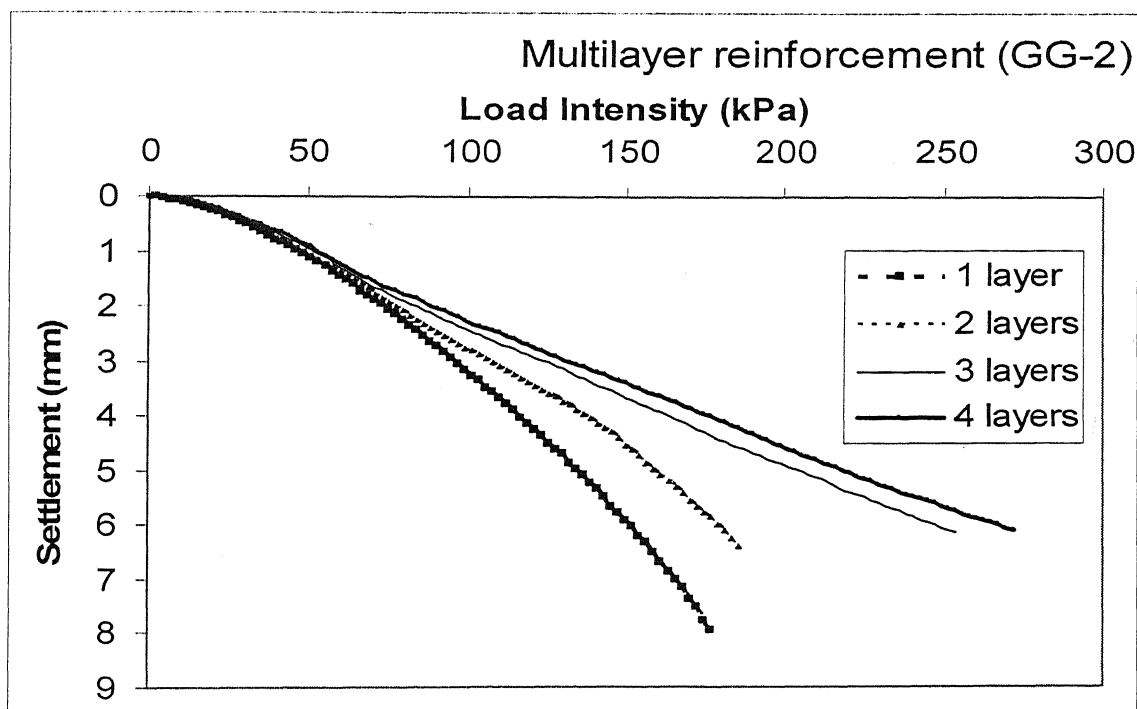


**Fig. 4.20:** Load-settlement Curve for Multilayer Reinforcement (GG-2)

As can be seen from the plot in Fig. 4.17 and 4.18 that there is no further reduction in settlement up to 35 kPa or so for GT-1 and up to 50 kPa for GT-2 even if number of layers is increased from 1 to 4. Even with further increase in load the settlement does not reduce significantly if the Number of layers is increased from 3 to 4 for GT-1 as well as for GT-2.

From the plots in Fig. 4.19 and 4.20, it can be seen that there is no further reduction in settlement up to 35 kPa or so for GG-1 and up to 65 kPa for GG-2 even if number of layers is increased from 1 to 4. With further increase in load the settlement does not reduce significantly if the number of layers is increased from 3 to 4 for GG-1 as well as for GG-2. Pattern of the plots is found to be similar for all types of reinforcement.

#### 4.10 EFFECT OF MULTIPLE LAYERS ON $BCR_s$

Plot for  $BCR_s$  and Number of Layers (N) for GT-1, GT-2, GG-1 and GG-2 is given in Fig 4.21. Load-settlement plots with 3 and 4 layers of reinforcement were not



curves but almost a straight line. The load was applied for these model tests till settlement of more than 6 mm was reached. The applied load could not cause failure due to experimental constraints, therefore the ultimate bearing capacity could not be ascertained. However, the bearing pressure for all types of model tests has been obtained from the load-settlement curves at 6 mm and  $BCR_s$  determined as the ultimate settlement for unreinforced sand was found to be 6mm.

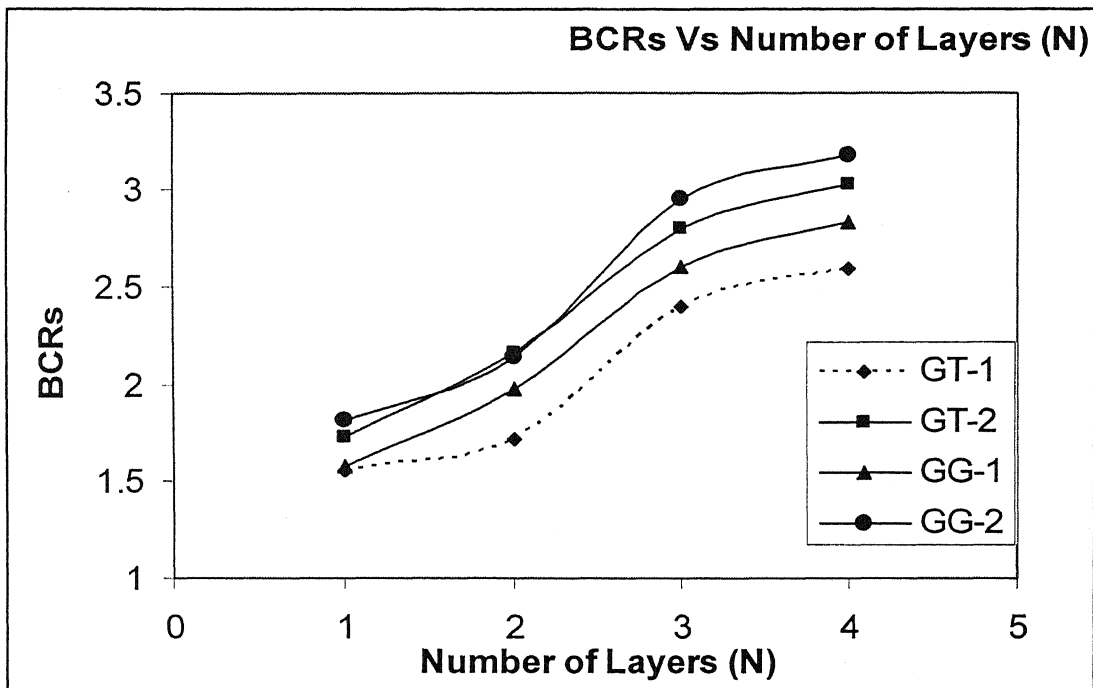


**Fig. 4.21:** Plot between  $BCR_s$  and Number of Layers for GT-1, GT-2, GG-1 and GG-2

As can be seen from the figure that  $BCR_s$  increases significantly if the No. of layers is increased from 2 to 3 for GT-1 as well as for GT-2. For GT-1 the increase is 40 % and for GT-2 it is 30 %. Increase in  $BCR_s$  is not found significant for GT-1 if the No. of layers is increased from 1 to 2 or 3 to 4 which is 10.3 % and 7.9 % respectively. The increase in  $BCR_s$  for GT-2 is not found significant if the number of layers is increased from 3 to 4 which is 7.8 %. Therefore, the optimum number. of layers for GT-1 and GT-2 is 3.  $BCR_s$  is varying from 1.55-2.59 for GT-1, 1.73-3.02

for GT-2. The  $BCR_s$  for 3 layers is found to be 2.4 and 2.8 for GT-1 and GT-2 respectively. Increase in  $BCR_s$  from GT-1 and GT-2 is found maximum for two layers.

For GG-1 and for GG-2,  $BCR_s$  increases significantly if the number of layers is increased from 2 to 3. The increase in  $BCR_s$  is not found significant for GG-1 and GG-2 if the No. of layers is increased from 3 to 4 which is 8.8 % and 8 % respectively. Therefore, the optimum number of layers for GG-1 and GG-2 is 3. The  $BCR_s$  is varying from 1.57-2.83 for GG-1 and 1.81-3.18 for GG-2. The  $BCR_s$  for 3 layers is found to be 2.6 and 2.95 for GG-1 and GG-2 respectively. Increase in  $BCR_s$  from GG-1 and GG-2 is found maximum for single layer.

#### 4.11 EFFECT OF MULTI LAYERS ON PRS

Plot between percentage reduction in settlement (PRS) and number of layers (N) for GT-1, GT-2, GG-1 and GG-2 is given in Fig. 4.22.

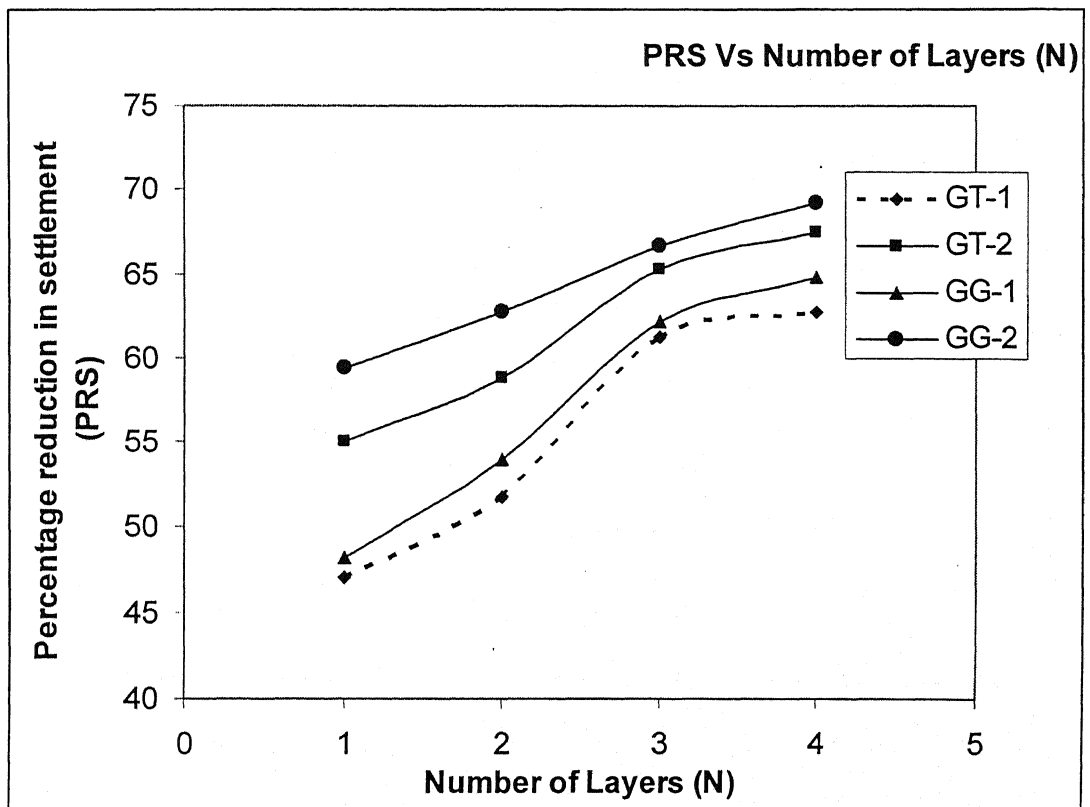


Fig. 4.22: Plot between PRS and Number of Layers for GT-1, GT-2, GG-1 and GG-2

As can be seen from the figure that percentage reduction in settlement (PRS) is significant if the number of layers is increased from 2 to 3 for GT-1 as well as for GT-2. The increase in PRS for GT-1 is 18 % and for GT-2 is 11 %. However, the PRS is not significant for GT-1 and GT-2 if the number of layers is increased from 1 to 2 or 3 to 4. The PRS is 47 with single layer and increases up to 62.7 with four layers for GT-1 whereas PRS is 55 with single layer and increases up to 67.5 with four layers for GT-2. The PRS with 3 layers for GT-1 and GT-2 is 61.2 and 65.3 respectively.

For GG-1 and for GG-2, the percentage reduction in settlement (PRS) is significant if the number of layers is increased from 2 to 3. The increase in PRS for GG-1 is 15 % and for GG-2 is 8 %. However, the PRS is not significant if the number of layers is increased from 1 to 2 or 3 to 4. The PRS is 48.2 with single layer and increases up to 64.8 with four layers in case of GG-1 whereas PRS is 59.3 with single layer and increases up to 69.2 with four layers in case of GG-2. The PRS with 3 layers for GG-1 and GG-2 is 62.2 and 67.7 respectively. From the settlement criteria also the optimum number of layers is found to be 3 for all types of reinforcement.

#### **4.12 DETERMINATION OF MODULUS OF SUBGRADE REACTION (K)**

Modulus of subgrade reaction (k) is defined as the pressure per unit deformation of the subgrade at a specified deformation or pressure level.

$$k = p/\Delta, \text{ where } p \text{ is pressure (kN/m}^2\text{), and } \Delta \text{ is deformation (m)}$$

Modulus of subgrade reaction (k) of unreinforced sand bed and reinforced sand bed for single layer with all types of reinforcements at all depth ratios ( $u/B$ ) has been determined by taking two points in the initial region of the curves and calculating the tangent of those points. The values of modulus of subgrade reaction (k) for reinforced sand bed are given in  $\text{kN/m}^2/\text{m}$  in the Table 4.4 below. The

modulus of subgrade reaction of unreinforced sand bed is determined as  $40.2 \times 10^{-3} \text{ kN/m}^2/\text{m}$

**Table 4.4**

Modulus of subgrade reaction for all types of Reinforcement at all Depth Ratios

<b>u/B</b>	<b>GT-1</b> ( $\times 10^{-3}$ )	<b>GT-2</b> ( $\times 10^{-3}$ )	<b>GG-1</b> ( $\times 10^{-3}$ )	<b>GG-2</b> ( $\times 10^{-3}$ )
0.15	46.5	52.6	49.1	61.4
0.3	47.4	54.4	51	63.1
0.5	51	55.3	57.7	68.0
0.7	47.4	50.0	55	66.2
0.85	45.7	49	51	57.7
1.0	44.2	47.8	47.4	55.3

From the above table it can be observed that modulus of subgrade reaction ( $k$ ) increases up to the depth ratio of 0.5 and thereafter it decreases till depth ratio is one for all types of reinforcements. The value of  $k$  at  $u/B = 0.5$  works out to be 26.9 % and 37.6 % higher than the  $k$  value of unreinforced sand for GT-1 and GT-2. Similarly, value of  $k$  for GG-1 and GG-2 is higher by 43.5 % and 69 % respectively. The range of increase of value  $k$  for all depth ratios is 9.9-26.9 % and 18.9-37.6 % for GT-1, and GT-2 respectively. Similarly, the range of increase of  $k$  value for GG-1 and GG-2 is 17.9-43.5 % and 37.6-69 % respectively.

#### **4.13 CONCLUDING REMARKS**

In this chapter results on tests conducted on materials were brought out. Load-settlement response of model tests at various depth ratios for single layer and multiple layers has been presented. Bearing capacity ratio and percentage reduction in settlement with single and multiple layers for all types of reinforcement were discussed. Modulus of subgrade reaction ( $k$ ) of unreinforced sand bed and reinforced sand beds have also been determined. Conclusions drawn have been reflected in the next chapter.

## CONCLUSIONS

The model tests were conducted as described in chapter 3. Based on the tests results and discussion presented in chapter 4, following conclusions are drawn from the study.

1. Ultimate bearing capacity of sand bed can be significantly increased by reinforcing the sand bed with any type of geosynthetic layer i.e. geotextile or geogrid.
  2. The effective depth for placing geosynthetic is  $B$ . The placement of geosynthetic beyond the depth  $B$  from the base of the footing is not beneficial.
  3. For single-layer reinforced sand bed there is an optimum embedment depth of the reinforcement layer at which the ultimate bearing capacity is the highest. The model tests results indicated that optimum embedment depth for GT-1, GT-2, GG-1 and GG-2 is  $B/2$ .
  4. There is a significant increase in  $BCR_u$  with depth of placement for all the four reinforcements studied. The increase in  $BCR_u$  from GT-1 to GT-2 at different corresponding depth ratios ( $u/B$ ) is not found significant even if the tensile strength of GT-2 is more than 2.5 times than that of GT-1. The reason for this is that mobilization of tensile force depends on the interfacial friction between sand and geotextile and that remains the same for GT-1 and GT-2. Similarly, the increase in  $BCR_u$  from GG-1 to GG-2 at different corresponding depth ratios ( $u/B$ ) is also not found very significant even if the tensile strength of GG-2 is more than 2.3 times than that of GG-1.
2. The reason for this is that mobilization of tensile force depends on effective bond

due to interlock of sand particles in the aperture of geogrid and the aperture size remains the same for GG-1 and GG-2.

5. For GT-1 and GT-2, significant improvement is observed in  $BCR_s$  at all settlement ratios ( $s/B$ ) for  $u/B = 0.3, 0.5$  and  $0.7$  than for other depth ratios. However,  $BCR_s$  is more prominent for  $s/B \geq 3$ . For GG-1 and GG-2 significant improvement is observed in  $BCR_s$  at all settlement ratios ( $s/B$ ) and at all depth ratios. However, it is more prominent for  $s/B \geq 3$ .

6. The percentage reduction in settlement (PRS) for single layer reinforced sand bed at various depth ratios ( $u/B$ ) ranges from 21 to 47 % for GT-1 and 32 to 55 % for GT-2. Similarly, PRS ranges from 31 to 48 % for GG-1 and 40 to 59 % for GG-2. Maximum PRS is observed at  $u/B = 0.5$  and found to be 47 % and 56 % for GT-1 and GT-2 respectively. For GG-1 and GG-2 the maximum PRS is observed at  $u/B = 0.5$  and found to be 48 % and 59 % respectively.

7. In multilayer reinforcement,  $BCR_s$  increases significantly if the number of layers is increased from 2 to 3 for GT-1, GT-2, GG-1 and GG-2. The increase in  $BCR_s$  is 40 % for GT-1 and 30 % for GT-2 whereas for GG-1 and GG-2 it is 38 % and 32 % respectively. However, the increase is not found to be significant if the number of layers is increased from 3 to 4 for all types of reinforcement. Optimum number of layers, therefore, for all types of reinforcement is 3. The  $BCR_s$  for 3 layers for GT-1 is 2.4 and for GT-2 it is 2.8 whereas  $BCR_s$  is 2.6 and 2.95 for GG-1 and GG-2 respectively.

8. Maximum increase in percentage reduction in settlement (PRS) for all types of reinforcement is observed if the numbers of layers is increased from 2 to 3. The increase in PRS is not significant if the number of layers is increased from 1 to 2 or 3 to 4 therefore, from settlement criteria also the optimum number of layers for all types

of reinforcement is 3. The value of PRS increases from 47 with single layer to 63 with four layers in case of GT-1 whereas the corresponding figures for GT-2 are 55 and 68. Similarly, the value of PRS increases from 48.2 with single layer to 64.8 with four layers in case of GG-1 and the corresponding figures for GG-2 are 59.3 and 69.2. The value for PRS for 3 layers for GT-1 is 61.2 and for GT-2 it is 65.3 whereas it is 62.2 and 67.7 for GG-1 and GG-2 respectively.

9. The range of increase in the modulus of subgrade reaction,  $k$  for all depth ratios is 9.9-26.9 % and 18.9-37.6 % for GT-1 and GT-2 respectively. Similarly, the increase of  $k$  value for GG-1 and GG-2 is 22.1-43.5 % and 36-69 % respectively.

## **SCOPE FOR FURTHER STUDY**

Model tests can be conducted with varied densities of sand.

Experiments can be conducted with different sizes of square footing to validate the results of BCR and PRS.

Tests can be conducted with different types of geotextiles and geogrids and comparison drawn amongst them.

## APPENDIX-A

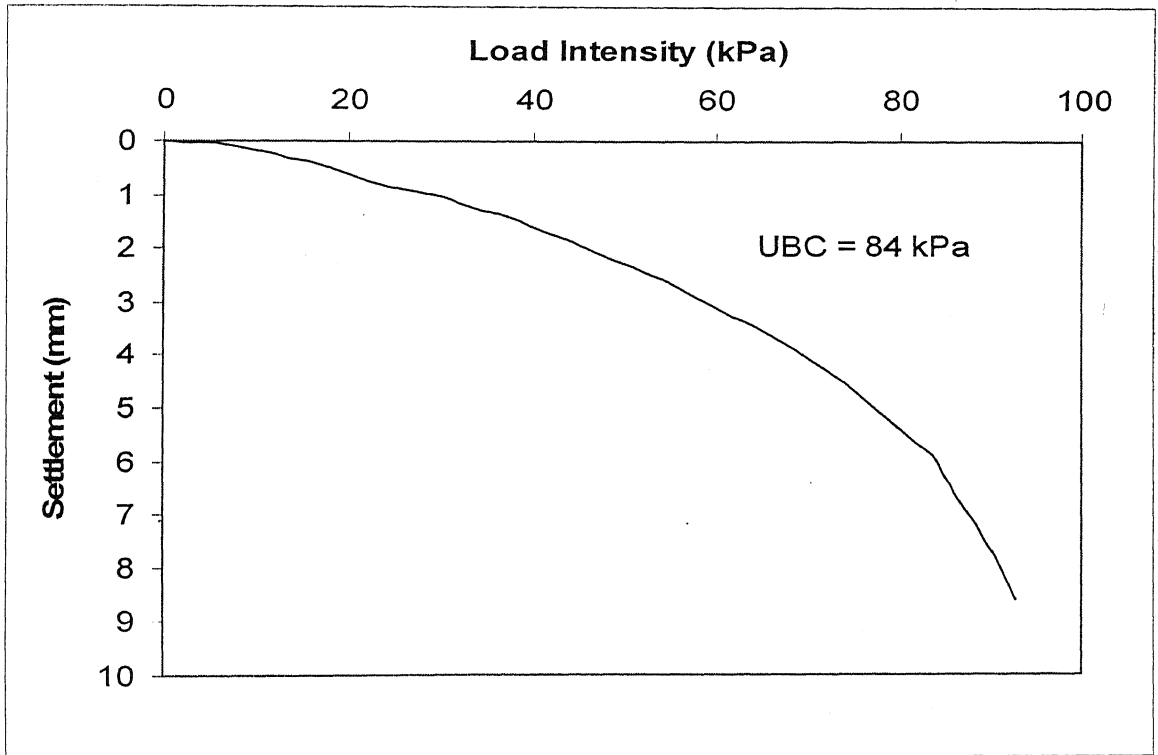


Fig. A.1: Load-Settlement Curve for Unreinforced Sand Bed

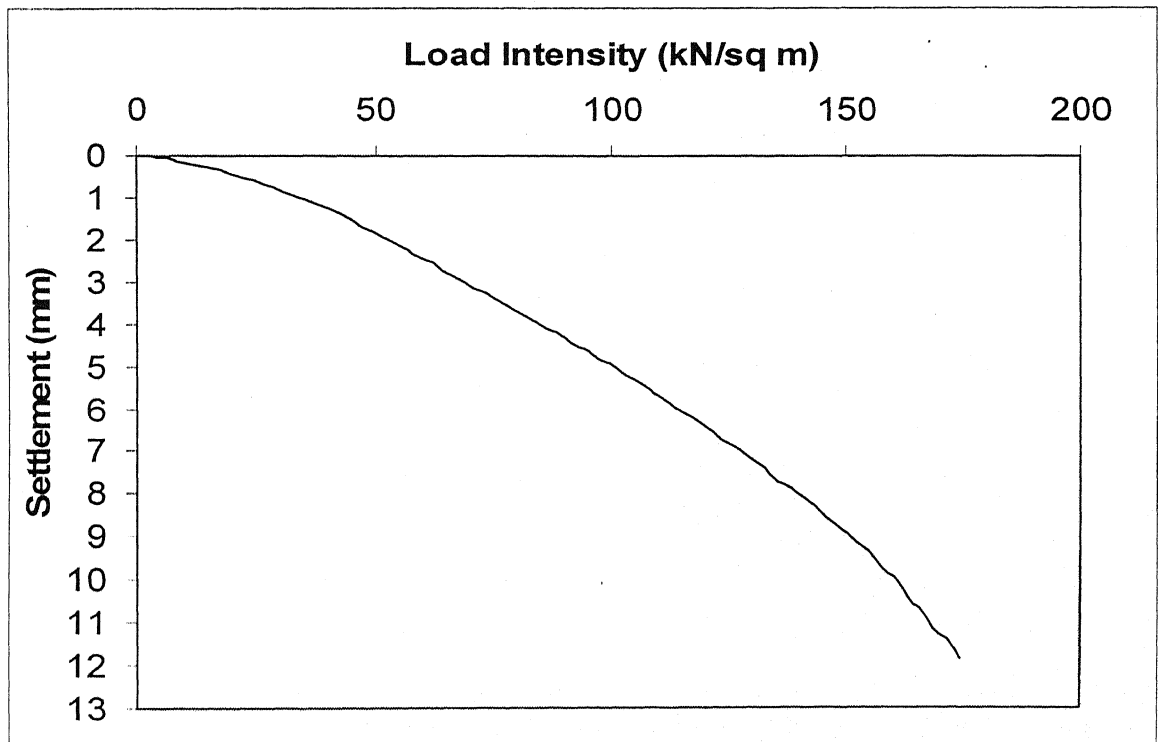


Fig. A.2: Load-Settlement Curve for GT-1 at  $u/B = 0.15$



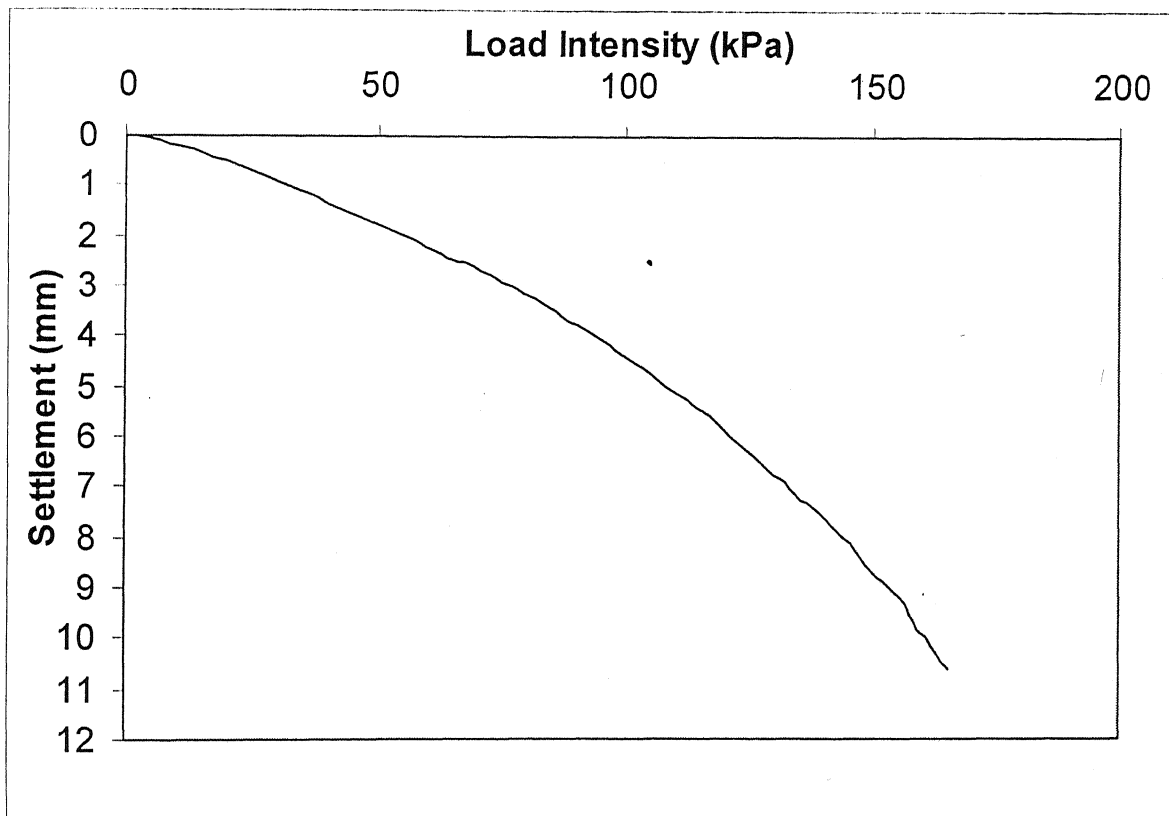


Fig. A.3: Load-Settlement Curve for GT-1 at  $u/B = 0.3$

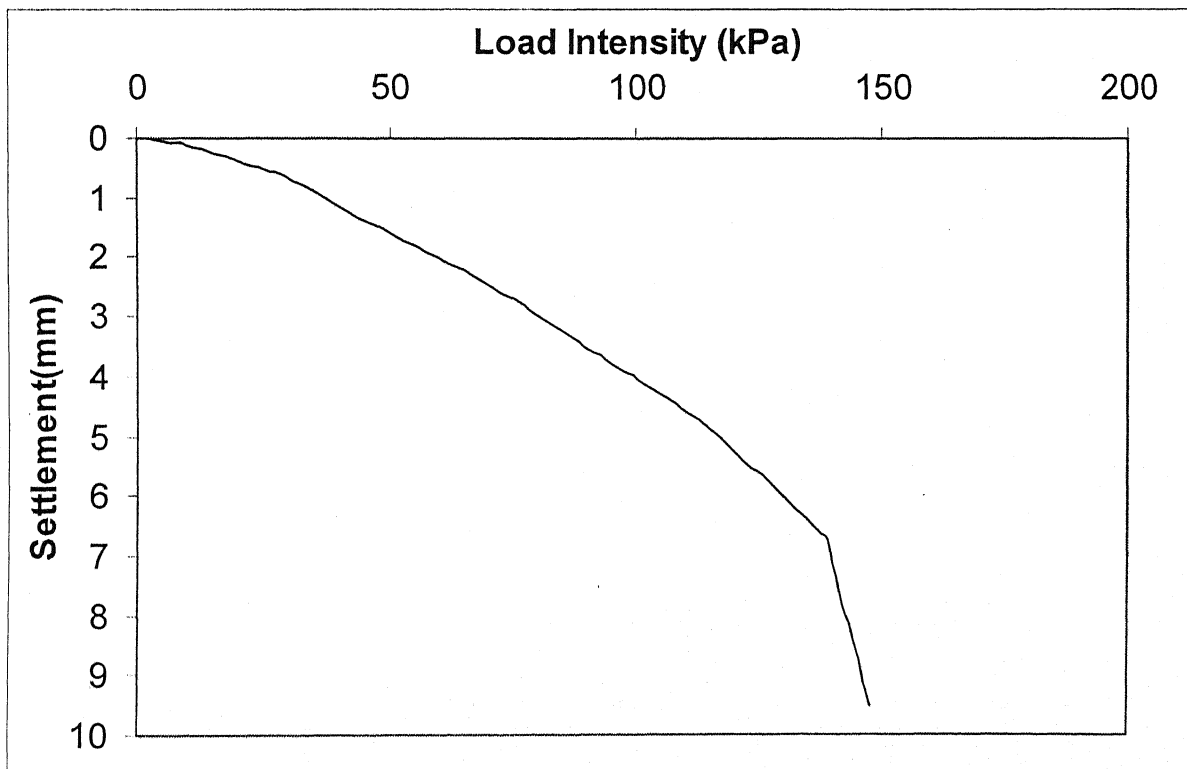


Fig. A.4: Load-Settlement Curve for GT-1 at  $u/B = 0.5$

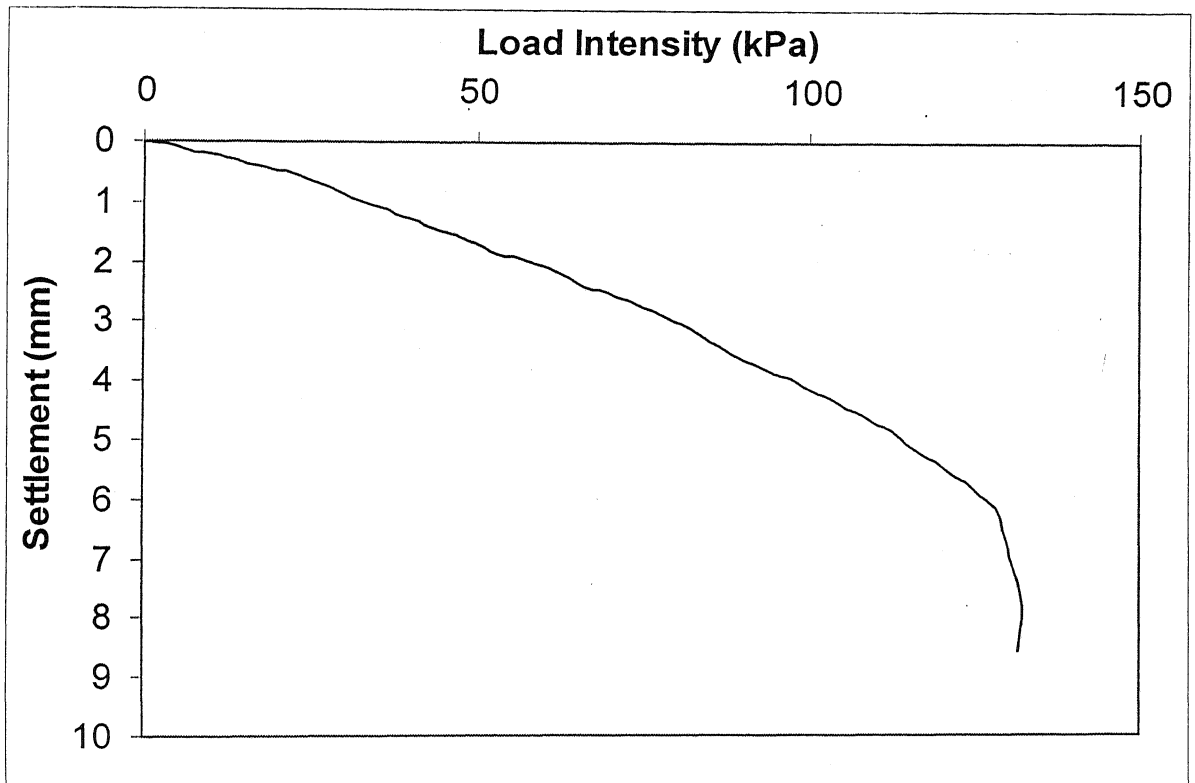


Fig. A.5: Load-Settlement Curve for GT-1 at  $u/B = 0.7$

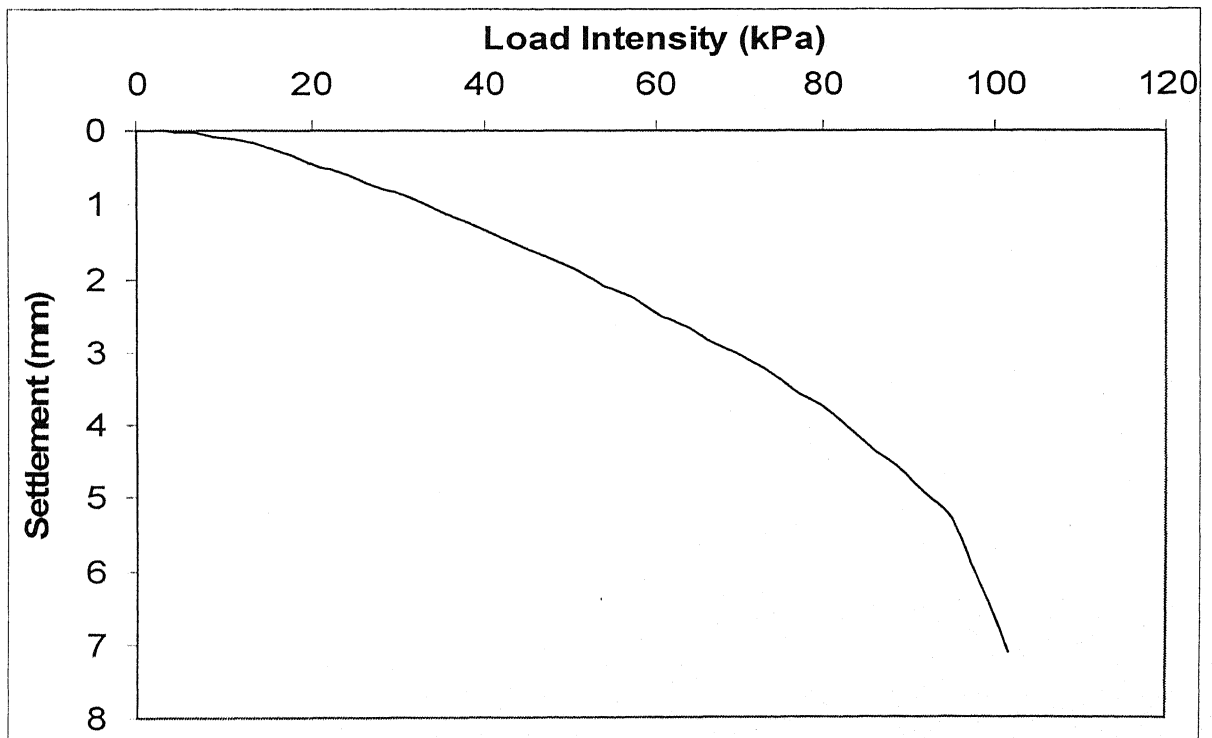


Fig. A.6: Load-Settlement Curve for GT-1 at  $u/B = 0.85$

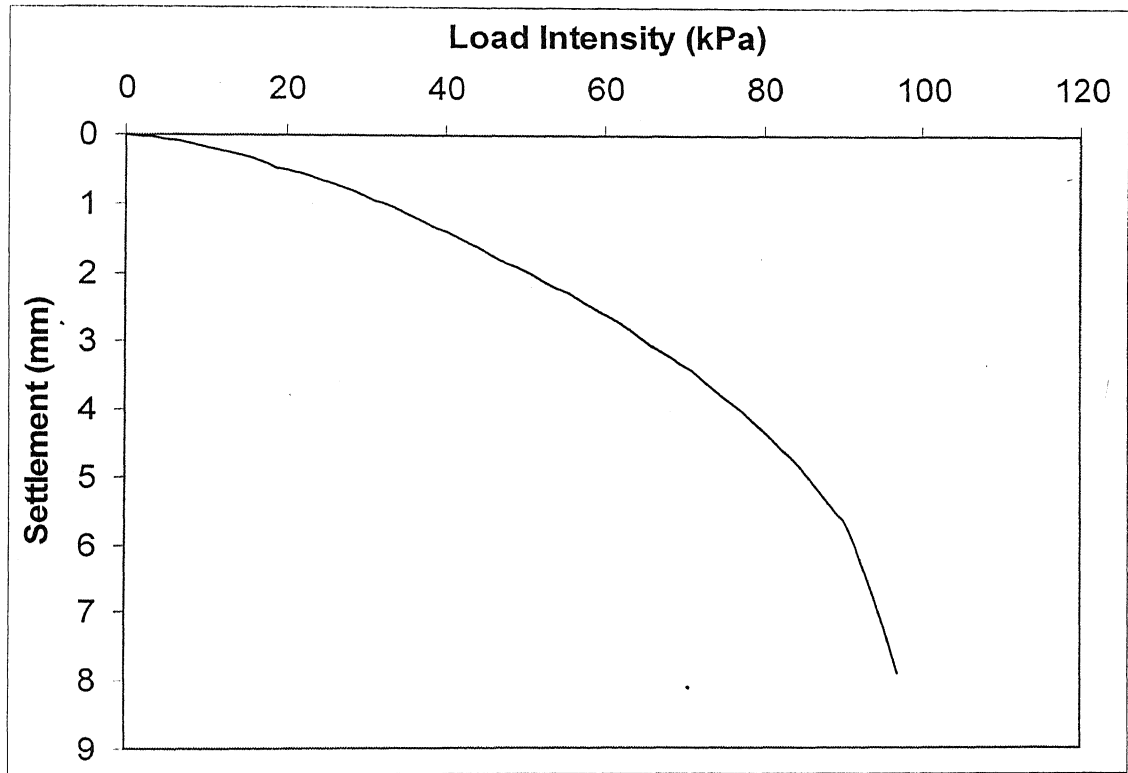


Fig. A.7: Load-Settlement Curve for GT-1 at  $u/B = 1.0$

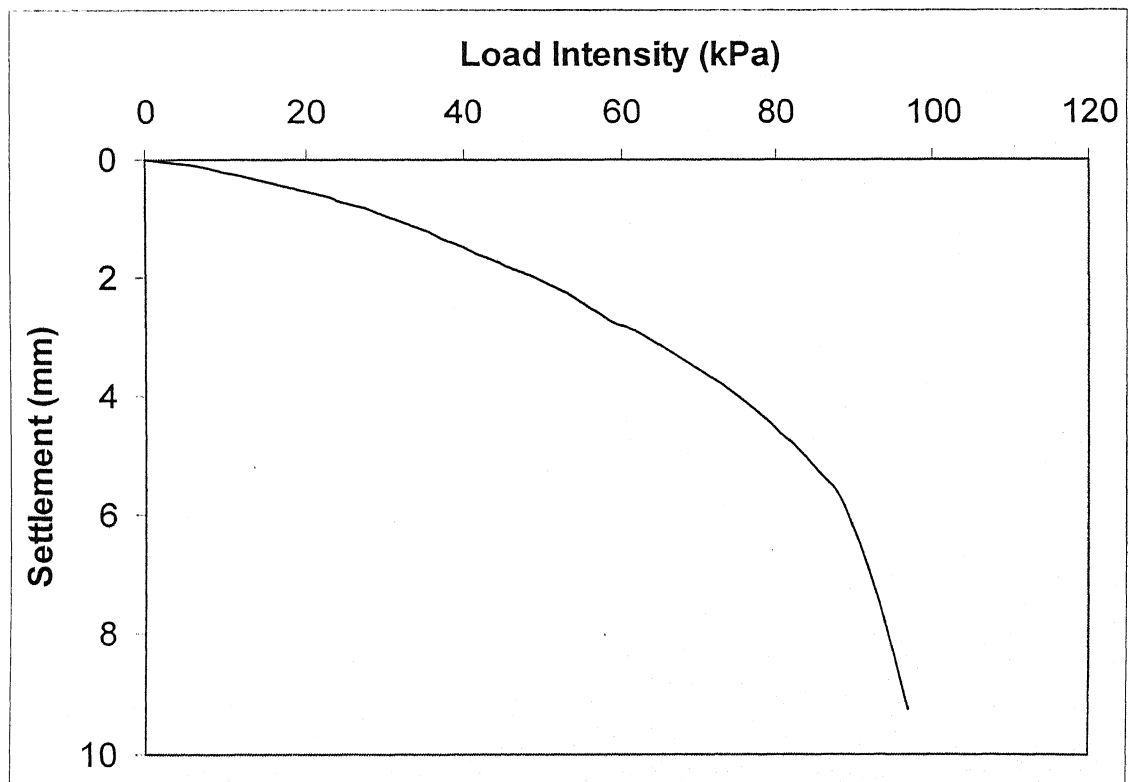


Fig. A.8 : Load-Settlement Curve for GT-1 at  $u/B = 1.2$

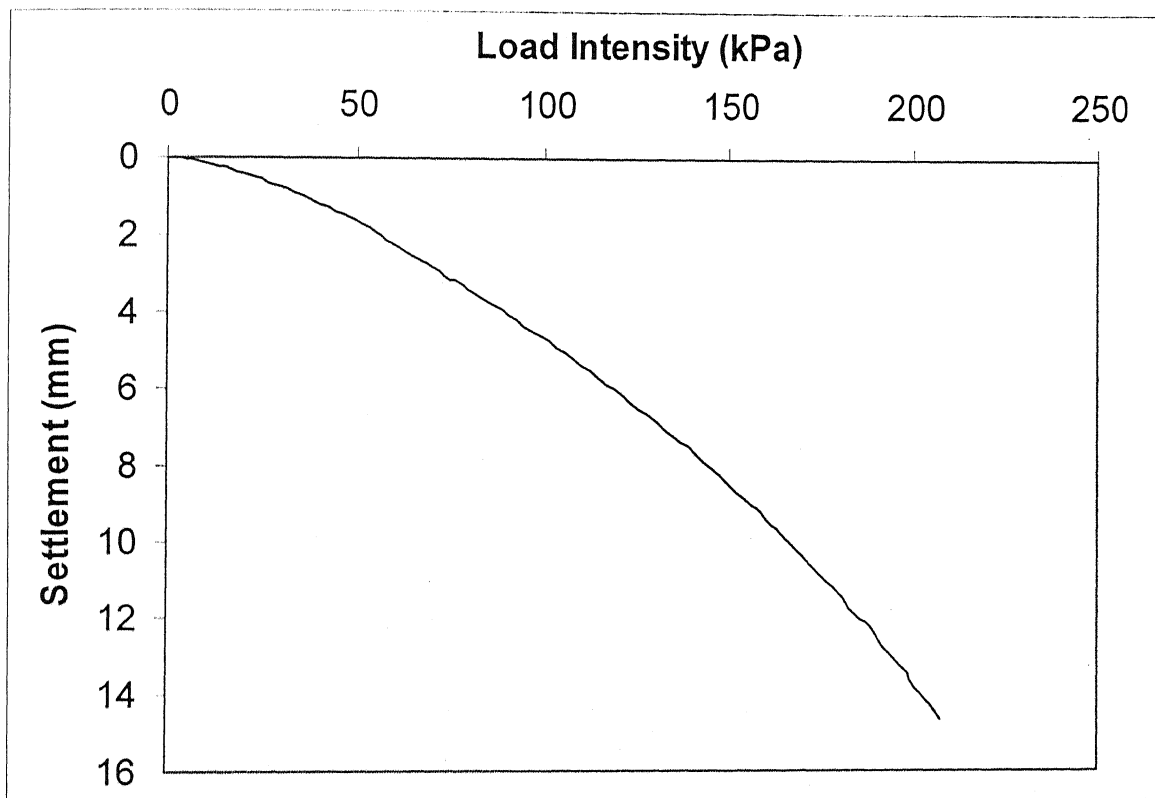


Fig. A.9: Load-Settlement Curve for GT-2 at  $u/B = 0.15$

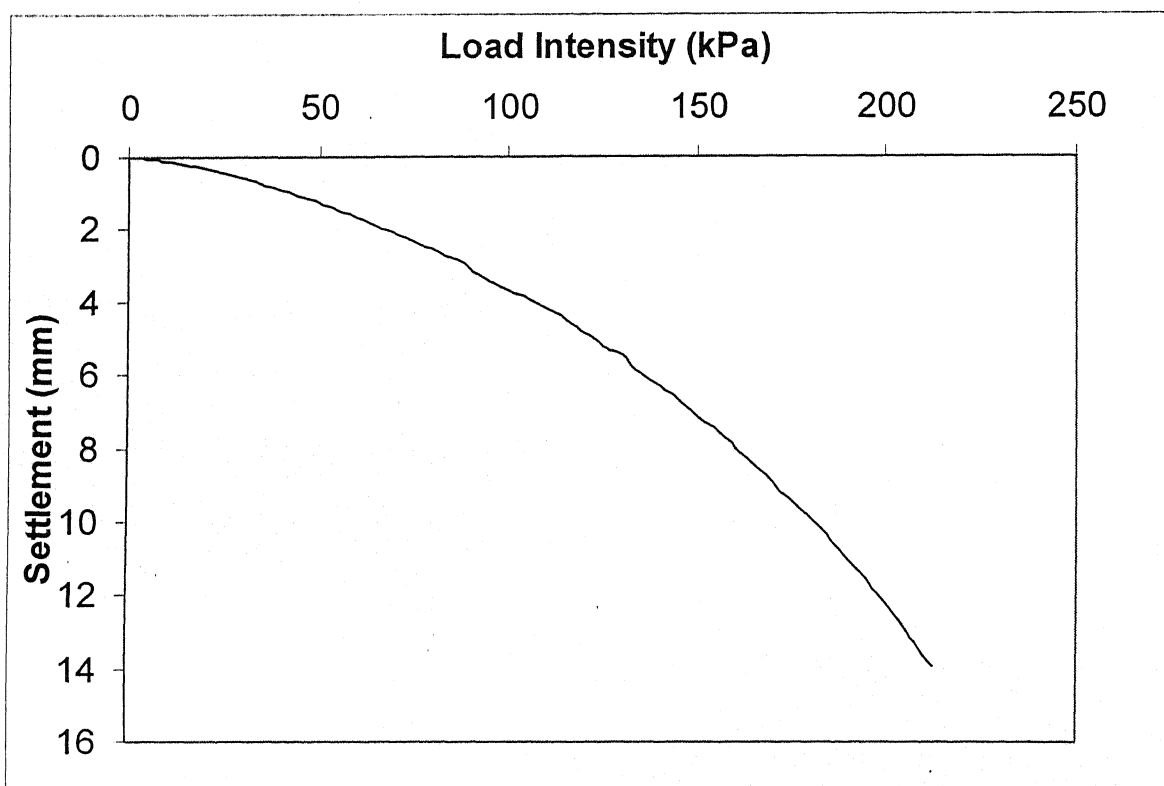
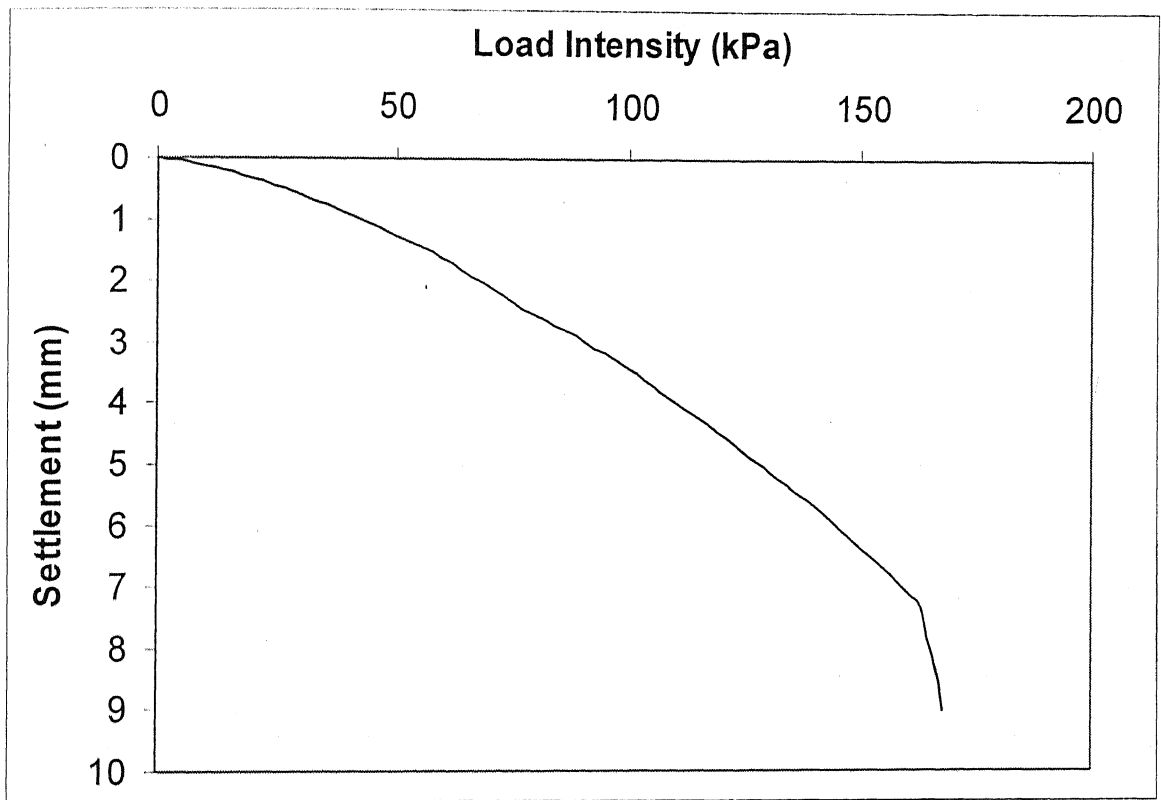
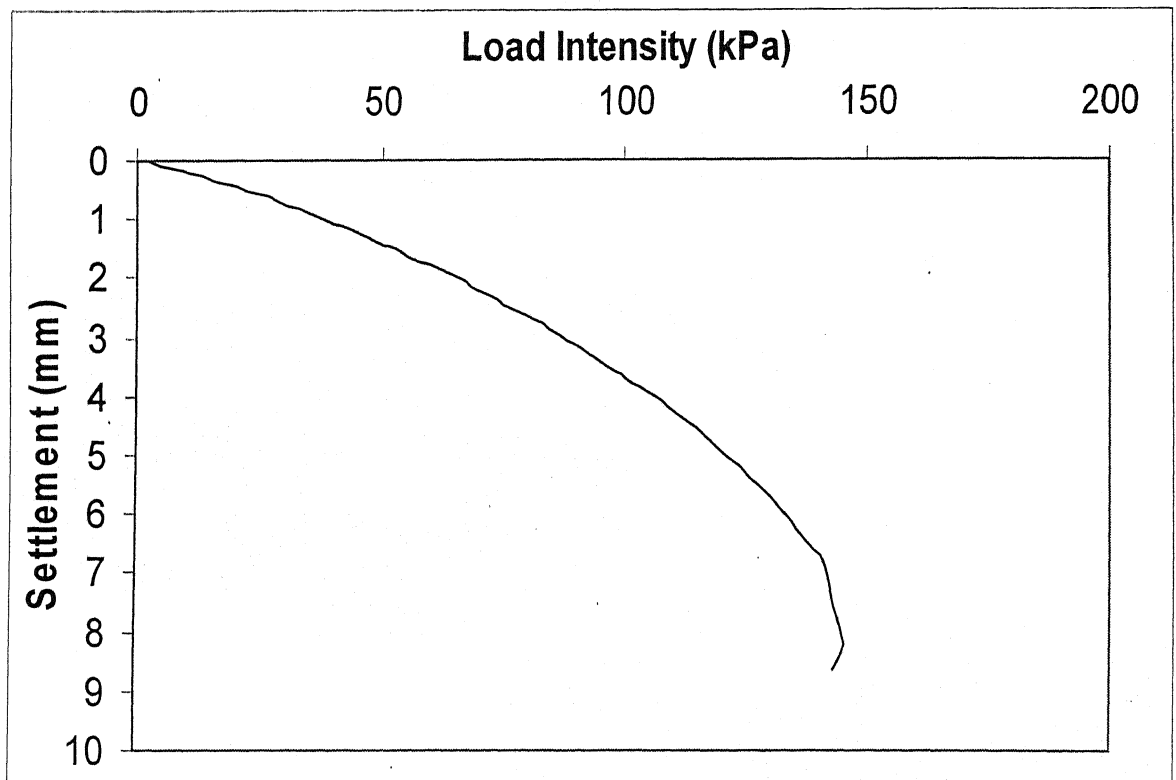


Fig. A.10: Load-Settlement Curve for GT-2 at  $u/B = 0.3$



**Fig. A.11:** Load-Settlement Curve for GT-2 at  $u/B = 0.5$



**Fig. A.12:** Load-Settlement Curve for GT-2 at  $u/B = 0.7$

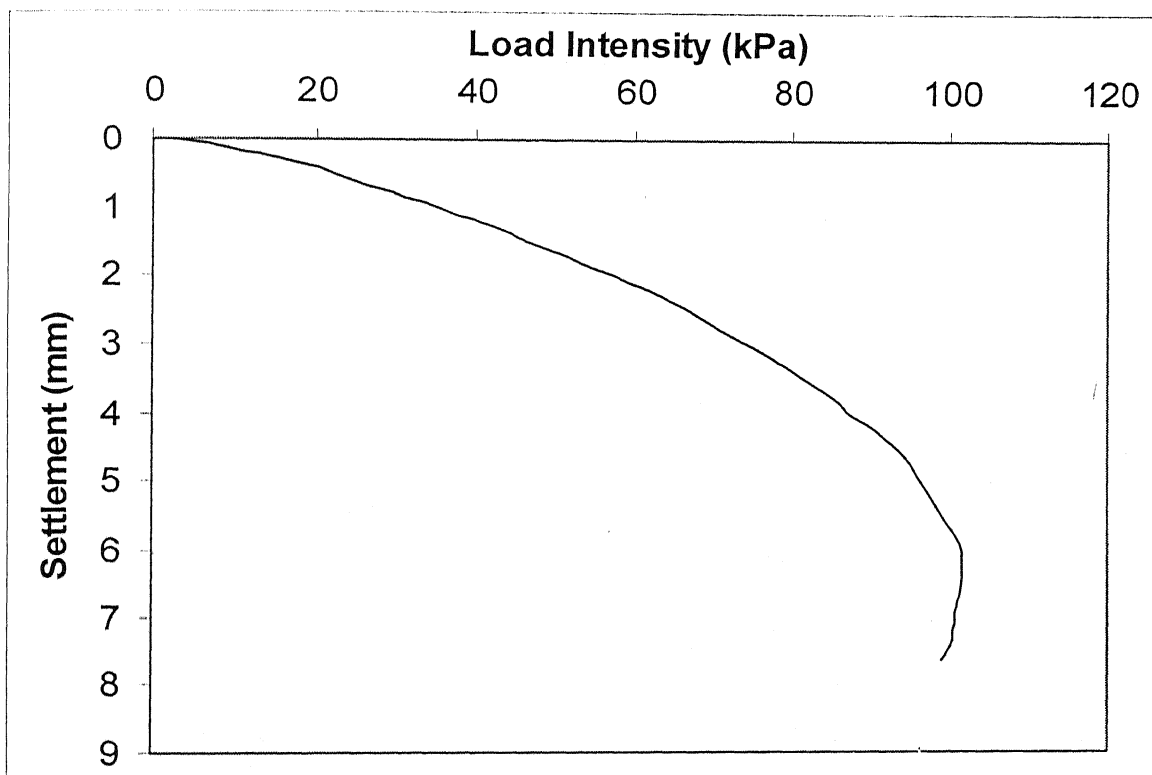


Fig. A.13: Load-Settlement Curve for GT-2 at  $u/B = 0.85$

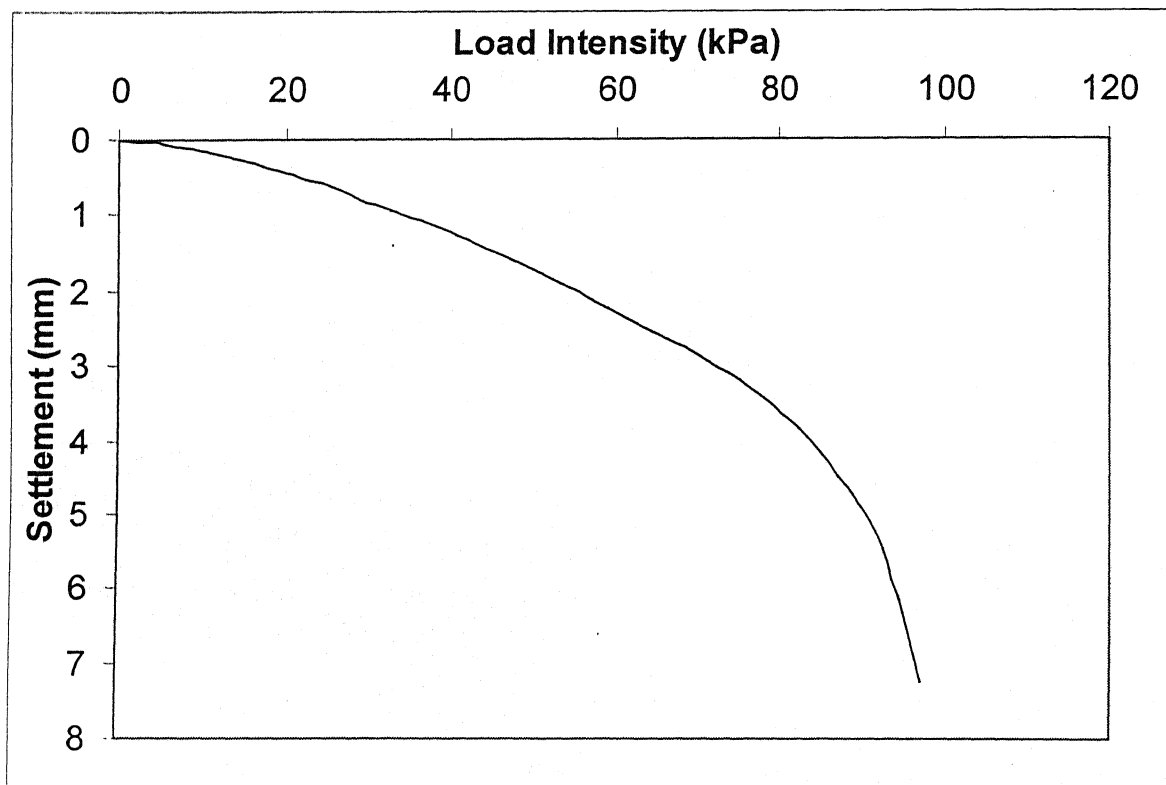


Fig. A.14: Load-Settlement Curve for GT-2 at  $u/B = 1.0$

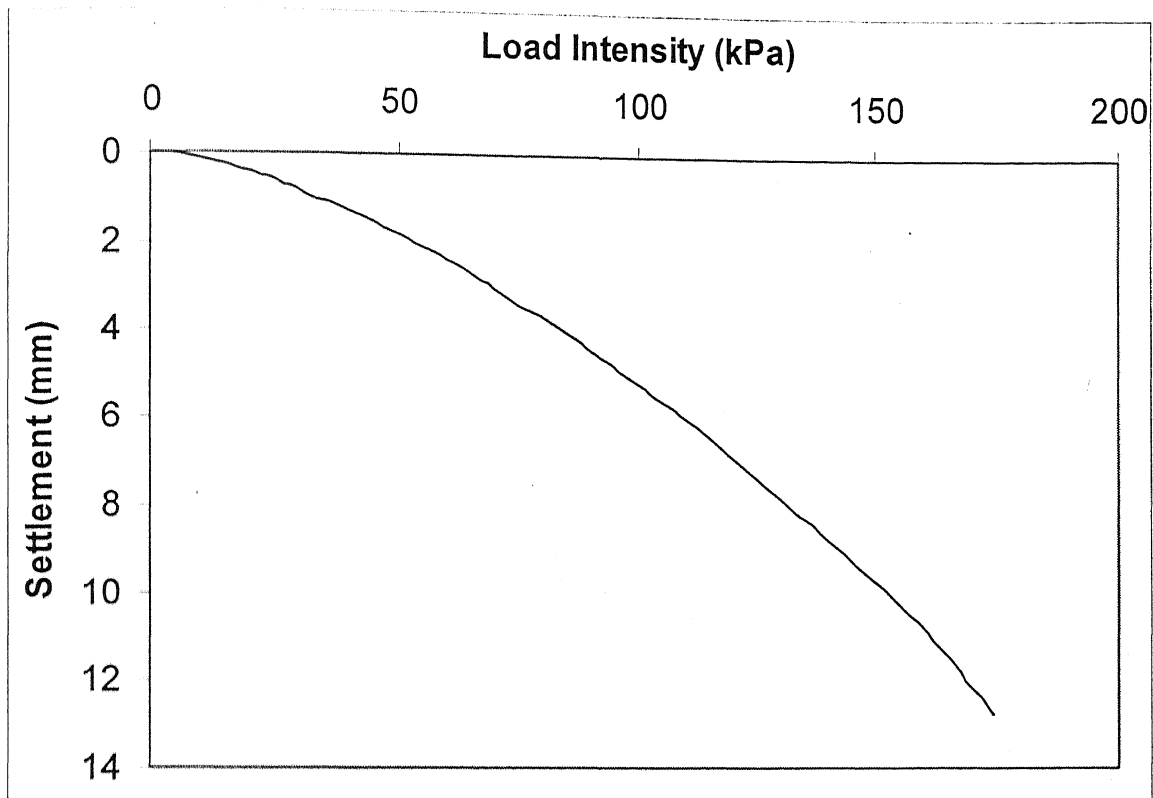


Fig. A.15: Load-Settlement curve for GG-1 at  $u/B = 0.15$

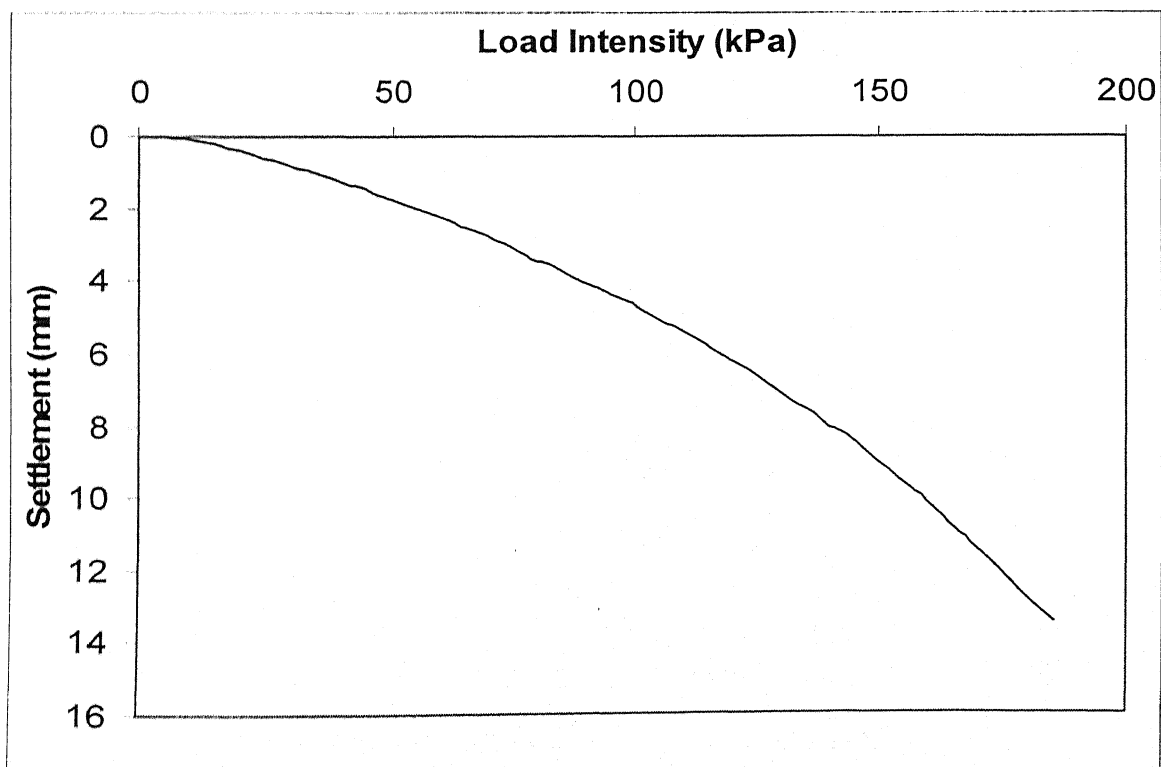


Fig. A.16: Load-Settlement curve for GG-1 at  $u/B = 0.3$

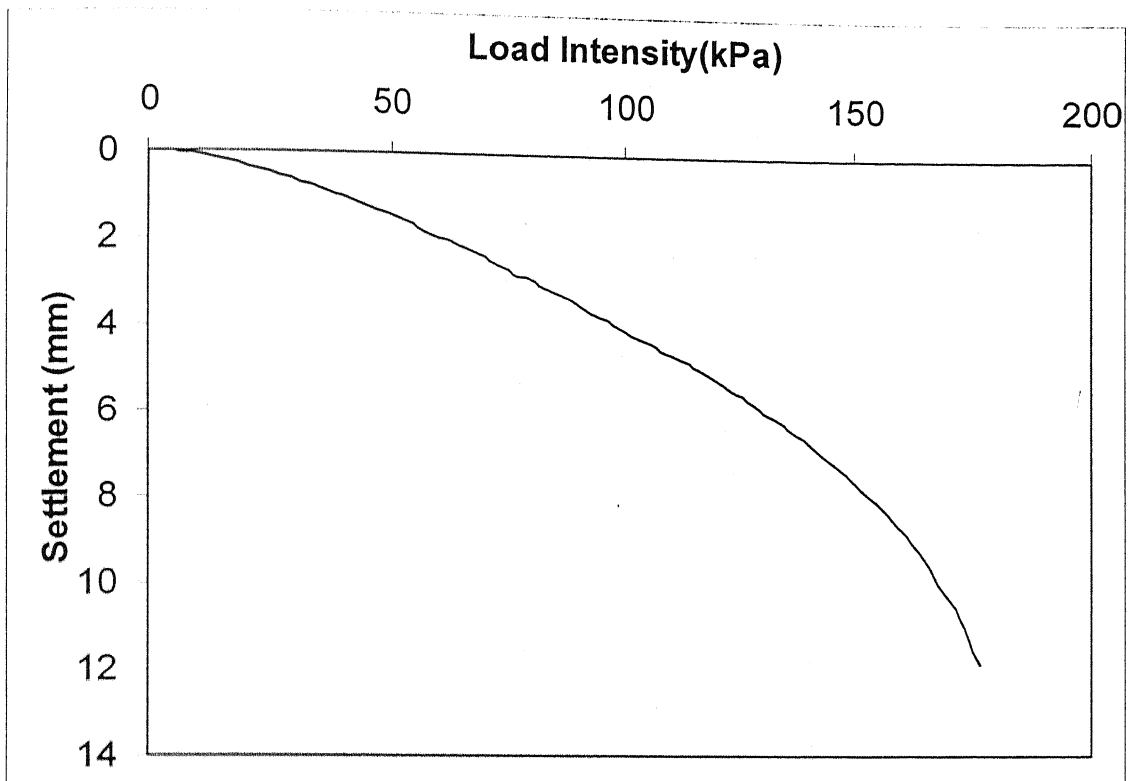


Fig. A.17: Load-Settlement curve for GG-1 at  $u/B = 0.5$

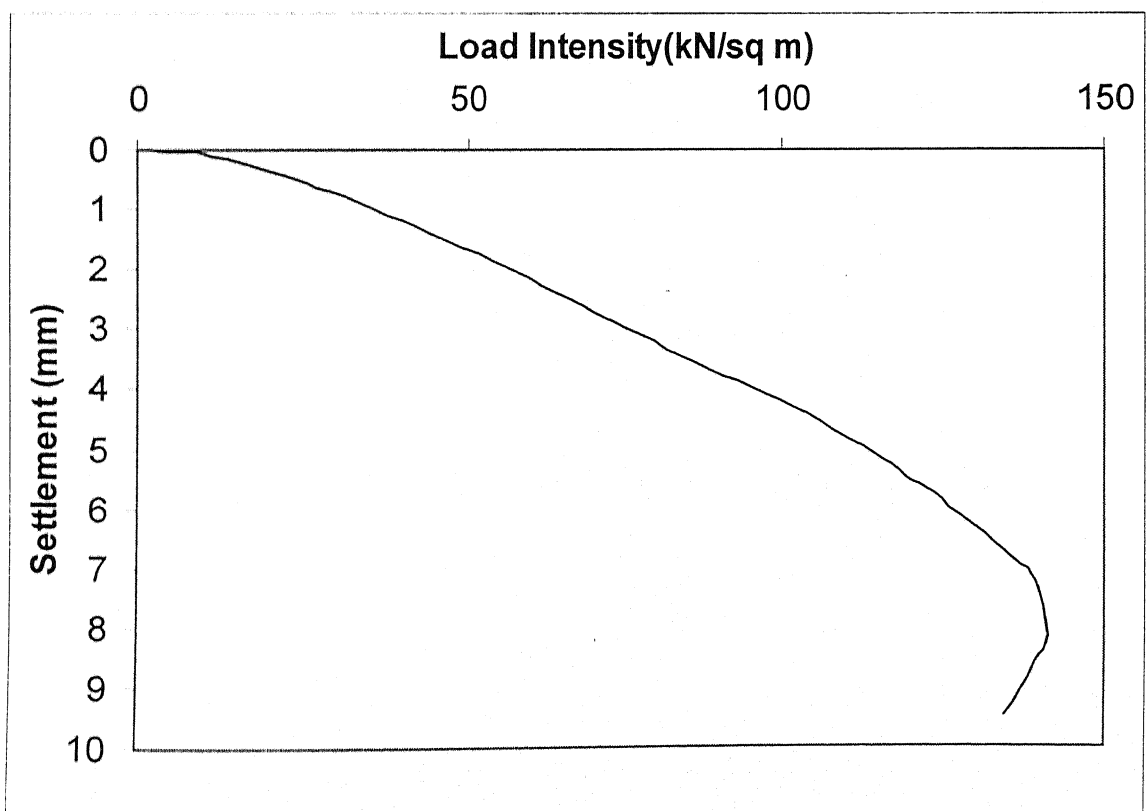


Fig. A.18: Load-Settlement curve for GG-1 at  $u/B = 0.7$



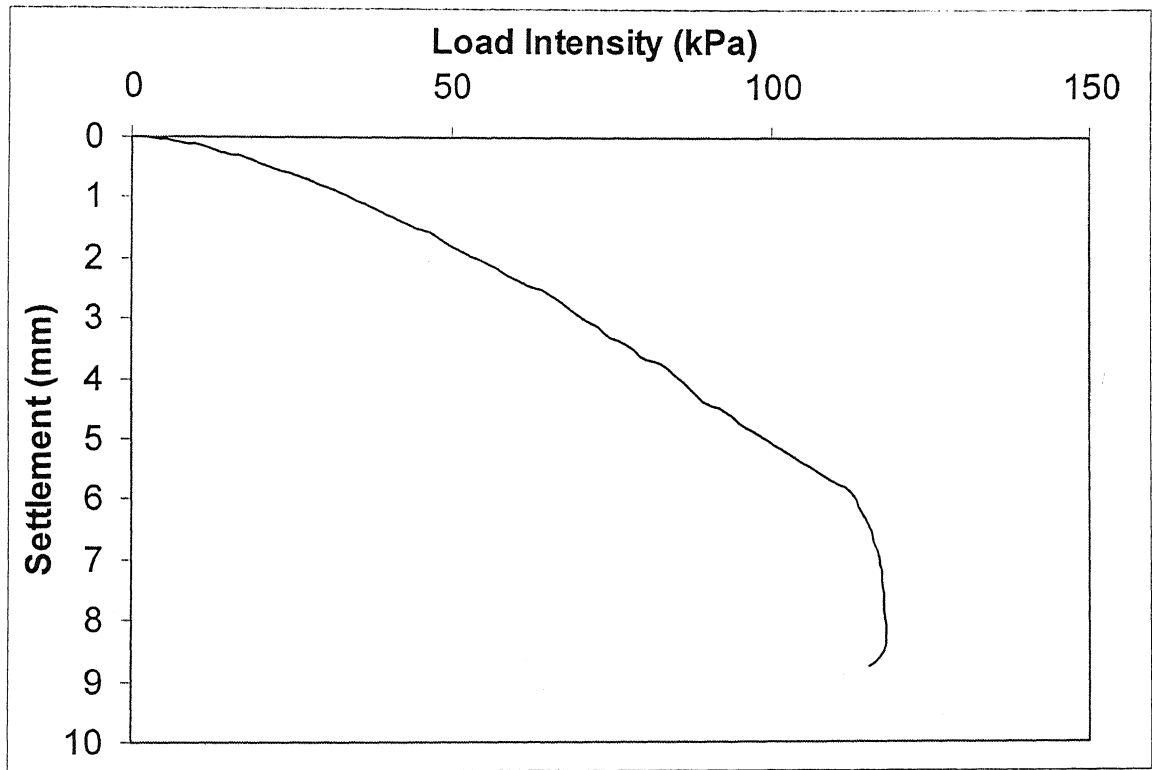


Fig. A.19: Load-Settlement curve for GG-1 at  $u/B = 0.85$

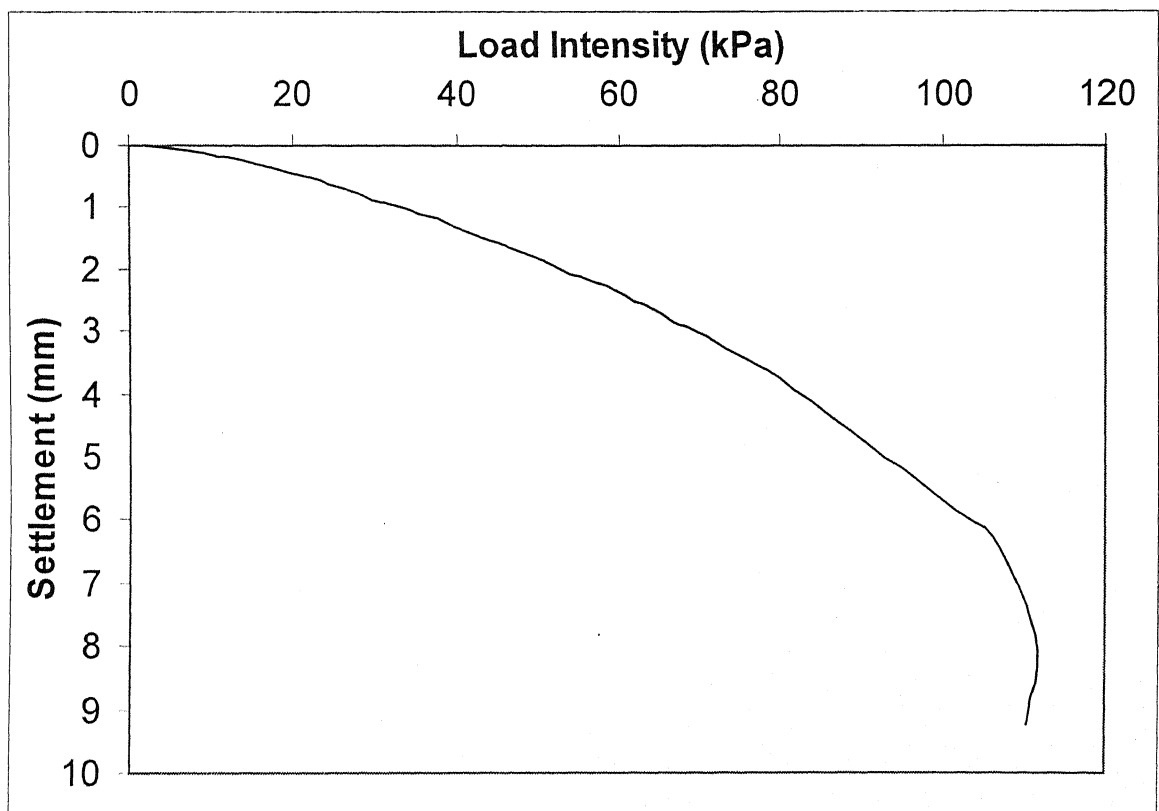
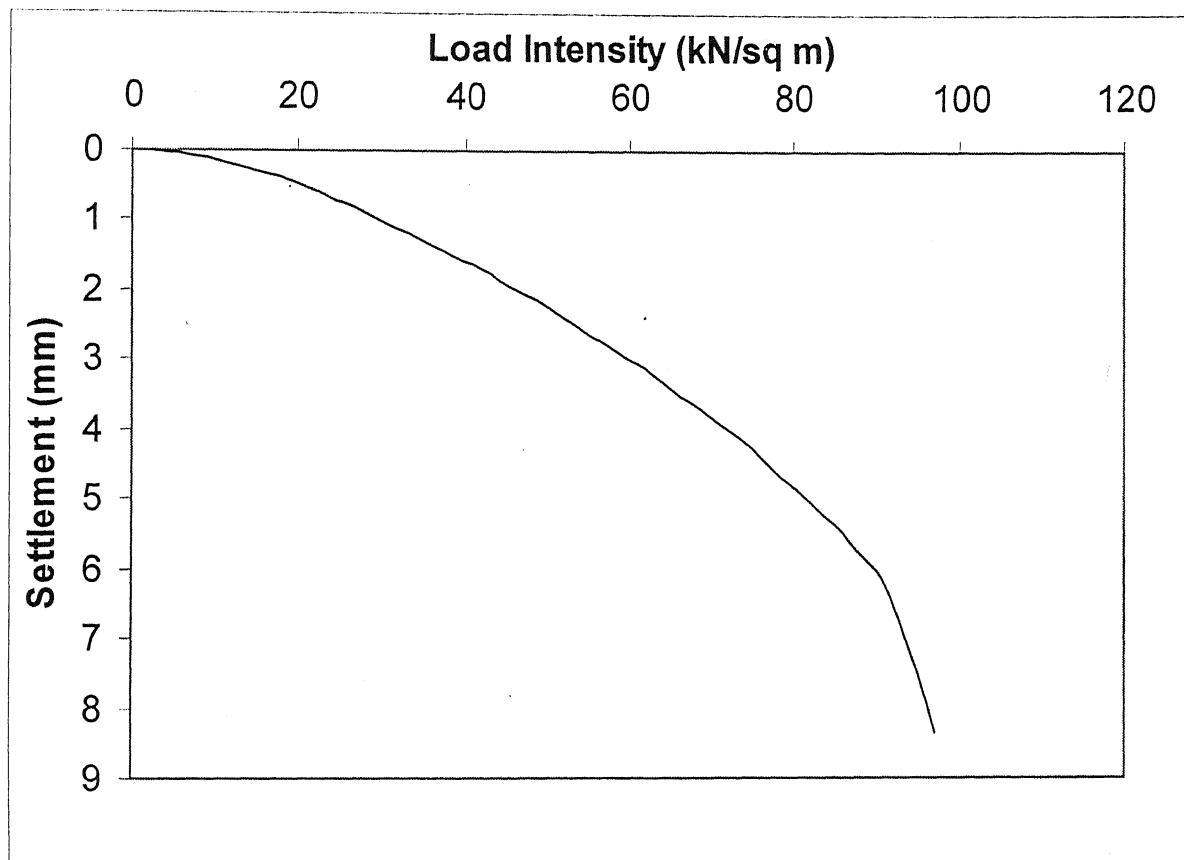


Fig. A.20: Load-Settlement curve for GG-1 at  $u/B = 1.0$



**Fig. A.21:** Load-Settlement curve for GG-1 at  $u/B = 1.2$

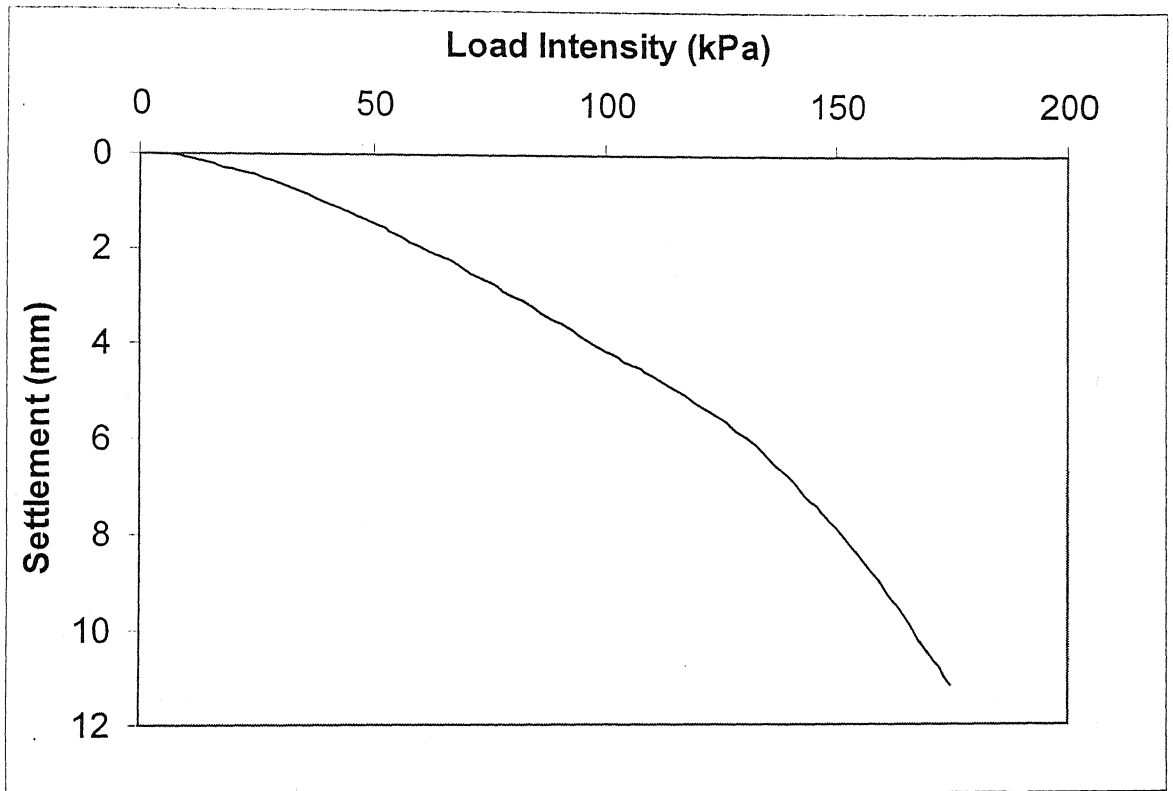


Fig. A.22: Load-Settlement Curve for GG-2 at  $u/B = 0.15$

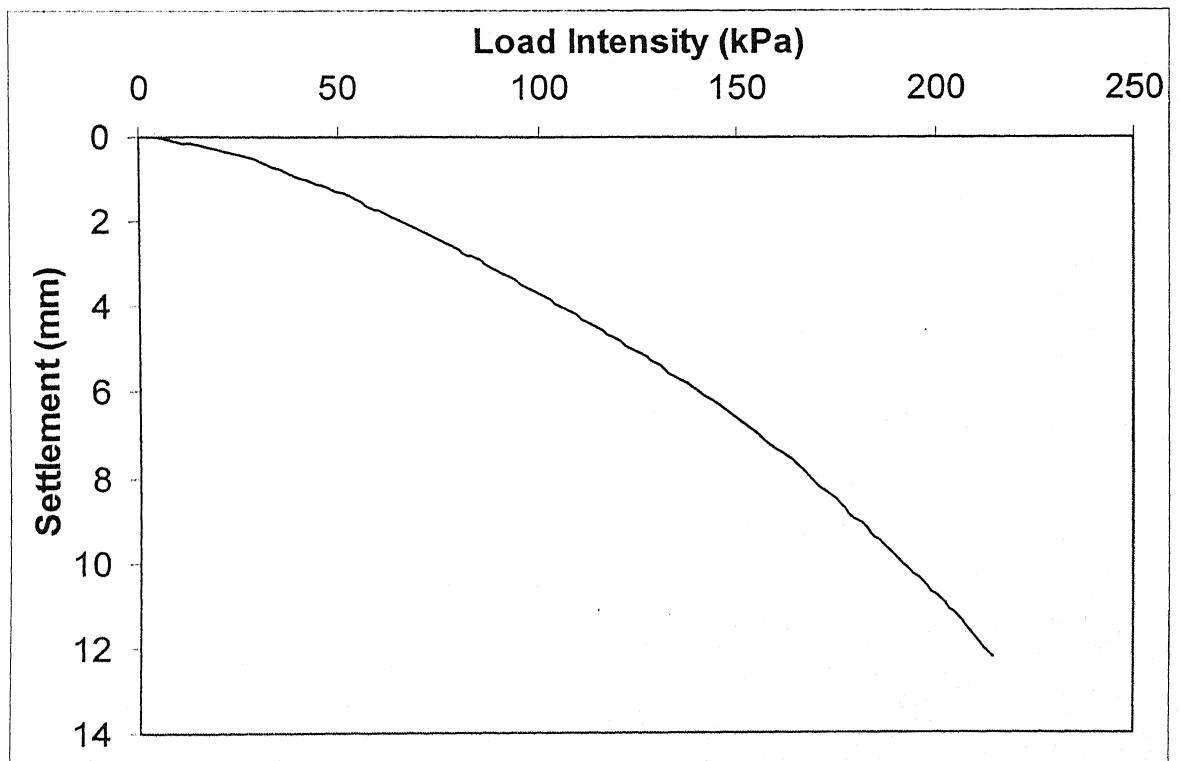


Fig. A.23: Load-Settlement Curve for GG-2 at  $u/B = 0.3$

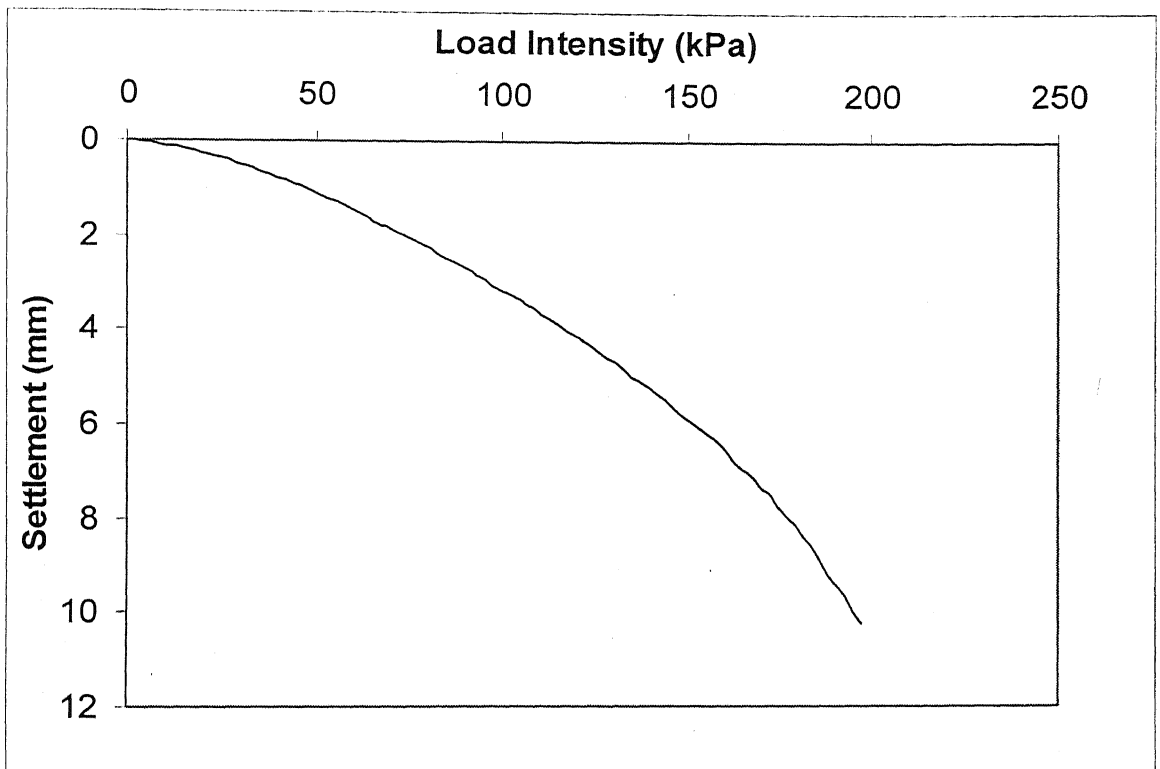


Fig. A.24: Load-Settlement Curve for GG-2 at  $u/B = 0.5$

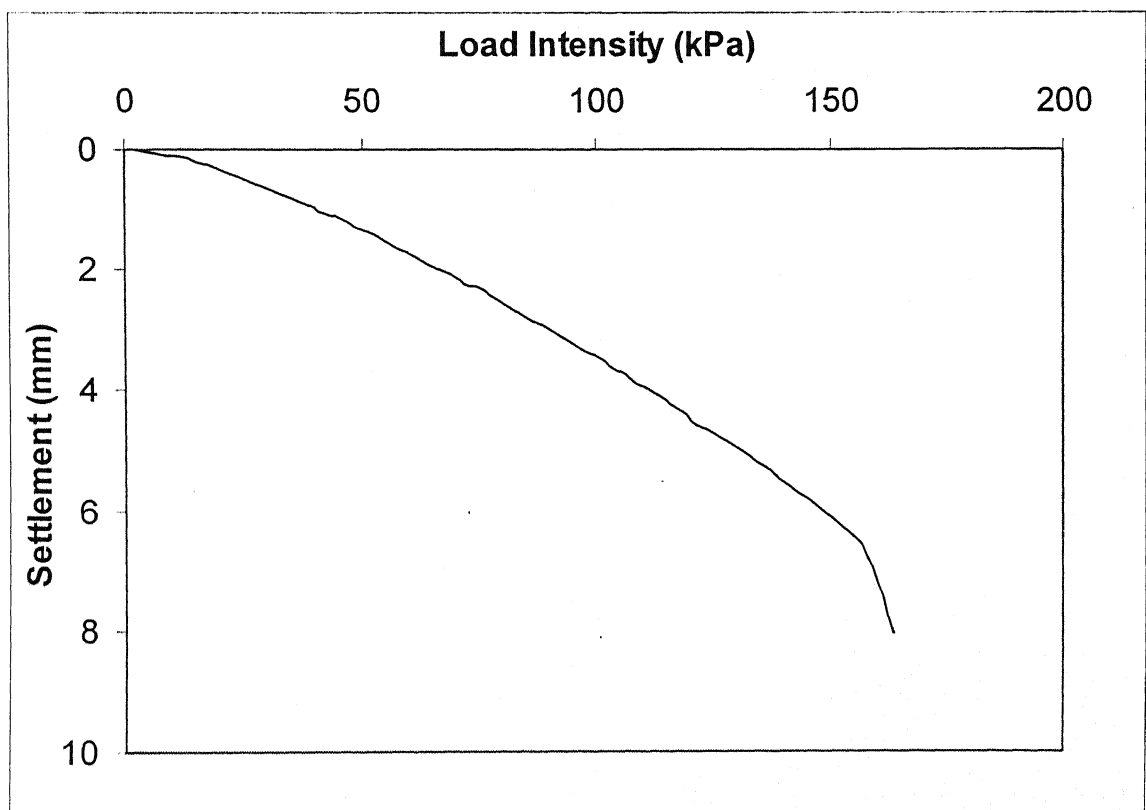


Fig. A.25: Load-Settlement Curve for GG-2 at  $u/B = 0.7$

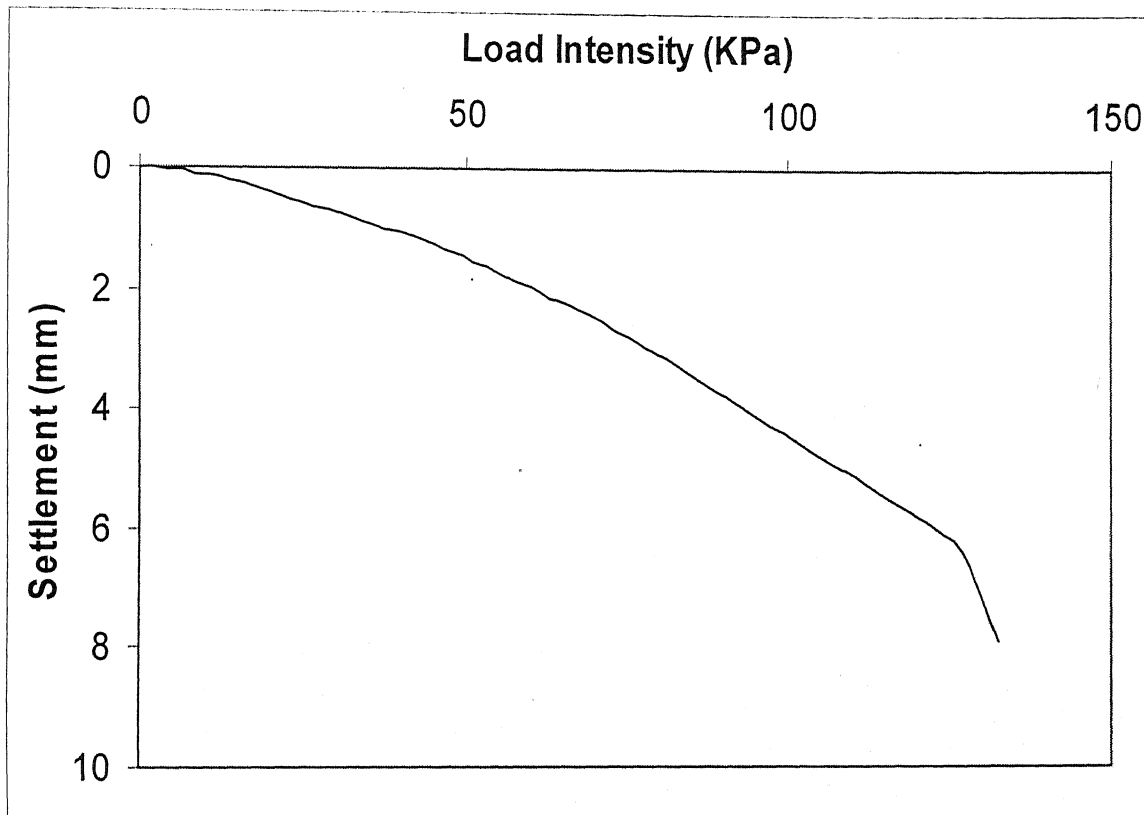


Fig. A.26: Load-Settlement Curve for GG-2 at  $u/B = 0.85$

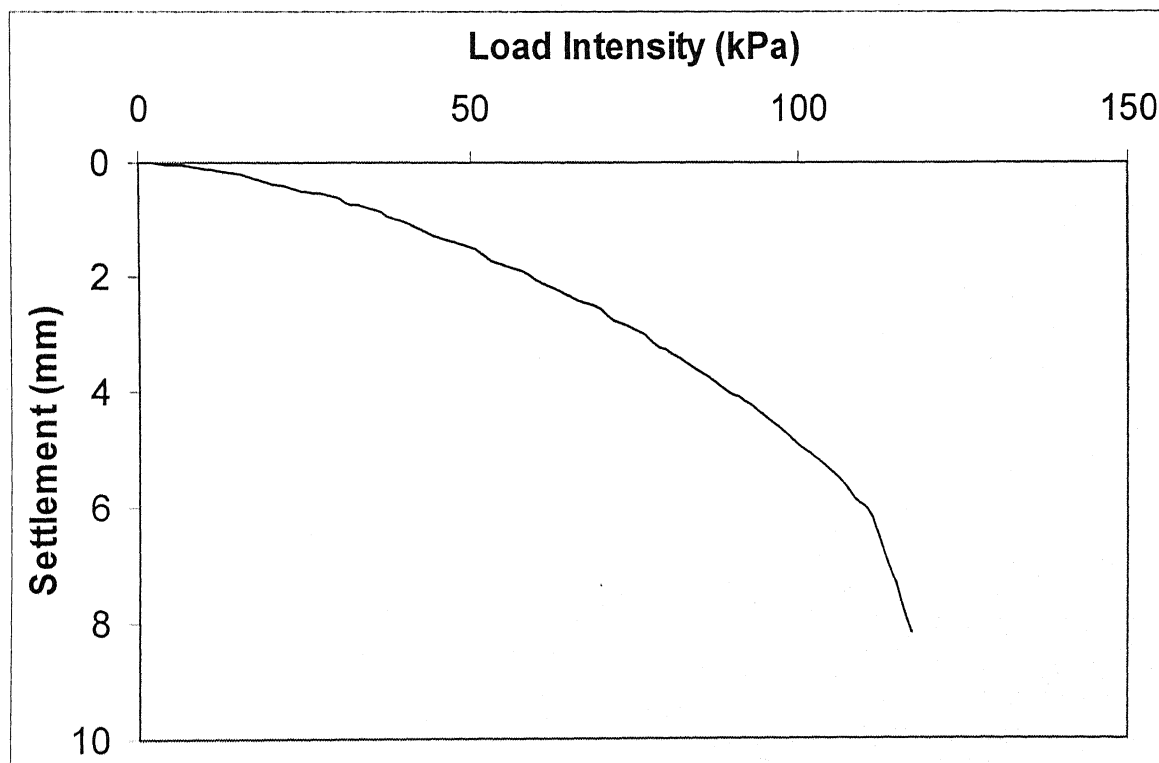


Fig. A.27: Load-Settlement Curve for GG-2 at  $u/B = 1.0$

**Table A.1**

Ultimate Bearing Capacity and Bearing Capacity Ratio  
at Different Depth Ratios ( $u/B$ ) for GT-1, GT-2, GG-1 and GG-2

$u/B$	GT-1		GT-2		GG-1		GG-2	
	$q_{u(R)}$	$BCR_u$	$q_{u(R)}$	$BCR_u$	$q_{u(R)}$	$BCR_u$	$q_{u(R)}$	$BCR_u$
0.15	126.70	1.508	143.9	1.713	128.36	1.528	135	1.607
0.3	130.80	1.557	154	1.833	133	1.583	146.4	1.743
0.5	139.60	1.662	163.54	1.947	150	1.786	167.6	1.995
0.7	128.20	1.526	141.44	1.684	139.2	1.657	156.9	1.868
0.85	95.00	1.131	101.7	1.211	112.7	1.342	126	1.500
1	90.61	1.079	92.82	1.105	106.1	1.263	110.5	1.315
1.2	88.40	1.052	—	—	90.61	1.079	—	—

## APPENDIX-B

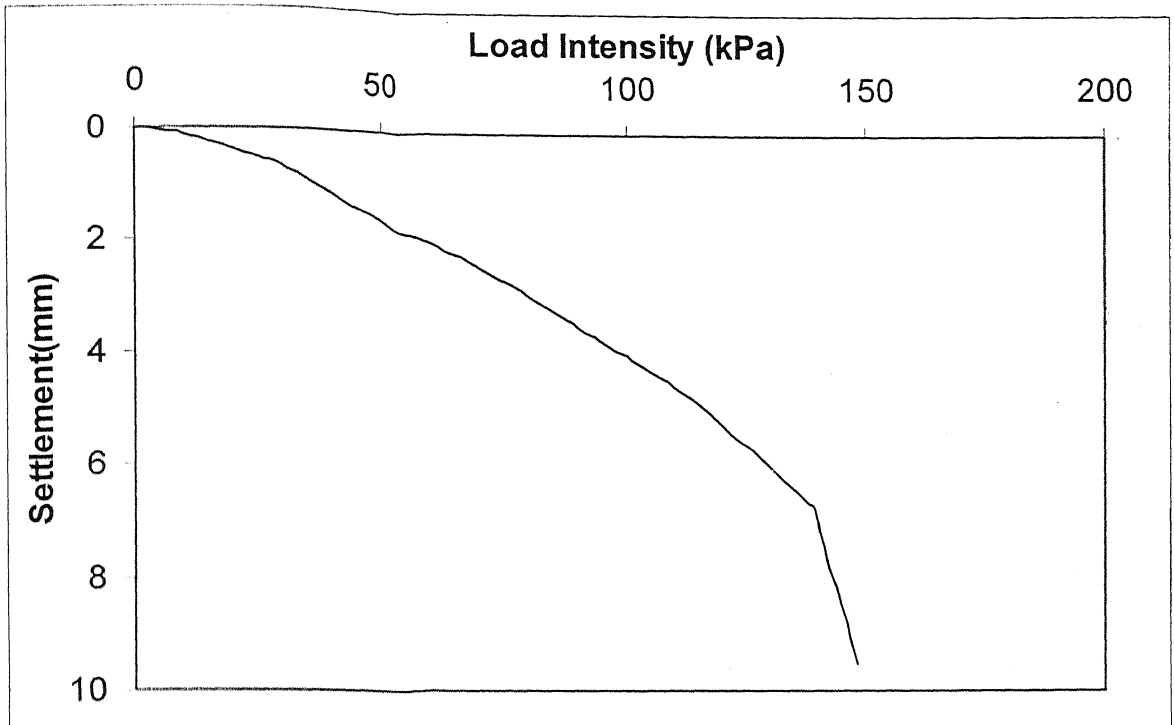


Fig.B.1: Load-Settlement Curve for One Layer for GT-1 at  $u/B = 0.5$  and  $h/B = 0$

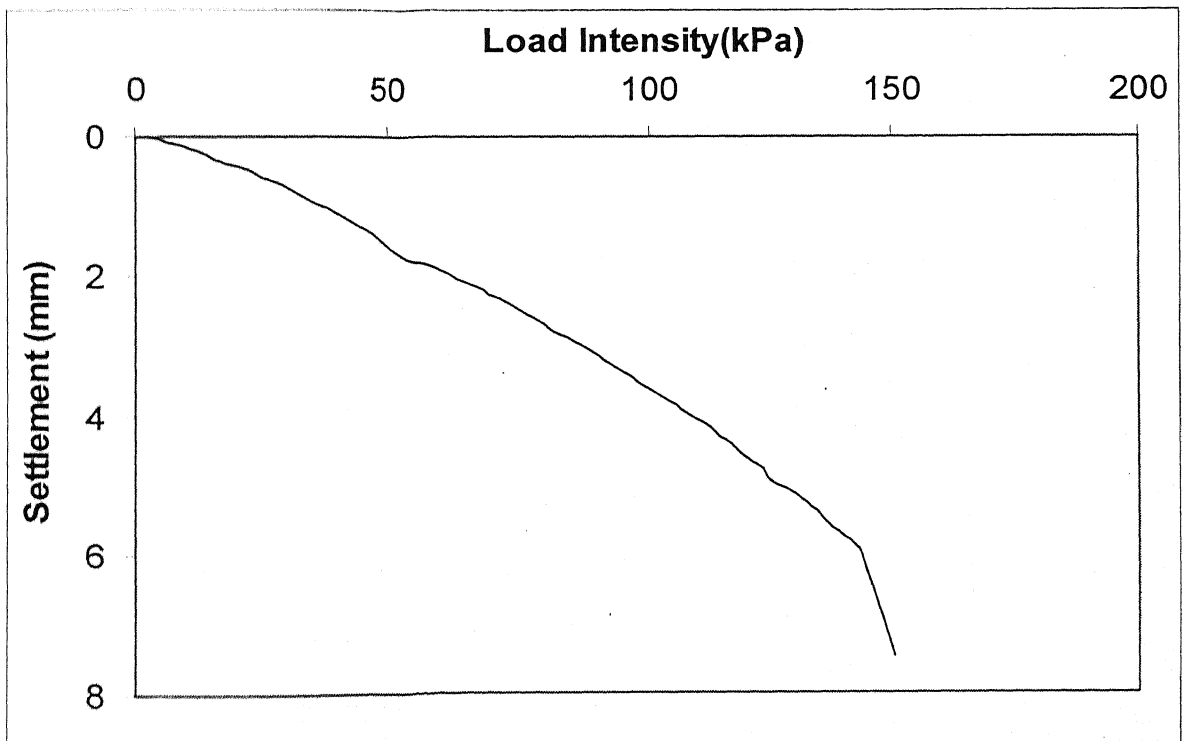
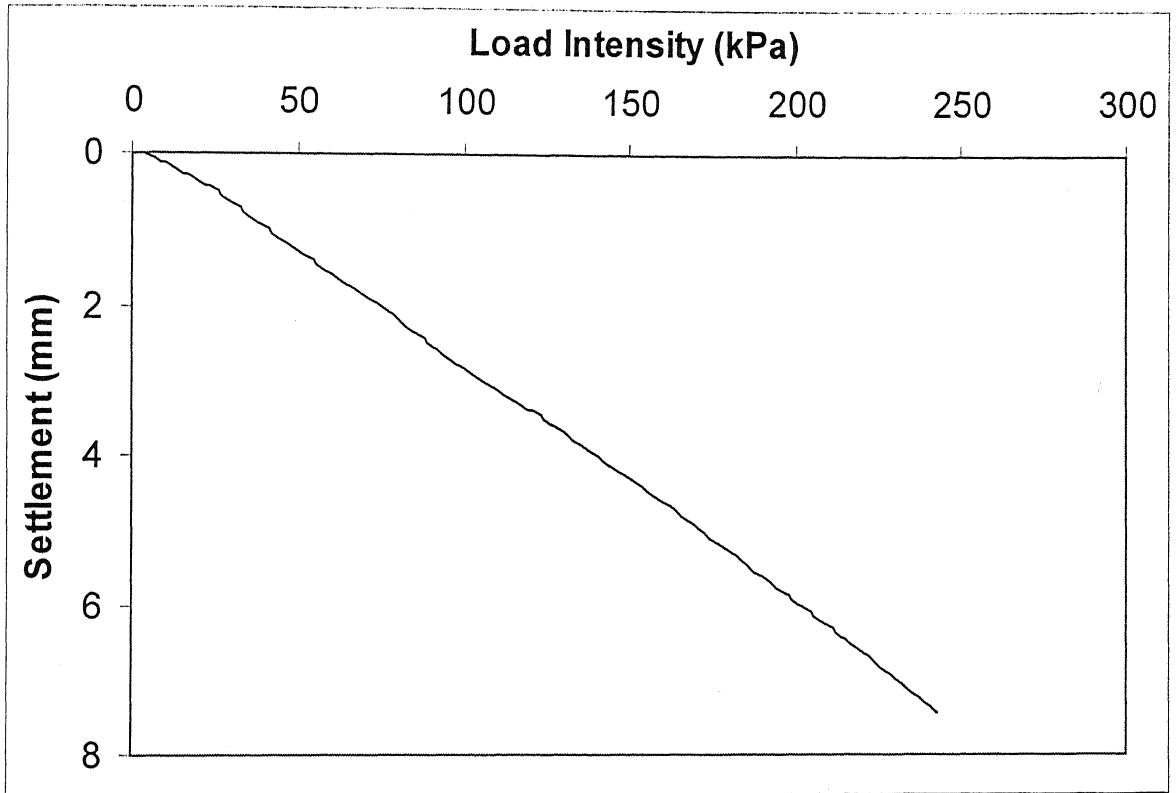
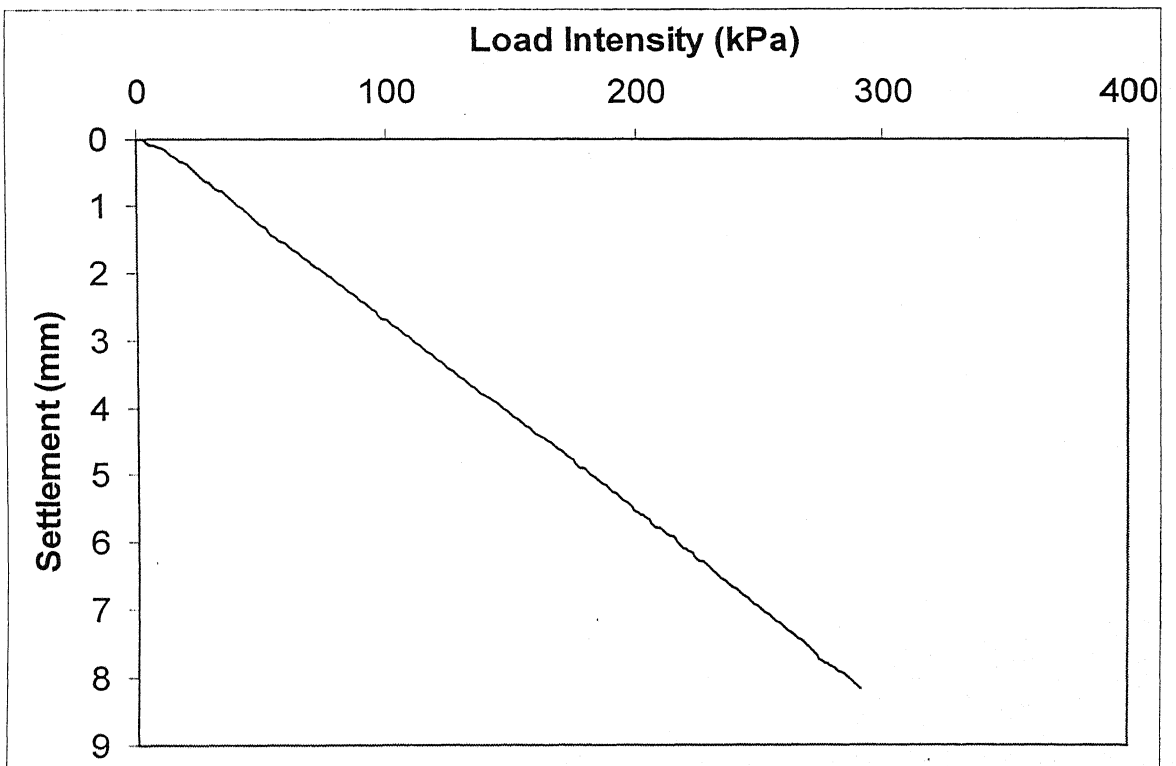


Fig.B.2: Load-Settlement Curve for Two Layers for GT-1 at  $u/B = h/B = 0.5$



**Fig.B.3:** Load-Settlement Curve for Three Layers for GT-1 at  $u/B = h/B = 0.33$



**Fig.B.4:** Load-Settlement Curve for Four Layers for GT-1 at  $u/B = h/B = 0.25$



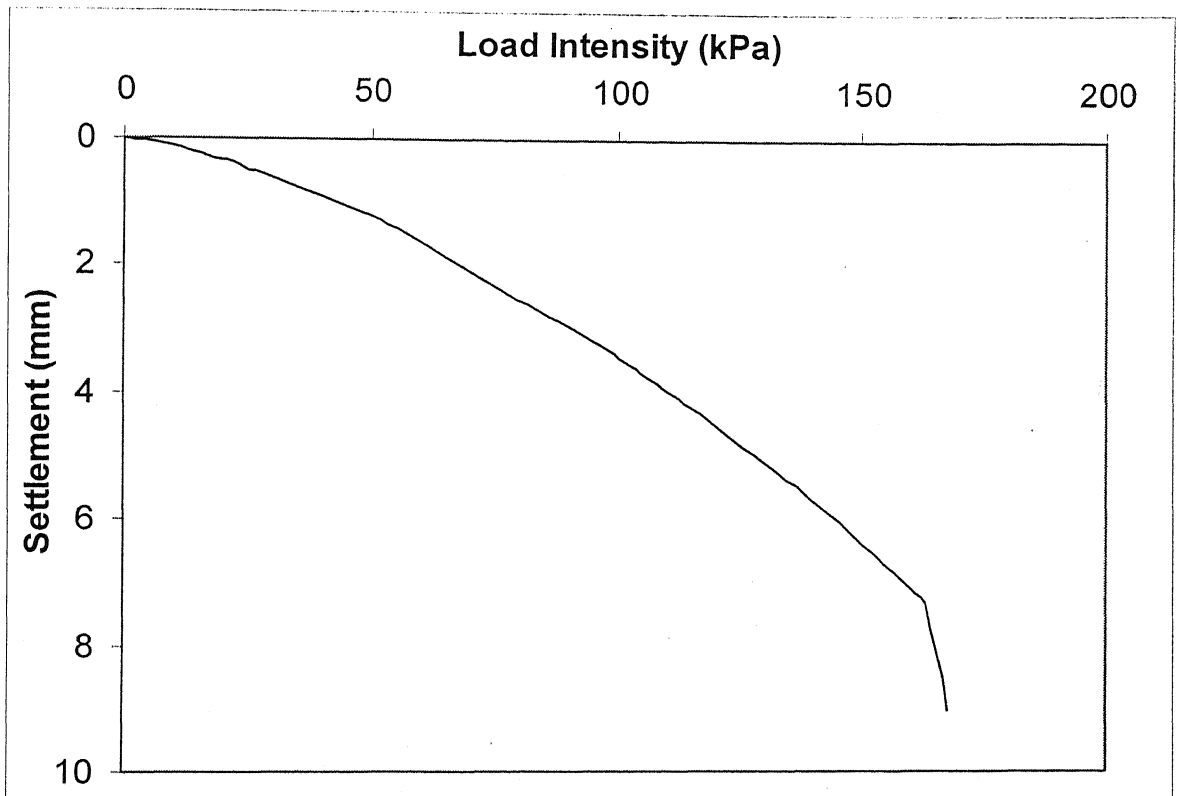


Fig.B.5: Load-Settlement Curve for One Layer for GT-2 at  $u/B = 0.5$  and  $h/B = 0$

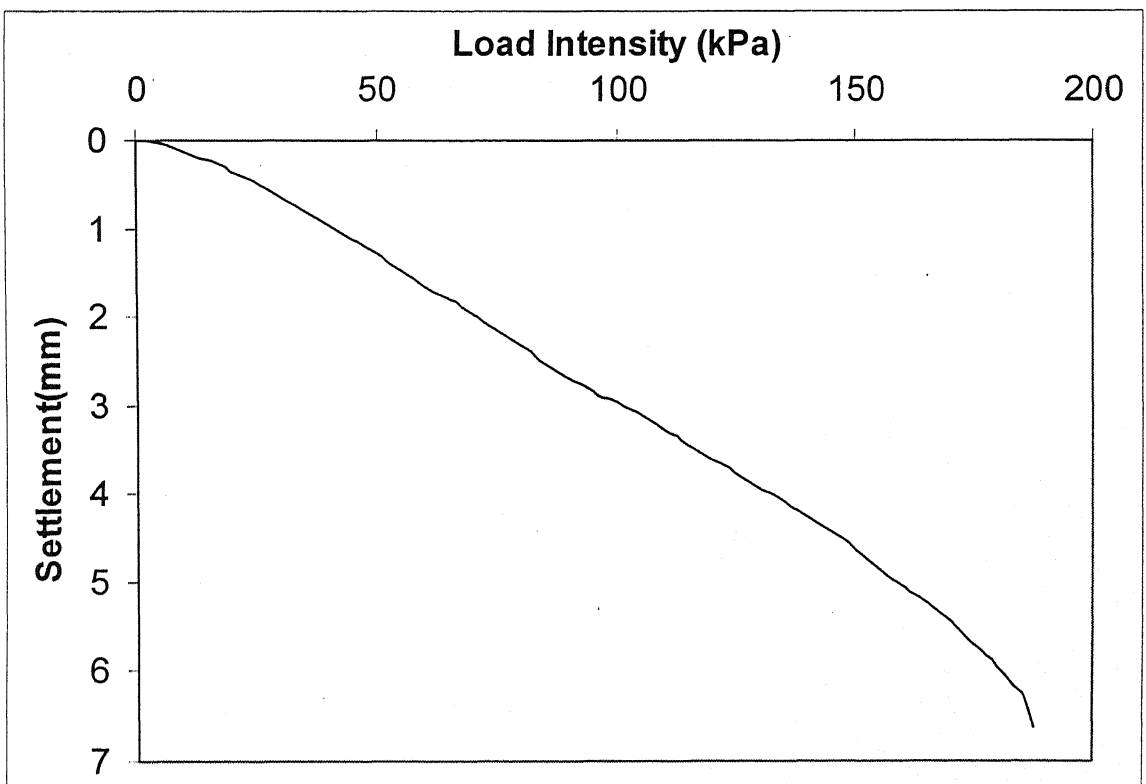
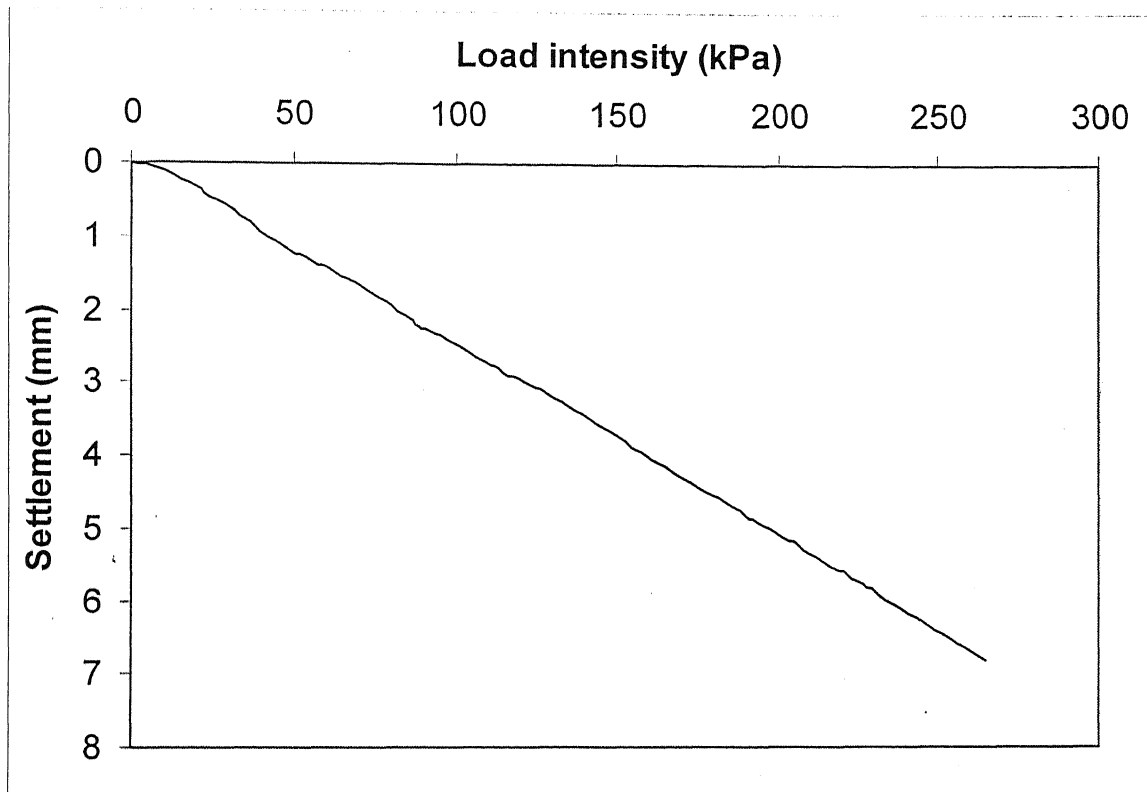
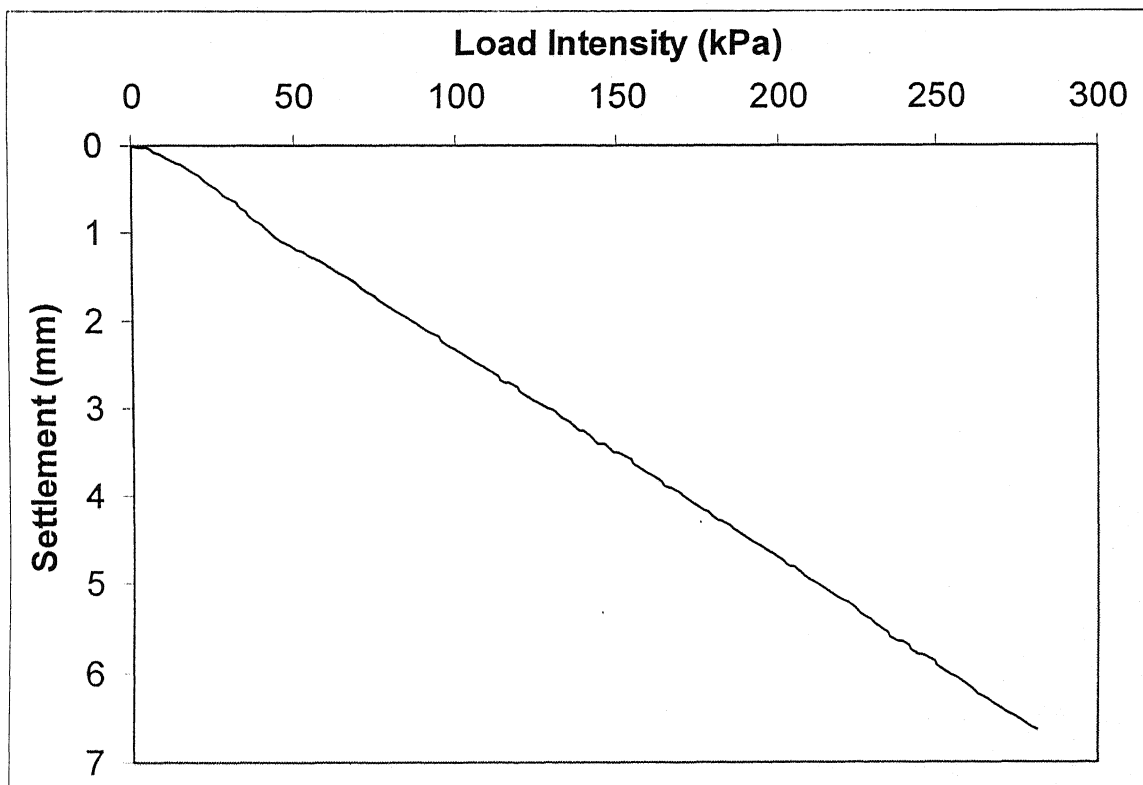


Fig.B.6: Load-Settlement Curve for Two Layers for GT-2 at  $u/B = h/B = 0.5$



**Fig.B.7:** Load-Settlement Curve for Three Layers for GT-2 at  $u/B = h/B = 0.33$



**Fig.B.8:** Load-Settlement Curve for Four Layers for GT-2 at  $u/B = h/B = 0.25$

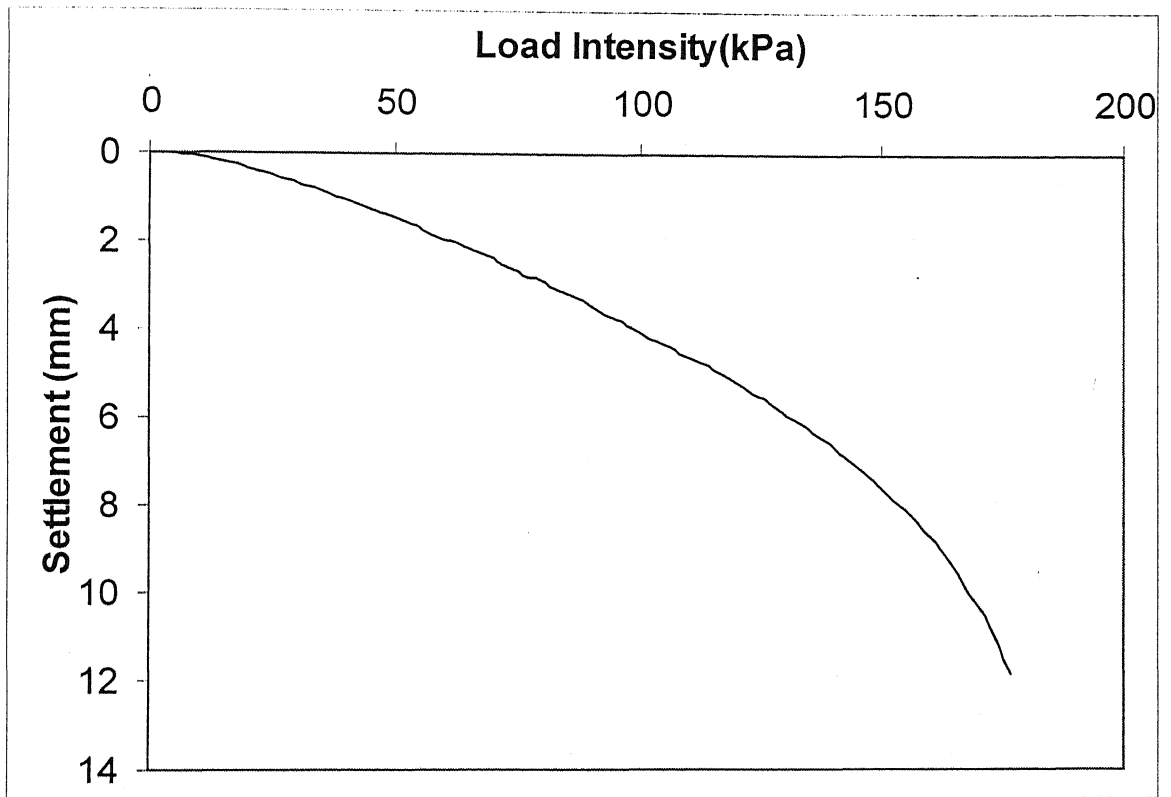


Fig.B.9: Load-Settlement Curve for One Layer for GG-1 at  $u/B = 0.5$  and  $h/B = 0$

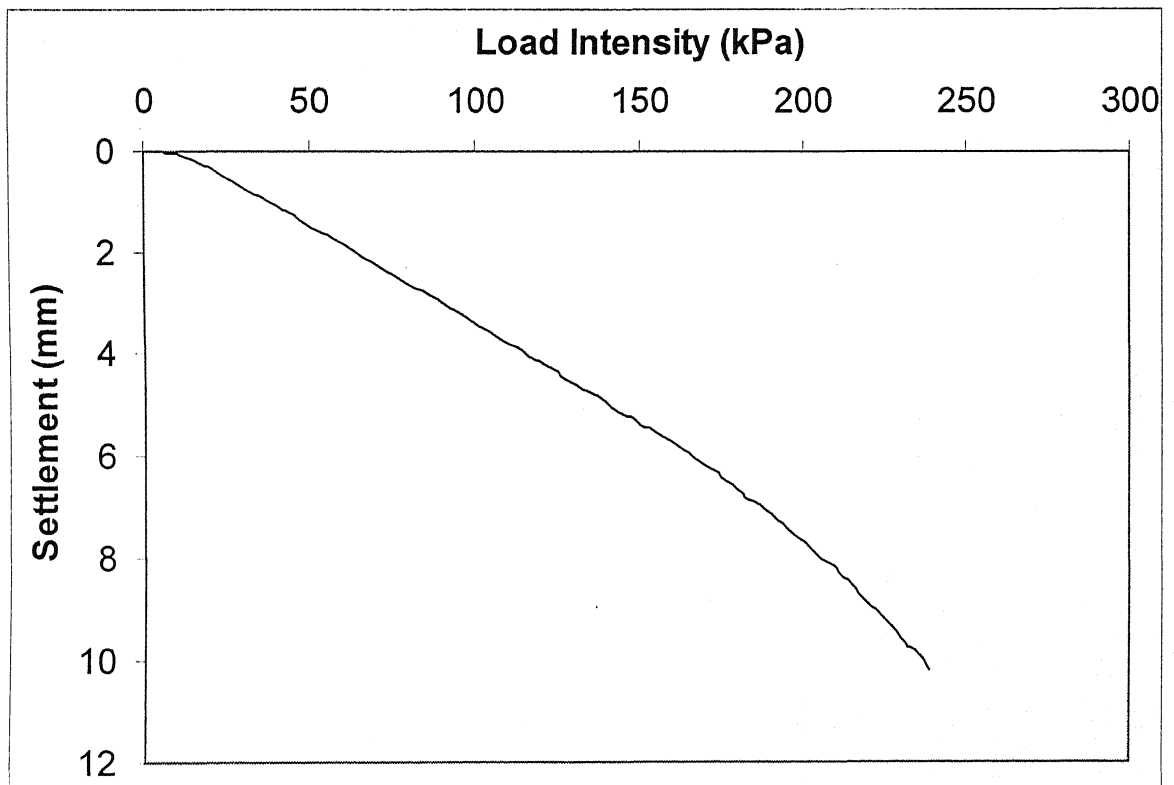


Fig.B.10: Load-Settlement Curve for Two Layers for GG-1 at  $u/B = h/B = 0.5$

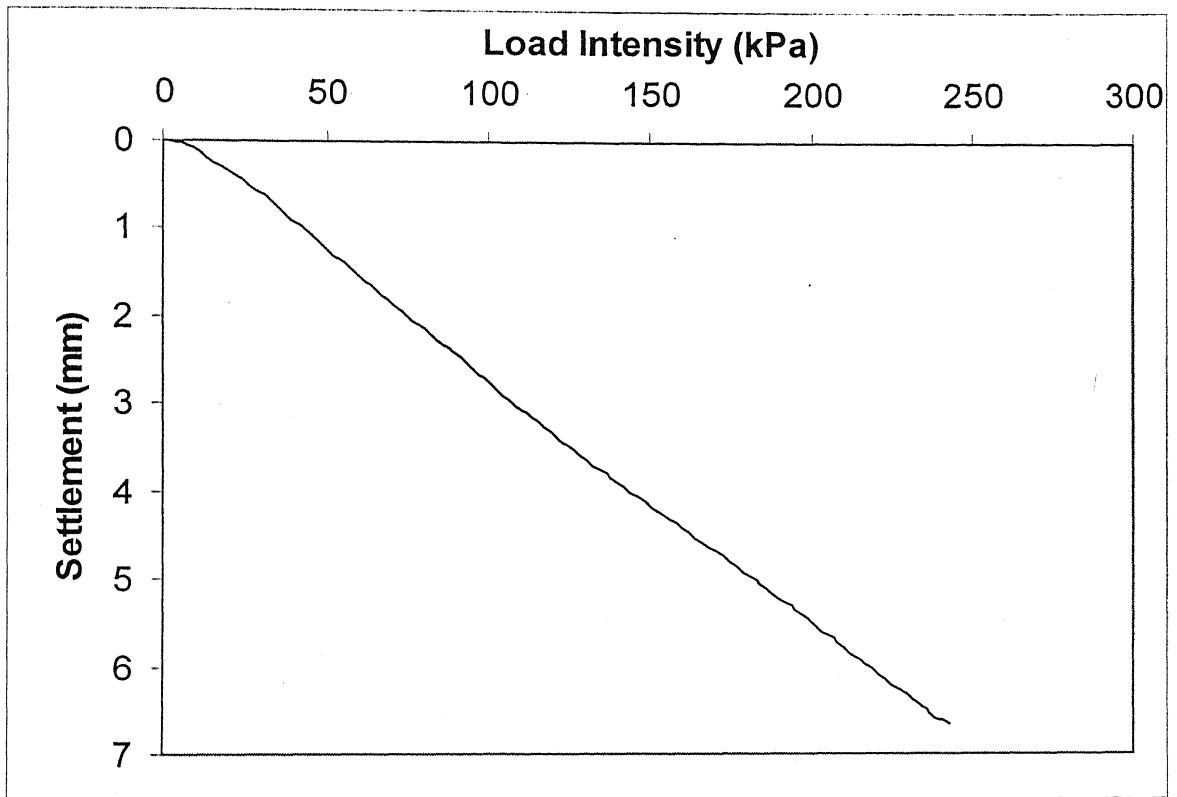


Fig.B.11: Load-Settlement Curve for Three Layers for GG-1 at  $u/B = h/B = 0.33$

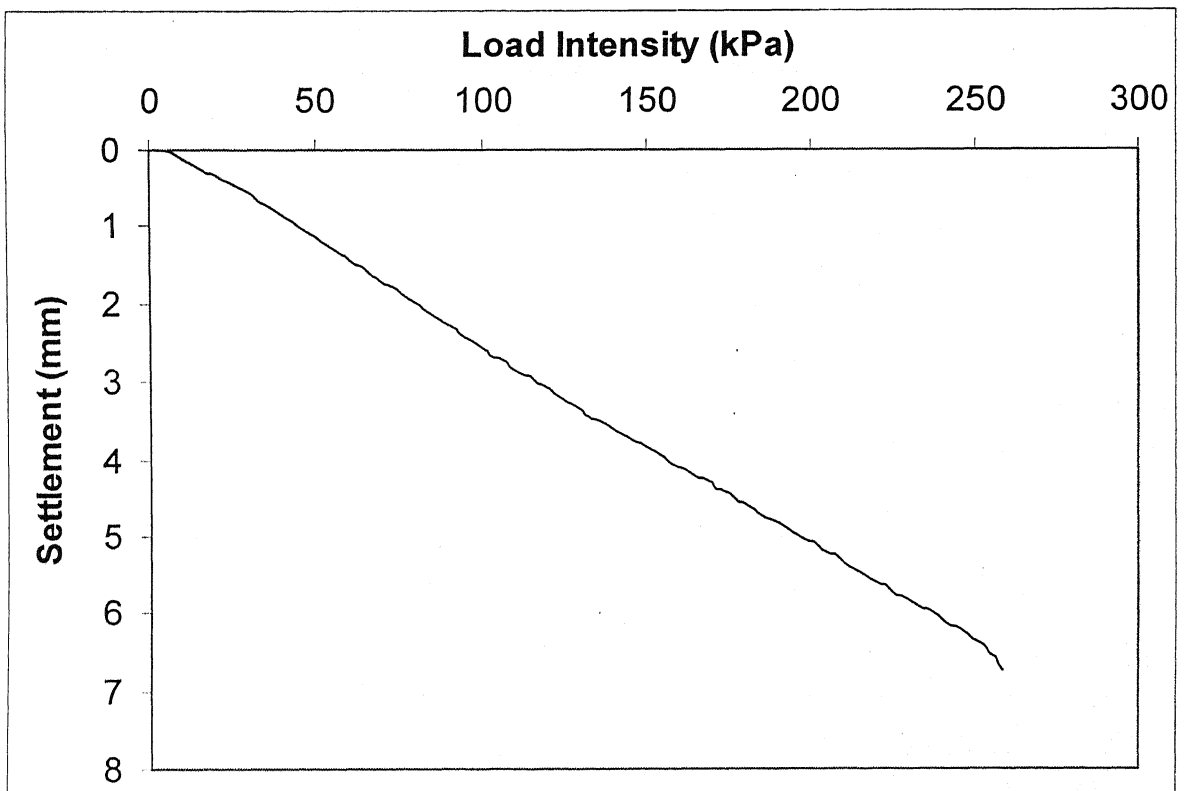
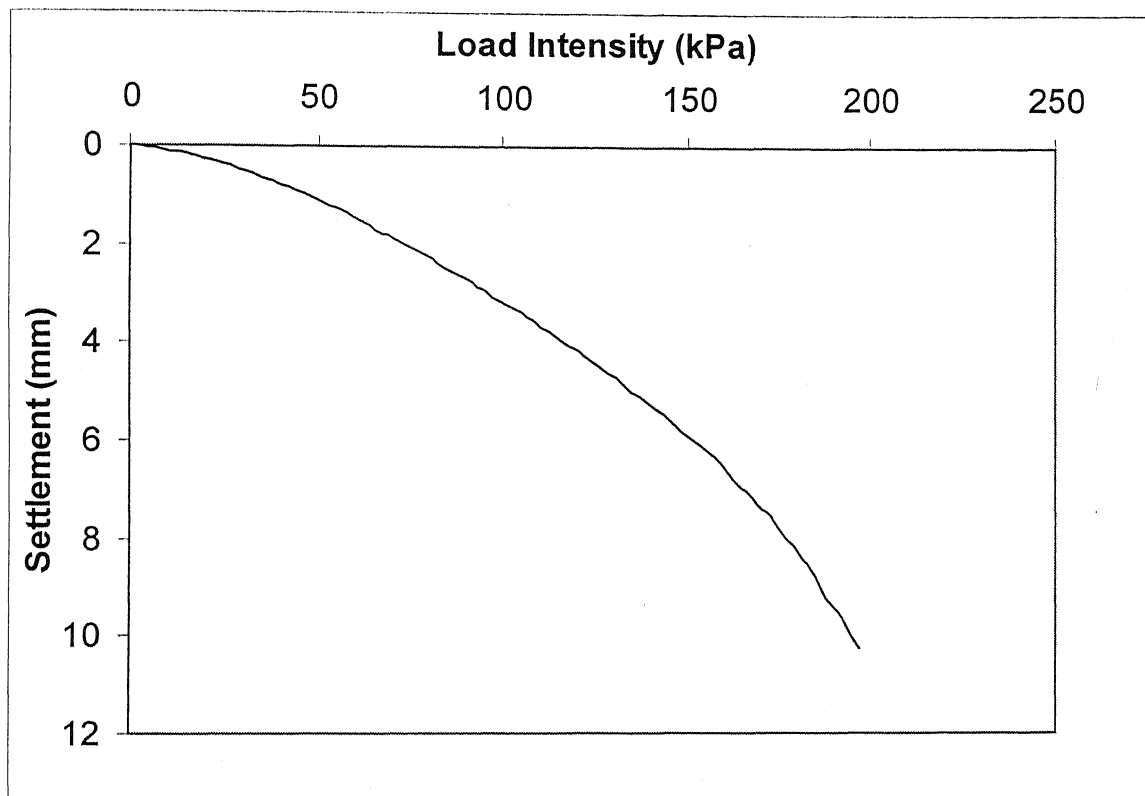
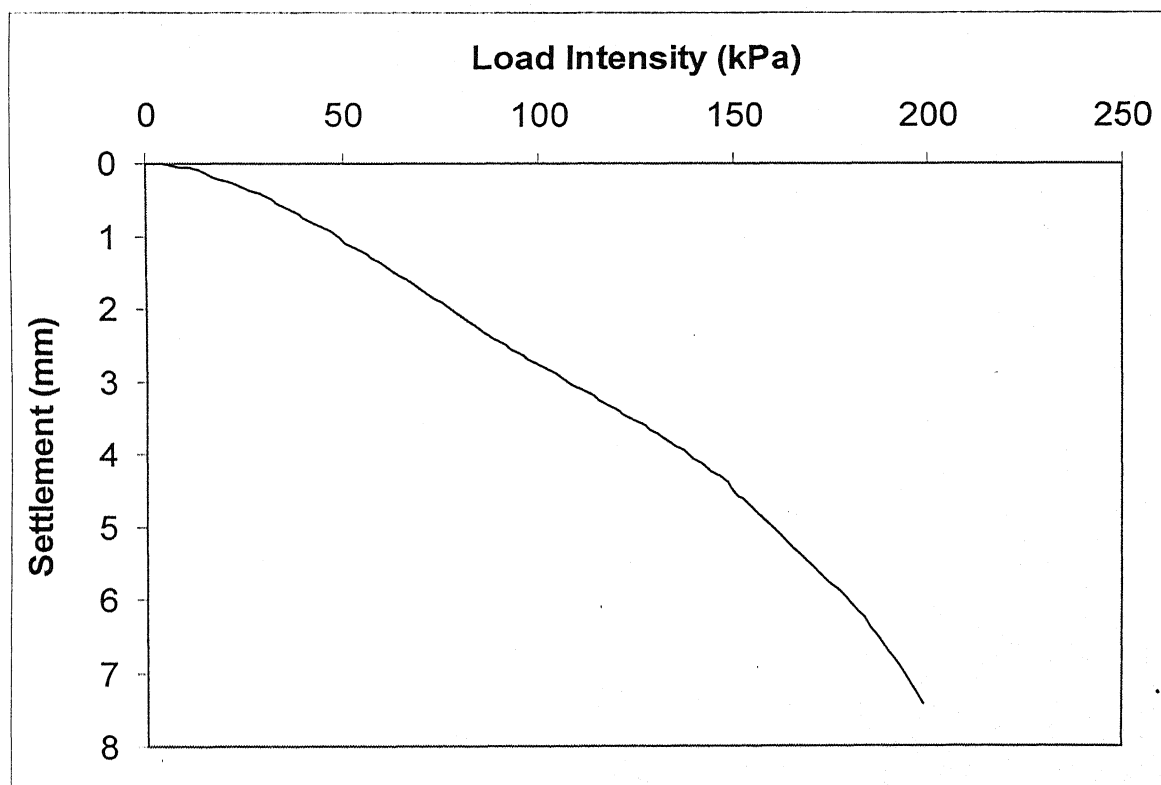


Fig.B.12: Load-Settlement Curve for Four Layers for GG-1 at  $u/B = h/B = 0.25$



**Fig.B.13:** Load-Settlement Curve for One Layer for GG-2 at  $u/B = 0.5$  and  $h/B = 0$



**Fig.B.14:** Load-Settlement Curve for Two Layers for GG-2 at  $u/B = h/B = 0.5$

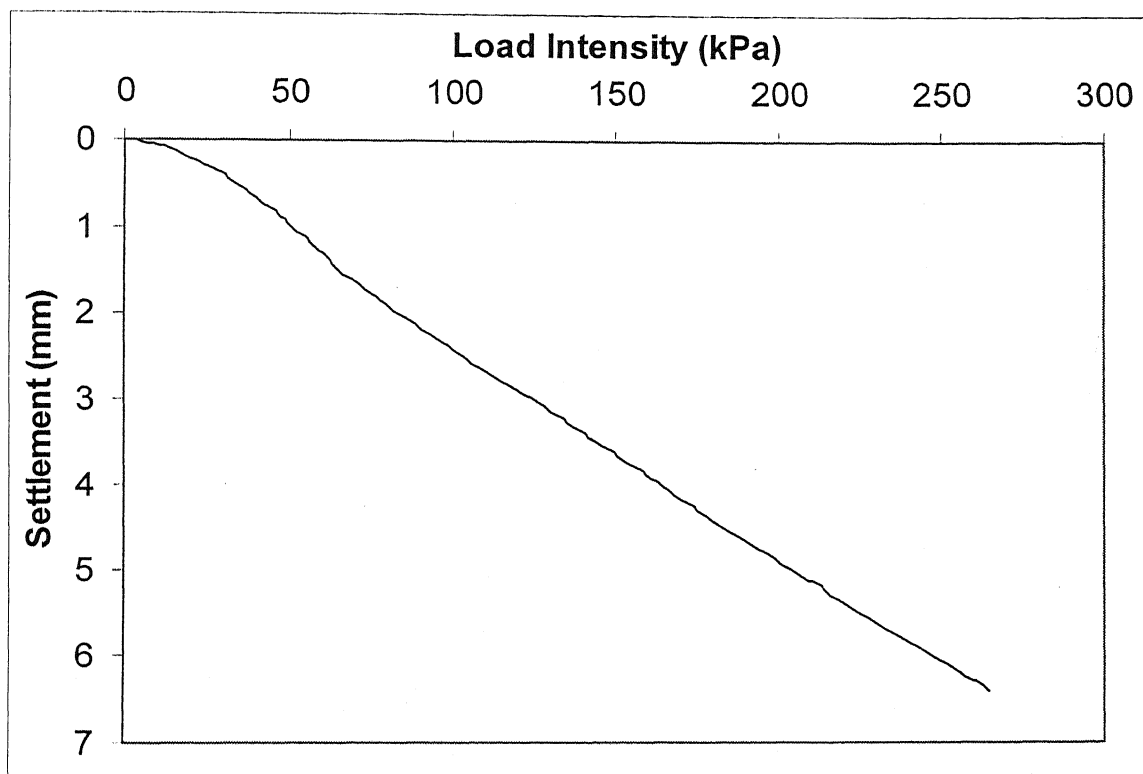


**Fig.B.15:** Load-Settlement Curve for Three Layers for GG-2 at  $u/B = h/B = 0.33$

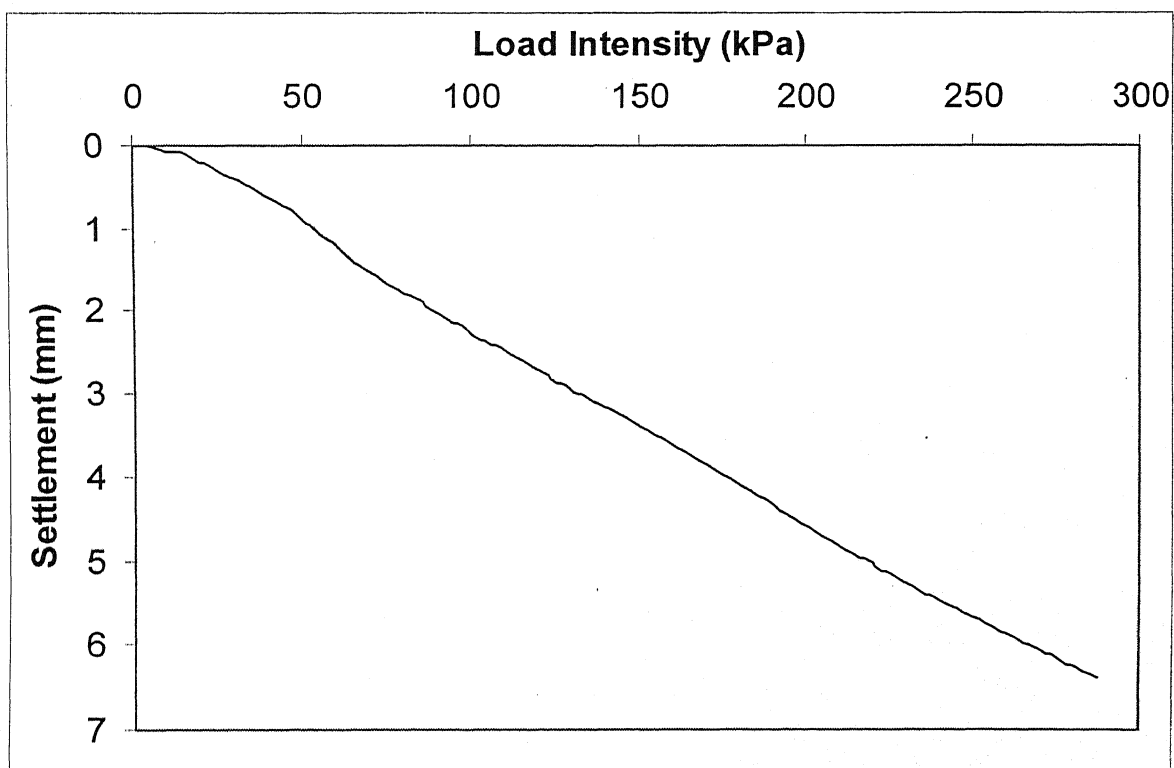


**Fig.B.16:** Load-Settlement Curve for Four Layers for GG-2 at  $u/B = h/B = 0.25$

**Table B.1**

Bearing Pressure at 6mm and Bearing Capacity Ratio  
for Number of Layers for GT-1, GT-2, GG-1 and GG-2

Number of Layers	GT-1		GT-2		GG-1		GG-2	
	$q_{(R)}$	$BCR_s$	$q_{(R)}$	$BCR_s$	$q_{(R)}$	$BCR_s$	$q_{(R)}$	$BCR_s$
1	130	1.55	145.3	1.73	131.5	1.57	152	1.81
2	143.65	1.71	181.1	2.16	165.2	1.97	179.4	2.14
3	201.6	2.40	235.1	2.80	218.3	2.60	247.5	2.95
4	217.7	2.59	253.7	3.02	237.9	2.83	267.4	3.18

## REFERENCES

- Akinmusuru, J.O. and Akinbolade, J.A. (1981). Stability of Loaded Footings on Reinforced Soil, *Journal of Geotechnical Engineering Division, ASCE*, Vol. 107, . No.GT6, 819-827.
- Arora, K. R. (2002). Soil Mechanics and Foundation Engineering. Standard Publishers Distributors, Delhi.
- Benrabah, A. and Gielly.J. (1996). Behavioural Study of a Reinforced Analogical Soil Under External Loads. *Geotextiles and Geomembranes*,14, 43-56.
- Binquet, J. and Lee, K.L. (1975). Bearing Capacity Tests on Reinforced Earth Slabs. *Journal of Geotechnical Engineering Division, ASCE*, Vol. 101, No. GT12, 1241-1255.
- Das, B. M (1985). *Advanced Soil Mechanics*. McGraw-Hill Book Co., Singapore.
- Das, B. M (1989). Foundation on Sand Underlain by Soft Clay with Geotextile at Sand-Clay Interface. *Geosynthetic 89' Conference, Vol 1, San Diego*, 203-13
- Das, B.M. (1999). *Principles of Foundation Engineering, 4<sup>th</sup> Edition*. PWS Publishing, USA.
- Das, B.M. and Khing, K.H. (1994). Foundation on Layered Soil with Geogrid Reinforcement-Effect of a Void. *Geotextiles and Geomembranes*, 13, 545-553.
- Das, B.M. and Shin, E.C. (1994). Strip Foundation on Geogrid-Reinforced Clay: Behavior under Cyclic Loading. *Geotextiles and Geomembranes*, 13, 657-667.
- Das, B.M., Maji, A. and Shin E.C. (1998). Foundation on Geogrid-Reinforced Sand-Effect of Transient Loading. *Geotextiles and Geomembranes*, 16, 151-160.
- Dash, S.K., Krishnaswamy, N.R. and Rajagopal, K. (2001). Bearing Capacity of Strip Footings Supported on Geocell-Reinforced Sand. *Geotextiles and Geomembranes*, 19, 235-256.
- Dembicki, E., Jermolowicz, P. and Niemunism, A. (1986). Bearing Capacity of Strip Foundation on Soft Soil Reinforced by Geotextiles. *Proceedings of 3<sup>rd</sup> International Conference on Geotextiles*, Vienna, 205-209.
- Dey, A and Basudhar. P.K. (2005). Flexural Response of Beams on Reinforced Sand Beds with Variable Subgrade Modulus. M. Tech. Thesis. Indian Institute of Technology, Kanpur
- Fragaszy, R.J. and Lawton, E. (1984). Bearing Capacity of Reinforced Sand Subgrades. *Journal of Geotechnical Engineering Division, ASCE*, Vol. 110, No. 10, 1500-1507.



- Ghosh, C. and Madhav, M.R. (1994 a). Reinforced Granular Fill-Soft Soil System: Confinement Effect. *Geotextiles and Geomembranes*, 13, 727-741.
- Ghosh, C. and Madhav, M.R. (1994 b). Reinforced Granular Fill-Soft Soil System: Membrane Effect. *Geotextiles and Geomembranes*, 13, 743-759.
- Guido, V.A., Chang, D.K. and Sweeney, M.A. (1986). Comparison of Geogrid and Geotextile Reinforced Earth Slabs. *Canadian Geotechnical Journal*, 23, 435-440.
- Huang, C. C and Hong, L. L. (2000). Ultimate Bearing Capacity and Settlement of Footings on Reinforced Sandy Ground. *Soils and Foundations*, Vol. 40, No. 5, 65-73.
- Huang, C. C. and Tatsuoka, F. (1988) "Prediction of bearing capacity in level sandy ground reinforced with strip reinforcement" *International Geotechnical Symposium on Theory and Practice of Earth Reinforcement, Fukuoka, Japan*, 191 - 196.
- Khing, K.H., Das, B.M., Puri, V.K., Cook, E.E. and Yen, S.C. (1993). The Bearing-Capacity of a Strip Foundation on Geogrid-Reinforced Sand. *Geotextiles and Geomembranes*, 12, 351-361.
- Khing, K.H., Das, B.M., Puri, V.K., Yen, S.C and Cook, E.E. (1994). Foundation on Strong Sand Underlain by Weak Clay with Geogrid at the Interface. *Geotextiles and Geomembranes*, 13, 199-206.
- Kurian, N.P, Beena, K.S. and Kumar, R.K. (1997). Settlement of Reinforced Sand in Foundations. *Journal of Geotechnical and Geoenvironmental Engineering Division, ASCE*, Vol. 123, No. 9, 818-827.
- Love, J.P, Burd., H. J, Milligan. G. W. E. and Houlsby. G.T. (1987). Analytical and model studies of reinforcement of a layer of granular fill on a soft clay subgrade. *Canadian Geotechnical Journal*, 24, 611-622.
- Maheshwari, P., Basudhar, P.K., and Chandra, S (2004). Analysis of beams on reinforced granular beds. *Geosynthetic International*, 11, No. 6, 470-480.
- Mandal, J.N. and Sah, H.S. (1992). Bearing Capacity Tests on Geogrid-Reinforced Clay. *Geotextiles and Geomembranes*, 11, 327-333.
- Meyerhof, G. G. (1974). Ultimate Bearing Capacity of Footings on Sand Layer Overlying Clay. *Canadian Geotechnical Journal*, 11, 223-229.
- Omar, M.T., Das, B.M., Puri, V.K. and Yen, S.C. (1993a). Ultimate Bearing Capacity of Rectangular Foundations on Geogrid Reinforcement. *Canadian Geotechnical Journal*, 16, 246-252.

Omar, M.T., Das, B.M., Puri, V.K. and Yen, S.C. (1993b). Ultimate Bearing Capacity of Shallow Foundations on Sand with Geogrid Reinforcement. *Canadian Geotechnical Journal*, 30, 545-549.

Poorooshasb, H.B. (1991). Load Settlement Response of a Compacted Fill Layer Supported by a Geosynthetic Overlying a Void. *Geotextiles and Geomembranes*, 10, 179-201.

Puri, V.K., Yen, S.C., Das, B.M. and Yeo, B. (1993). Cyclic Load-Induced Settlement of a Square Foundation on Geogrid-Reinforced Sand. *Geotextiles and Geomembranes*, 12, 587-597.

Ranjan. G and Rao. A. S. R. Rao (1991). Basic and applied Soil Mechanics, Wiley Eastern Limited, New Delhi.

Samtani. N. C. and Sonpal. R. C. (1989). Laboratory Tests of Strip Footing on Reinforced Cohesive Soil. *Journal of Geotechnical Engineering Division, ASCE*, Vol. 115, No.9, 1326-1330.

Shukla, S.K. and Chandra, S. (1994 b). A Study of Settlement Response of a Geosynthetic-Reinforced Compressible Granular Fill-Soft Soil System. *Geotextiles and Geomembranes*, 13, 627-639.

Unnikrishnan, N., Rajagopal. K., Krishnaswami.N.R (2002). Behaviour of Reinforced Clay under Monotonic and Cyclic loading. *Geotextiles and Geomembranes*, 20, 117-133.

Yetimoglu, T., Wu, J.T.H. and Saglamer, A. (1994). Bearing Capacity of Rectangular Footings on Geogrid-Reinforced Sand. *Journal of Geotechnical Engineering Division, ASCE*, Vol. 120, No. 12, 2083-2099.

Yoo, C. (2001). Laboratory Investigation of Bearing Capacity Behavior of Strip Footing on Geogrid-Reinforced Sand Slope. *Geotextiles and Geomembranes*, 19, 279-298.